

Analysis and Design
of
Electrically Small Loop Antennas
for
LF and MF Applications

Open Source Hardware Engineering

Version 7
Winter, 2022

Contents

1	Introduction	3
2	Antenna Modeling	9
3	Output Coupling	19
4	Noise	29
5	Air Core Loops	39
6	Permeability	50
7	Ferrite Core Loops	62
8	Ferrite Sleeve Loops	88
9	Design Strategies	111
10	Example Analyses	119
A	Symbols	126
B	Double-Tuned Transformers	128
C	Noise Bandwidth	130
D	Antenna Noise Output	132
E	Exact Resonant Loop Analysis	138
F	Miscellaneous	145
G	Axial Field Polynomial Fits	155
H	Worked Examples	157
I	Matlab/Octave Scripts	173

Revision History

This document is a work in progress. Here's a list of changes.

Version 7, Winter, 2022 Corrected error in loss tangent formula (Permeability chapter).

Version 6, Winter, 2022

- Updates to chapter on FSL antennas.
- Changed limits where proximity effect calculations are accurate (figure 5.2).
- Added info about proximity effects and Medhurst's data to Miscellaneous appendix.

Version 5, Winter, 2022

- Experimental verification of FSL antenna analysis added.
- FSL chapter modified extensively.
- Many minor edits and corrections.

Versions 4, 4.1 Spring 2022

- Many changes and additions to the chapter on Air Core loops.
- More re-working of examples. This work is not yet finished.
- Many edits and corrections, too numerous to mention.
- (4.1) Bug fix in Matlab/Octave script `SolenoidAcResistance`.

Version 3, Winter 2021

- Rev 3.1 added calculation of Q to Matlab/Octave example in Appendix E.
- Chapters have been re-ordered.
- Chapter on Noise has been updated with more information on the variation of noise with seasons of the year, and an example observation of sferics.
- Appendix D has been reworked; it contained errors and the analysis was confusing.
- Analysis in appendix E has been reworked in favor of computer analysis. The previous equations were very complex and prone to error.
- Errors in Appendix H have been cleaned up.
- Matlab/Octave scripts added with ITU noise data.

Version 2, Winter 2020

- Many small changes and text edits.
- None of the underlying simulation data or curve fits has been altered.
- Example calculations have been updated to include losses in capacitors used to resonate loop antennas in the LF band.
- Example calculations for loop using 77-material updated to fix problems with self resonance.
- Section added about self resonance in ferrite loop antennas.
- Chapter on models updated with discussions of capture area and quality factor.
- Appendix with resonant loop analysis updated with better definition of resonance, and sample calculation of Q away from resonant frequency.

Chapter 1

Introduction

This article explores the design of receiving loop antennas for the LF (30 to 300kHz) and MF (300kHz to 3MHz) frequency bands. This may also be useful for some VLF applications (3 to 30kHz). Typical examples are antennas for the AM broadcast band (approximately 500 to 1700kHz), or single-frequency designs at 60kHz or 75.5kHz, to receive time signals transmitted by NIST station WWVB in the United States, or DCF77 in Europe.

As with the design of anything, the process begins with a preferably explicit, but perhaps more often, implicit set of specifications. It is not uncommon to begin with only a vague, unwritten idea of specifications. For example, a project might start with the thought “I need a better antenna for my AM radio”. Several questions are lurking inside this idea which must be dealt with for the project to succeed.

- What signal or signals are to be received?
- What are the ambient noise levels?
- What receiver(s) will be used with the antenna?
- How much time is available for the project?
- What are the limits on cost?
- How large can the antenna be?
- Is an electrically small loop antenna the best choice?

Often, the answer to some of these questions will be vague. Regarding size, one might only be able to say something like “tell me how big it needs to be, and I’ll tell you if I can live with it.” As with most engineering problems, there are plenty of trade-offs to be made.

Unfinished Work

This article is still a work in progress, though we feel it is far enough along to publish at this point.

The directional behavior of these kinds of loop antennae is not currently examined in this article, and that is important for some applications. Future versions of this document may be expanded to cover this topic as well.

Signal Strength

The question of which signals are to be received is tougher than it first appears. What the antenna designer really wants to know is the field strength of the signal at the antenna. This is typically the electric field magnitude in units of micro-volts per meter. For example, the requirement might be to receive the AM broadcast on 850kHz from KOA in Denver, Colorado on a typical night in Modesto, California. This then becomes a problem in radio propagation with questions such as:

- What is the frequency? (850kHz)
- What is the transmit power? (50kW)
- What is transmit field strength? (362mV/m at 1km)
- Is the transmit antenna omni-directional, or if not, what does the pattern look like? (non-directional)
- Is the propagation mode ground or sky-wave? (Huh?)
- What is the path loss? (What?)

Answers to some of the easier questions are included above from the FCC AM station query page on the Internet. But the signal strength cannot be estimated without answers to all of those questions, and those having to do with propagation over long distances are not so easily dealt with. It is a complex topic, and beyond the scope of this article. Luckily, in many cases it's not necessary to work these propagation problems because there are alternate ways to estimate the signal strength at the receiving location.

Never Mind

Reality beats theory every time, and examples of signal reception in the same vicinity using antennas and radios with known parameters can provide rough estimates of signal field strength. In the AM broadcast band, regulations published by the FCC provide hints about signal strength. In other cases, signal strength maps may be available regarding the signal of interest.

Noise

A major role is played by noise in the design of loop antennas. Signal output levels from the antenna must be adequate to overcome the contributions of various noise sources. These sources may be broadly categorized as being either external or internal to the antenna and receiver. Noise external to the antenna comes from many sources and includes cosmic, atmospheric, thermal and man-made variants. Noise categorized as internal includes thermal noise (from many different sources) or shot noise generated in electronic amplifiers.

At frequencies of interest for the purposes here (MF and LF), it is often the case that atmospheric noise dominates, and therefore places a lower bound on the weakest signal which can be received. Data published by the International Telecommunications Union (ITU) [ITU-R] can be used to estimate these noise levels. Depending on the receiving site, man-made noise can also be a limiting factor. A following chapter on noise looks at this in more detail.

In cases where atmospheric noise (i.e. lightning discharge) is a limiting factor, a directional antenna may provide better results. Electrically small antennas are limited in their gain (see Chu) and therefore, directionality. This is a case where bigger (a *lot* bigger) is better, and beyond the scope of consideration here.

Size

Loop antennas can be broadly categorized by size. An electrically small loop is one whose size is quite small compared to a wavelength at the frequency of operation. The word “small” is a fuzzy term but here we take it to mean something on the order of 5-10% of a wavelength (0.05 to 0.1λ), at the highest frequency of operation. For example at 1710kHz ($\lambda = 175\text{m}$) a small loop would be no larger than 9 to 18 meters maximum dimension.

For purposes of this article, consideration is further limited such that the total length of wire is no more than 5-10% of a wavelength. It may be possible to push this up as far as 20%, but some of the small-antenna assumptions begin to break down at this point and the accuracy of formulas begins to degrade.

For antennas that tune the entire AM broadcast band (up to 1710kHz), this requires the antenna’s main loop to be wound with no more than about 20m (65 feet) of wire.

For the remainder of this article, only electrically small loop antennas are considered in which both the size and total wire length are limited. The word *loop* will only refer to such designs unless otherwise noted.

Bigger Loops

Design equations used here are based on the approximation that current in the loop wire is roughly in phase at all places in the loop. Loops using more wire will violate this assumption and the equations used will become inaccurate.

For example, we've built a large octagonal loop containing 32m of wire and it works quite well over the entire AM broadcast band. However, estimates of sensitivity made from information in this article are of questionable accuracy at the upper end of the AM band.

Magnetic Coupling

A common technique used to enhance the performance of portable and tabletop AM broadcast receivers is to place the receiver's internal loop antenna in the vicinity of a large air core loop which has been tuned to resonance. This provides magnetic coupling between the receiver's internal ferrite core antenna and the external loop. A theoretical analysis of this configuration is presented which helps to understand what sort of performance can be expected from it.

FSL Antennas

A relatively new, trendy antenna design is the *Ferrite Sleeve Loop*. These seem to have sprung up in hobbyist/amateur radio circles and have received much praise from users. This article presents what may be the first theoretical analysis of these designs.

Motivation

This article was originally intended to be a rewrite and clean up of a previous treatise on loop antennas (see [CIA]). As we got into the article however, it became clear that some of the analysis presented therein was just plain wrong. So that idea was dropped, although some of the drawings and original text have survived in this final result.

A fair bit of research was consulted in the process and it's all referenced in the bibliography. In addition to [CIA], a master's thesis from [Bolton] played a major role in some of the material regarding ferrite core loops.

Theoretical/Mathematical Content

Overall, the math content of this article is not too deep. It is provided in an attempt to provide an intuitive understanding of loop antennas.

For the most part, simple algebra is about the extent of math used here. We also assume a fundamental understanding of AC circuit theory, and complex numbers. The reader will also find it useful to have a very basic understanding of electromagnetic fields and radio wave propagation. Some calculus is also used, but has been limited as much as possible.

Attachments

A zip file has been attached to the original PDF file in which this article is distributed. It may be extracted using the `pdftk` utility, and other PDF viewers may also be able to extract it. Contained in the zip file are Matlab/Octave scripts and data files which implement functions related to ferrite core antennas which are described herein to compute the μ_{rod} and F_{ext} parameters.

Summary and Conclusions

The original motivating article ([CIA]) concludes that in general, the ferrite cored antenna is comparable to an air core antenna when its maximum dimension is somewhat larger (1.2 - 1.8 times) than the air core antenna diameter. In general, we found this to be an accurate statement. The choice between air and ferrite core antennas often depends upon the value that is placed on size. In the limit, air core antennas can be made large enough that it's not practical to build a ferrite core antenna with the same performance.

The line geometry of ferrite antennas results in reduced stray capacitance to nearby objects, so there may be less E-field noise pickup. Furthermore, E-field shielding of a line geometry can be simpler than for an air core loop.

Some design considerations push for a large number of coil turns, yet the higher inductance can make simultaneously achieving a high Q value and acceptable self-resonance frequency difficult with air core designs. This is less of an issue with ferrite core antennas.

Characteristics of ferrite materials introduce problems not found in air-core antennas.

- Ferrite is hard and brittle.
- Its permeability varies with temperature.
- Hum pickup is possible due to ferrite's non-linear B-H curve.
- Permeability can be altered by mechanical shock and stress, vibration and exposure to high level AC or DC magnetic fields.

In many or most situations, it is possible to avoid these issues with careful design.

The largest readily available ferrite rods that will work at MW frequencies (e.g. AM broadcast) are in the range of 1/2 inch (12.7mm) diameter and 7 or 8 inches (200mm) long.

For lower frequencies it may be possible to re-purpose ferrite rods designed for use in RF welding of pipes. These are sometimes called *ferrite impeder cores* and may be useful at frequencies up to a few hundred kHz at most. However, they are very difficult to find online for purchase, and only seem to be available in lengths up to 200mm. To be useful two such cores would need to be stacked, doubling the price, which is quite high. We found some slotted hollow cores online, 40 x 200mm with 20mm ID for about \$36US each. The reduced size of a ferrite antenna would need to be very important to justify that kind of price. Our analysis of Ferrite Sleeve antennas would be of some use here, since these cores often are available as hollow tubes, and have more realistic aspect ratios than do typical FSL designs.

Chapter 2

Antenna Modeling

A simple concept is used to estimate the voltage induced in a loop antenna by an incoming radio signal. More accurate results can be had with expensive simulation software, but this is of questionable value for the purposes of this article.

Propagating radio signals are Transverse Electro-Magnetic (TEM) plane waves. See the entry in Wikipedia or many other resources on the Internet for more detail about TEM plane waves. For a plane wave propagating in free space or air, the magnitudes of electric and magnetic fields have a known ratio. This ratio is often called the impedance of free space, and has a numerical value of about 377 ohms.

By way of example, if the electric field strength of a propagating TEM wave is known to be 1 volt-per-meter (1 V/m), then the magnetic field strength will be 1 V/m divided by 377 ohms or about 0.0027 A/m (amperes-per-meter). For the sake of completeness, the impedance of free space is defined by the permeability and permittivity of free space:

$$Z_o = \sqrt{\frac{\mu_o}{\epsilon_o}} \approx 377\Omega$$

Also useful is this relationship between free space permittivity, permeability and the speed of light:

$$\sqrt{\mu_o\epsilon_o} = \frac{1}{c}$$

and the relationship between frequency and wavelength (also in free space):

$$\lambda = \frac{c}{f}$$

Another concept used here is that of the *phase constant*. It represents how much the phase of a TEM wave changes per unit distance of travel. In the MKS system, it is in units of radians per meter and assigned the greek letter beta. A wave propagating in free space or air will go through a full 360-degree (or 2π radians) rotation over a

distance equal to it's wavelength. This relationship can be expressed in several ways by making substitutions for the wavelength:

$$\beta = \frac{2\pi}{\lambda} = \frac{2\pi f}{c} = \frac{\omega}{c} = \omega \sqrt{\mu_o \epsilon_o} \quad (2.1)$$

Magnetic Fields

There is really only one magnetic field that can be directly measured, and it is a vector field usually represented by the symbol \mathcal{B} . Thus, people talk about B-fields and whether it's vector nature matters or not is often taken as a matter of context. Except for introductory remarks, this article will only be concerned with the magnitude of the field and it will be referred to by the capital letter B. In the MKS system of units, it has units of Teslas.

Confusion may arise however because there is another *conceptual* magnetic field. It is also a vector field and is symbolized as \mathcal{H} , and it's magnitude will be referred to as the H-field. It has units of amperes per meter, or A/m. This field is not always directly measurable, but the conceptual difference between H and B-fields is quite useful when working with ferrite materials.

The chapter on permeability explores this topic. For now, it is adequate to keep in mind that in general, B-fields and H-fields are not the same thing.

Effective Height

The key parameter which characterizes the ability of an electrically small loop antenna to convert radio signals (aka TEM plane waves) into voltages is *effective height*. It tells us how much voltage is induced in the antenna coil in the presence of a radio signal of known field strength.

In a magnetic loop antenna, the open-circuit voltage (V_{oc}) induced by the incoming signal is determined by a vector dot product between the signal's magnetic field vector (\mathcal{H}) and the antenna's effective height, which is a vector, aligned with the loop's axis.

$$V_{oc} = \mathcal{H} \cdot \vec{h}_e$$

For simplicity however, we assume the antenna has been rotated for maximum pickup, and the dot product can be replaced with a multiplication of the two vector magnitudes.

$$V_{oc} = H h_e$$

There may be a bit of confusion regarding electric and magnetic fields as relates to effective height. It is customary to describe TEM waves in terms of the electric field magnitude in volts per meter, not the magnetic field. A radio signal's strength

is not often described in units of micro-Teslas, or micro-Amperes per meter. Thus, the previous equation is not used and (2.2) below takes its place, with effective height in meters multiplying the E-field in volts per meter to yield open circuit voltage in volts.

More will be said about this in the chapter on permeability. For now it's sufficient to note that the open circuit voltage induced in a loop antenna is equal to the TEM wave's E-field magnitude multiplied by the loop's effective height:

$$V_{oc} = E h_e \tag{2.2}$$

under these two assumptions:

- The magnetic field and effective height vectors are co-linear so that maximum output voltage is obtained.
- The signal is propagating in, and the antenna is located in free space or air.

Capture Area

Another useful measure of antenna effectiveness is the idea of *capture area*. This concept is not used here, but a quick explanation as to why is in order. This is a way of quantifying how much *power* an antenna can extract from a propagating radio wave. In this case, the incoming signal strength is expressed in the plane perpendicular to propagation direction at the antenna in units such as watts per square meter. Full-sized antennas can have practical impedances and radiation resistances such that it's feasible to extract significant amounts of power from a radio signal. This idea of capture area makes sense in these circumstances.

Electrically small loops being considered here have such small values of radiation resistance that it's impractical to extract useful power from a radio signal. Most of the power ends up being dissipated in copper losses within the antenna and associated wiring.

Instead, small loops are more often used as magnetic field probes with high impedance voltage outputs. So, although it's possible to compute the capture area of a small loop, this parameter is of little use for our purposes. Instead, quantifying the linear relationship between an incoming signal's field magnitude and the output voltage from the loop is more useful.

Directional Behaviors

Electrically small loop antennas are not generally omnidirectional. In some applications, the ability to place an interfering signal in the null of an antenna pattern is useful. This document does not currently explore the directional behavior of loop antennas, although future updates may add information on this topic.

Loop Schematic Model

Figure 2.1 is the schematic equivalent of a small loop antenna that is used for this article. It contains the following components:

- A voltage induced by an incoming TEM plane wave.
- Loop self-inductance, L
- Wire and core losses, R_{loss} .
- Radiation resistance, R_{rad}
- Self resonance is modeled by placing a capacitor across the loop.

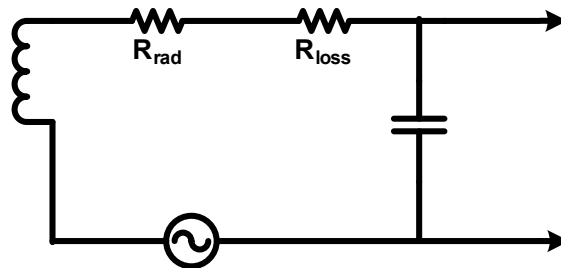


Figure 2.1: Simple loop antenna model

Estimation of loop inductance is left to later chapters. It is treated separately for air and ferrite core loops.

Loss resistance encompasses ohmic losses in the wire plus core losses when the coil is wound on a ferrite rod. Wire resistance will be increased above its direct current value by skin and proximity effects. Core losses can be significant when coils are wound on ferrite rods and in general cannot be neglected. These losses behave just like an additional resistance, including the generation of thermal noise.

For electrically small antennas, radiation resistance is typically in the range of micro-ohms and will be neglected.

Self resonance is a topic in itself but here it's modeled with a capacitor in parallel with the loop terminals. As long as the loop is operated well below its self resonance frequency (SRF), this capacitance will slightly alter the values of external components required to resonate the loop. Losses associated with this capacitance may also slightly lower the resonant Q , mainly in the case of ferrite cored loops. In many cases, it's possible to ignore this capacitance with the caveat that computed external component values may need to be slightly altered to compensate.

Quality Factor

Much of what follows will assume the loop is to be operated with external capacitance added to place it in resonance at the operating frequency. As such, the quality factor, or Q of the resonant loop is of major importance.

The Q of a circuit is frequency dependent, and is defined as the peak energy stored during one cycle divided by the total energy lost per cycle (see [Krauss] section 3.1 for example).

$$Q = 2\pi \frac{\text{Peak Energy Stored during cycle}}{\text{Energy Lost per cycle}}$$

For a series RLC resonant circuit, the Q at resonance is given by

$$Q = \frac{\omega L}{R} = \frac{1}{R \omega C}$$

This expression is only valid at the resonant frequency where equal amounts of energy are being stored in the inductor and capacitor. Calculation of Q requires finding the maximum combined stored energy in both L and C at any point during the cycle.

$$Q = 2\pi \frac{\text{Energy stored in C} + \text{Energy stored in L}}{\text{EnergyLost}}$$

At resonance of a high- Q circuit, stored energy is constant, moving back and forth between L and C during the cycle, with a small fraction of it being dissipated (typically as heat). As such, it's easiest to compute peak energy using either the peak capacitor voltage (when inductor current is zero), or vice versa.

A resonant loop will produce an output voltage higher by a factor of Q , but the calculation of Q must include capacitor losses and the loading effect of the receiver, preamp or whatever electronics is connected to the loop. The actual output voltage is given by

$$V_o = E Q h_e,$$

and we may define the resonant effective height as

$$h'_e = Q h_e \tag{2.3}$$

In the remainder of this document, we will denote both resonant and non-resonant heights by the same symbol, h_e , and the difference should be apparent according to the context.

Q Away From Resonance

The calculation of Q is generally assumed to be made at the resonant frequency of a circuit, but it can also be calculated at other frequencies. Away from resonance, the picture changes. At frequencies well below resonance, energy stored in the inductor is inconsequential. During a cycle, energy in the capacitor reaches a maximum, then nearly all of it gets returned, not to the inductor, but to the source during the next half of the cycle. Even less power is dissipated in the loss resistance away from resonance.

The calculated Q at these frequencies is higher than at resonance, but this is not of much use or interest as the circuit's behavior at resonance is the main concern. Expressions for Q away from resonance are worked out in Appendix E.

The Terminal Impedance Trap

A frequent misconception has it that the Q of a resonant circuit can be determined by measuring the terminal impedance, and that at resonance the Q is zero because the impedance is purely resistive. Plenty of energy is being stored in the circuit at resonance, so the Q cannot be zero.

Impedance analyzers often have the ability to measure the Q of inductors and capacitors. This is done in many cases by assuming the device under test is either an ideal capacitor or inductor with associated loss resistance. Q is estimated by finding the tangent of the phase angle between current and voltage. This method works as long as the test frequency is well away from any resonances of the device, but does not produce the correct result at and near resonance.

High Q Designs

When a high- Q loop is resonated with an external capacitor and connected to a receiver, estimating the Q at resonance requires consideration of additional losses. These include losses in the capacitor and the input impedance of the receiver. The formula for this is not simple and won't be attempted here. Instead, the result can be worked out using CAD tools such as Matlab, Octave or SPICE.

As demonstrated in the chapter on ferrite core loops, more complex models are required to accurately model loop behavior over a wide range of frequencies. This is not strictly necessary for single-frequency designs, but wide band loops (e.g. those used for AM band reception) may need to use more complex models to accurately predict Q at resonance.

Predicting Loss Resistance

Predicting the loss resistance of air core loops is feasible but both skin and proximity effects must be included in the calculation. Ferrite core loops are a different story.

We did not find any published techniques that gave a good estimate for at least one of the ferrite loops we built. While accurate prediction might be possible, we cannot recommend any methods, formulas or algorithms for this purpose.

Diminishing Returns

For resonant loops, Q at the tuned frequency has two major impacts on loop performance that must be traded off against one another. Higher values of Q produce a larger output voltage (proportional to Q), and output impedance (proportional to Q^2). At some point, the resonant impedance becomes large enough that receiver input impedance prevents any further increase in Q .

Higher values of Q result in a smaller 3dB bandwidth for the tuned loop. This is helpful up to a point, but tuned bandwidth can not in general be reduced below the signal bandwidth.

High values of Q also require more accurate loop tuning and can result in stability issues. In our experience, Q values above 150-200 or so start to become difficult to manage without automation through firmware or other means.

In-situ Measurement of Q

The most accurate way to determine the frequency response of a high- Q loop is to measure it in situ, i.e. while connected to an operating receiver. This removes any concerns about the accuracy of estimated parameters for the loop, capacitors, receiver and any other relevant components.

This is easily done with the aid of a signal generator and oscilloscope, as shown in figure 2.2. Depending on the frequencies involved, an expensive signal generator may not be required. We have done this successfully at 60kHz using an Arduino Uno¹ as the signal source, running some code which implements a fractional-N divider on the system clock.

The excitation loop can consist of a ferrite core with enough turns of wire to create a reasonable impedance at frequencies of interest. For example, 80-100 turns of wire on a 12.7x190mm core of 43 material worked well for us.

Depending on the signal source, a current limiting resistor and/or DC blocking capacitor may be necessary. If used, make sure the blocking capacitor value is much larger than what's required to resonate the test loop at frequencies of interest. Its impedance at test frequencies should also be much less than the current limiting resistor (if used).

The excitation loop is placed at a distance from the test loop such that a reasonable signal level is generated at resonance. This should be enough above the noise floor of the scope to give repeatable data, but not so large as to overload the receiver's input

¹To generate accurate frequencies, the ceramic resonator on the Uno must be replaced with a quartz crystal.

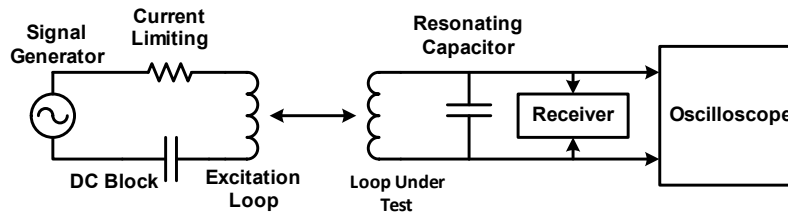


Figure 2.2: In-situ testing of frequency response

stages. Levels of a few hundred mV are typical. Loop spacings are typically on the order of 1-5 feet or so. Obviously, the excitation loop should not be so close as to significantly alter the characteristics of the test loop.

At typical frequencies (MW and below), the test loop will mostly see magnetic near-field components generated by the excitation loop.

The response data may be curve fit to an ideal resonant loop response to determine the resonant Q of the loop under test. For low-Q loops, it may help to correct the measured response with a $1/f$ term to compensate for increasing effective height versus frequency. Some samples of these measurements are shown in the Examples chapter.

Capacitor Losses

For designs with targeted resonant Q values of 50 to 100 or more, losses in the resonating capacitor must be considered. The ratio of loss resistance to reactance in a capacitor is called the loss tangent. This is frequency dependent and is usually expressed as a percentage. The inverse of this value represents an upper limit on the Q of a parallel resonant circuit for the capacitor. For example, a loss tangent of 1%, or 0.01 would limit the Q to no more than 100. In a resonant loop antenna, the loss resistance of the capacitor is in series with the loop's loss resistance, and this must be factored in as well.

The loss tangent is mostly a function of the dielectric material in the capacitor, and here is a quick rundown of what's typically available.

X7R MLCC These are not generally useful for anything but low-Q designs, as loss tangents are typically larger than 1%.

NPO/C0G Although the range of capacitance available is limited, these can have very low losses – 0.1% and less, and are very useful for MW band loops.

PPS Film (Polyphenylene Sulfide) Typical loss tangents below 100kHz can be fractions of a percent, and these are useful for designs with Q values less than 100 or so. Losses tend to increase above a few hundred kHz.

PP Film (Polypropylene) Loss tangents are very low, often less than 0.1%, and these are useful for designs with moderate to high Q.

Air Usually found in the form of variable capacitors, these units can have very low losses, but maximum capacitance values are usually in the range of a few hundred pF to a couple of nF. They are useful for MW band designs, and for fine tuning of lower frequency loops.

Polystyrene This material makes a very high performance capacitor, but such units are no longer generally available. Consider polypropylene as an alternative.

To have minimal effect on resonant Q, the loss tangent of the capacitor should be at least ten times less than $1/Q_L$ where Q_L is the ratio of reactance to resistance of the antenna coil in parallel with the receiver input impedance. This is often not possible with high-Q designs, and capacitor losses may end up causing a significant limit on achievable Q.

As an example, consider an air-core loop we built for 60kHz. It is 170mm in diameter with 83 turns of 22-gauge stranded wire. Measurements of the loop alone indicate an inductance of 1.034mH with AC resistance of 2.26 ohms at 60kHz – giving a maximum achievable Q of $\frac{2\pi \times 60,000 \times 0.001034}{2.26} \approx 173$.

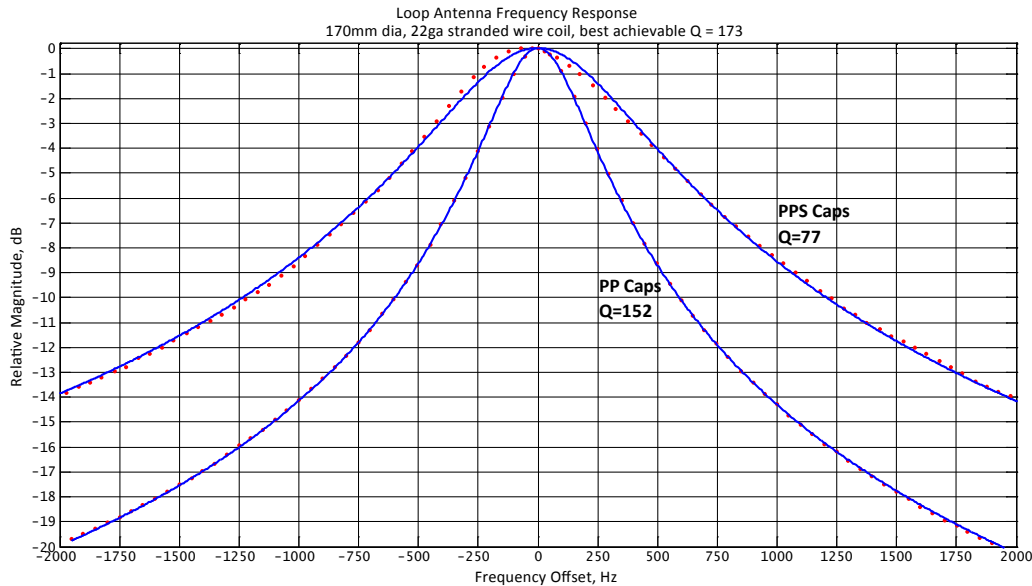


Figure 2.3: Effect of Capacitor Losses on Resonant Q

Measurements of resonant Q were made with two different resonating capacitor types. First a PPS film capacitor in parallel with some C0G units for fine tuning were tried, with a resulting Q of 77 at 60kHz, indicating a loss tangent of about 0.7%, which matches the manufacturer’s specified loss.

Switching to polypropylene film capacitors increased the Q to 152, which is consistent with a capacitor loss tangent of 0.08%, which is also in line with the specified loss tangent of 0.07%.

Figure 2.3 shows the measurements of these two configurations, with measured data points as red dots and fitted resonance models in blue. Using the best available capacitors (PP film) results in a 5.9dB increase in resonant effective height, compared to moderately low loss caps (PPS film).

Impedance Transformation

As shown in the appendix, for a simple series R-L-C circuit, loss resistance is transformed at parallel resonance into a much higher value – by a factor of Q^2 . In many cases, extremely high values of receiver input impedance are required to avoid lowering the overall loop Q at resonance.

When this is not practical, a second coupling loop with fewer turns may be added for connection to the receiver. This will transform the receiver input impedance to a higher value which better matches the loop’s tuned impedance.

For example, a 1:10 turns ratio ($N = 10$) on the output coupling loop would increase a receiver’s 300Ω input impedance by a factor of 10^2 up to $30k\Omega$, and that might be enough to avoid loading down the loop’s Q too much. This would simultaneously reduce the loop output voltage by a factor of ten (20dB).

Antennas versus Systems

While loop antenna performance in isolation can be modeled, in many or most cases this is not practical. The loop must be connected to a receiver to be useful, and the receiver’s input parameters can have a significant effect on overall performance. In practice then, it is only possible to predict and compare the performance of antenna-receiver combinations.

As an example, the overall resonant Q (and therefore effective height) must take into account the loss resistance of the receiver’s input. Two resonant loops may have a 10:1 ratio of Q values by themselves, but receiver input loss resistance may reduce that ratio to a much lower value, thus reducing benefit of one loop over another. Similar issues arise with parameters such as noise and bandwidth.

So, while this document is largely concerned with prediction of antenna performance, it is tacitly assumed that relevant parts of receiver performance will be integrated with these methods in predicting overall system performance.

Chapter 3

Output Coupling

Electrically large antennas (such as a half-wave dipole or large loop) have a practical radiation resistance (tens or hundreds of ohms), and copper losses are low compared to this. As a result, useful amounts of power may be extracted by a receiver.

In a small loop antenna, radiation resistance is minuscule compared to the loss resistance. A typical ratio of radiation to loss resistance is $100\mu\Omega/3\Omega$ which equates to an 84dB power loss compared to the power theoretically available from the antenna without the loss resistance. This explains why small loops are not used much in transmit mode.

Electrically small loop antennas in receive mode cannot be expected to provide useful *power* to the receiver. Instead, voltage or current must be sensed and amplified to provide a useful output. Typically, such loops are coupled to receivers in one of two ways: direct voltage output, or by magnetic coupling to a secondary loop.

Connecting a capacitor in parallel with the loop to resonate it at the operating frequency does two things. First, voltage developed in the loop is multiplied by the resonant Q; this is useful for direct voltage output. Secondly, current through the loop is maximized at resonance, and this maximizes induced fields for purposes of magnetic output coupling.

Direct Output

This can be done with or without resonating the loop. Parallel resonant circuits are most common, but it's also possible to configure the loop as a series resonant circuit.

Non-Resonant

If loop output levels are adequate, a low-noise amplifier may be connected directly across the loop's output. The input impedance only need be large compared to the loop reactance at frequencies of operation.

Amplifier input current noise must be managed since the loop may have a reactance of several thousand ohms or more at operating frequencies.

If noise issues can be managed, this scheme has an advantage in that the loop does not require tuning to match incoming signal frequencies. A non-resonant loop does not provide frequency-dependent filtering, and this may be a disadvantage if there are large undesired signals at other frequencies capable of overloading the amplifier.

Parallel Resonance

A capacitor can be placed across the loop terminals as in figure 3.1. This model includes a resistance, R_{tune} to represent losses in the added capacitor. Of course, the amplifier should have a high input impedance, Z_L , at the frequencies of interest – ideally, high enough not to significantly lower the loop’s resonant Q .

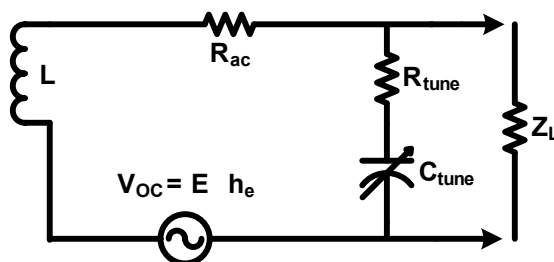


Figure 3.1: Parallel Resonant Loop Configuration

Resonating the loop increases its output voltage but also drastically increases the impedance through which this voltage is delivered. If the load impedance in figure 3.1 is ignored, there is a simple formula to express the loop’s quality factor:

$$Q = \frac{f_o}{B} = \frac{\omega_o L}{R}, \quad R = R_{ac} + R_{tune}$$

The first identity is the ratio of center frequency (f_o) to 3dB bandwidth (B), and the second is loop inductive reactance at resonance ($\omega_o L$) divided by loss resistance (R). At resonance, the loss resistance is transformed by the Q squared, so the loop’s output impedance appears to be:

$$Z_o = RQ^2 = R \left(\frac{f_o}{B} \right)^2 = R \left(\frac{\omega_o L}{R} \right)^2 = \frac{\omega_o^2 L^2}{R}$$

For a typical example, consider a loop with 20kHz bandwidth operating at 1MHz ($Q = 50$) and total loss resistance of 4Ω . At resonance, the output impedance will be $4\Omega \times 50^2 = 10k\Omega$.

While these equations are useful for getting a rough idea of overall Q , they don’t consider the load impedance, Z_L , or the fact it is connected at the junction between R_{ac} , R_{tune} . Including these additional factors make the equations considerably more

complex, and it will be simpler to use CAD tools such as Matlab/Octave or SPICE to analyze the overall circuit.

Series Resonance

A variation of resonant coupling involves adding a capacitor in series with the loop to cancel the loop reactance. In this case, the induced voltage in the loop generates a current which is then amplified as shown in figure 3.2.

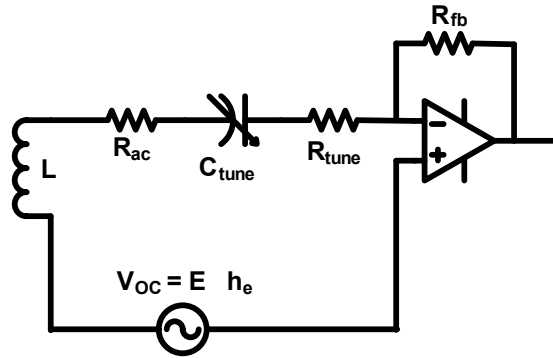


Figure 3.2: Series Resonant Loop Configuration

A typical schematic for this is shown in figure 3.1 where an operational amplifier is used. This type of design requires an amplifier with very low input current and voltage noise. These types of amplifiers do exist, but can be fairly expensive.

We're not aware of this design being used anywhere. The main advantage of this configuration would be improved rejection of atmospheric noise (sferics) in MW frequency applications. To get good sensitivity, loops with large non-resonant effective heights are required and this kind of design may or may not be practical.

Parallel vs Series Resonance

A significant difference in these two configurations is their behavior away from resonance. The parallel circuit (figure 3.1) has a constant low frequency gain of $1/Q$ at frequencies well below resonance. Gain rolls off at a rate of 40dB/decade well above resonance. Thus, unwanted signals and noise at lower frequencies are suppressed by a constant amount.

The series resonant configuration (figure 3.2) exhibits a gain curve that rolls off at a rate of 20dB/decade both above and below resonance. Compared to parallel resonance, this configuration does a better job of rejecting unwanted signals and noise at lower frequencies, but is not as good with higher frequencies. This is an accurate picture for internally generated voltages such as thermal noise. Where external signals

are concerned, the antenna's effective height varies linearly with frequency and that must be considered as well. This adds a 20dB/decade increasing slope to the gain at all frequencies.

These differences are shown in figure 3.3 for the parallel (left graph) and series (right graph) resonant configurations. External gains are plotted with solid lines, and internal gains are dashed.

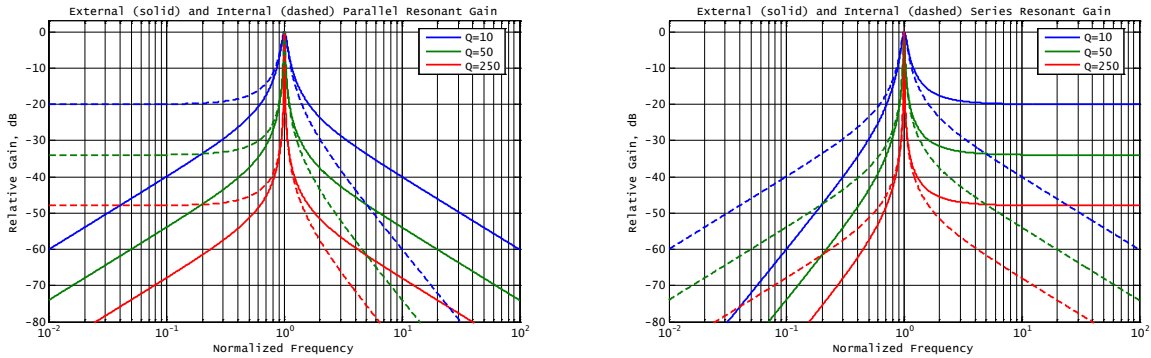


Figure 3.3: Behavior of Parallel and Series Resonant Loops

Where external signals are concerned, the parallel resonant configuration rejects unwanted signals and noise equally above and below resonance (20dB/decade). The series resonant design rejects low frequencies better (40dB/decade) than high (constant attenuation of $1/Q$). In the chapter on Noise, the effect of these behaviors on atmospheric noise will be investigated.

Modern AM Radios

Several portable/tabletop radios are commercially available today which make use of radio-on-a-chip integrated circuits (e.g. from Silicon Labs). These chips connect directly to a loop antenna and contain internally adjustable capacitance. The loop is automatically tuned to resonance by firmware in the radio chip. This makes it feasible to modify the radio by disconnecting the internal loop antenna and connecting a much larger external loop directly to the radio chip. It is only necessary to keep the loop inductance within limits acceptable to the radio chip.

Magnetic Coupling

This is usually done for one of two reasons.

- Loops may be wound with a low turn count secondary winding either adjacent to or interspersed with the main winding. The high main loop impedance can be lowered to a more convenient value by this method.

- A resonant loop may be coupled to the internal ferrite rod antenna of a portable or tabletop radio, by placing the radio in close proximity to the loop. This is convenient as it does not require any modification of the radio to achieve better sensitivity. The downside is that the loop must be manually tuned to the same frequency as the receiver.

Tuning the loop to resonance cancels the reactance of the coil so the voltage induced into the antenna by RF signals is applied across the total loop resistance, which is the sum of radiation resistance, copper resistance and ferrite losses (if present). A current flows in the loop equal to the induced voltage divided by the total resistance. This current then creates a magnetic field which is picked up by the secondary winding, which can be either a dedicated winding that's part of the loop structure, or the internal ferrite antenna in a portable radio.

In both scenarios, this is essentially a transformer and it will be analyzed that way. The transformer parameters of interest here are the inductance of primary, secondary, and mutual inductance. The reader may review the transformer model used here on many educational web sites or in standard entry-level engineering textbooks.

Figure 3.4 shows the transformer model. L_p, L_s are the open-circuited primary and secondary inductance. k is the coupling factor, V_p, V_s are the induced primary and transformed secondary voltages. Resistors represent winding resistance but core losses may need to be modeled as resistances in parallel with the windings; we don't consider that here for the time being. The second schematic shows the secondary components reflected into the primary side of the transformer.

First, consider the situation with the secondary open-circuited. Assume that the primary resistance R_p is negligible compared to the total inductive reactance and may be ignored. When tuned to resonance, the voltage across the primary is the induced signal voltage, V_p multiplied by Q . This voltage appears across the series combination of primary leakage ($(1-k)L_p$) and magnetizing (kL_p) inductance. These two components act as a voltage divider so that the voltage appearing across the magnetizing inductance is the induced primary voltage multiplied by the coupling factor. It is this reduced voltage which is transformed by the turns ratio into the secondary voltage, V_s .

Thus, signal voltage will be lost on the secondary side when the coupling factor is less than one. A coupling factor $k = 0.1$ means that only 10% of the induced primary voltage actually gets transformed, so there is a 20dB loss of signal. A transformer with induced primary voltage of $100\mu\text{V}$, $k = 0.5$, and a 5:1 turns ratio would provide an open-circuit voltage of $(100 \times 0.5 \times 0.2) = 10\mu\text{V}$ on the secondary.

Loaded Q

The second equivalent schematic in figure 3.4 must be used to determine the effect of receiver loading on the resonant Q . This is no longer a simple resonant circuit, and

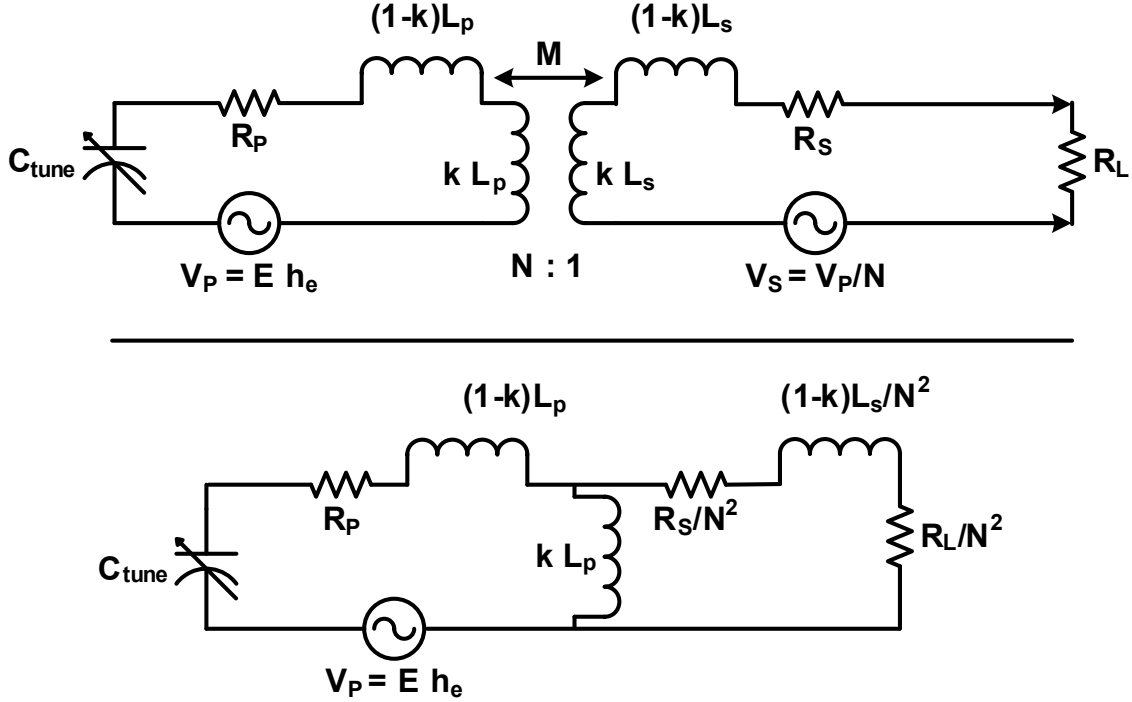


Figure 3.4: Transformer model including leakage inductance

an expression for the loaded Q will not be developed here. It's much easier in this case to use a SPICE simulation to determine the output voltage levels.

Coupled Windings

When secondary windings are located adjacent to or interspersed with an air core loop's main winding coupling factors between 0.5 and 0.8 are not uncommon. If it's not possible to measure k , assume a value in this range for typical designs. Multiple windings on ferrite rods will typically have higher coupling factors.

At resonance the loss resistance on the primary side is transformed by Q^2 , and can become very large. The transformer will scale this impedance as the square of the turns ratio, so the high impedance of a resonated loop is lowered to a more manageable value on the secondary side, although the output voltage is obviously also reduced by the turns ratio.

Consider a resonant loop with $200\mu\text{H}$ of inductance and Q of 100 tuned to resonance at 1MHz. Based on the Q value, loop resistance would be 12.6 ohms, and that would be transformed at resonance to $RQ^2 = 126\text{k}\Omega$. Using a 5:1 turns ratio on the secondary would reduce that by a factor of 25, down to about $5\text{k}\Omega$, while also reducing the output voltage (and equivalent effective height) by a factor of five (assuming $k = 1$). Obviously, the numbers would come out differently with a lower

coupling factor.

Coupling to a Radio's Internal Loop Antenna

Most portable/tabletop AM radios are supplied with an internal ferrite loop antenna. A common technique used to improve the sensitivity of these radios is to magnetically couple the internal antenna to an external loop which has been tuned to resonance.

The external loop acts as the primary winding of a transformer with the secondary being the antenna coil in the AM radio. Now both loops are tuned since ferrite antennas in these types of radios are resonated inside the radio – this is a double-tuned transformer. Analysis of a double-tuned transformers is complex and beyond the scope of this article. Readers should be aware that these types of circuits can behave in unexpected ways.

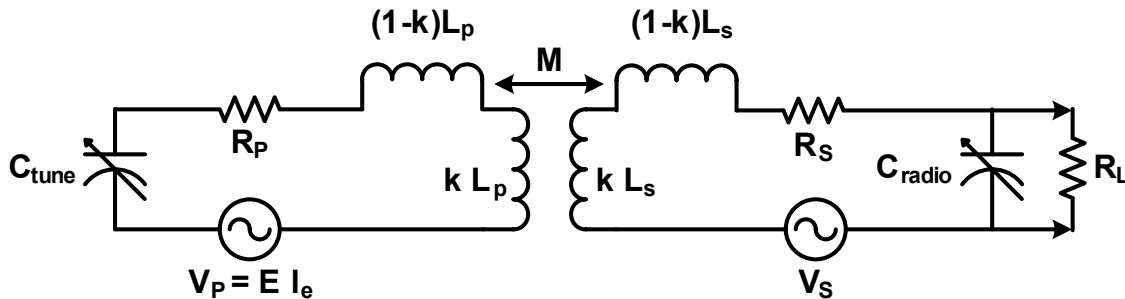


Figure 3.5: Double tuned transformer model

There is a critical coupling ratio where the output of the secondary is maximized. The frequency response of the circuit changes significantly above and below the critical coupling ratio. Below we show three different frequency responses from a double-tuned transformer with both primary and secondary having $Q = 100$, tuned to 1MHz. Critical coupling in this case is $k_c = 0.01$. The three responses represent coupling factors less than, equal to and more than critical. These responses can occur as the portable radio is moved towards and away from the external loop.

The horizontal axis is 10kHz per division and we observe the following:

- The red response has $k = k_c/3$. The bandpass may be a bit too narrow for an AM signal without distortion of the audio spectrum.
- In blue, coupling is critical, with the classic flat-top passband shape. This is a reasonable bandwidth for AM broadcast signals. The signal voltage is about 2dB higher than in the over- and under-coupled cases.
- The green response is over-coupled ($k = 3k_c$), and the bandwidth is now wider than necessary for a 10kHz AM signal spacing. Tuning the external loop slightly

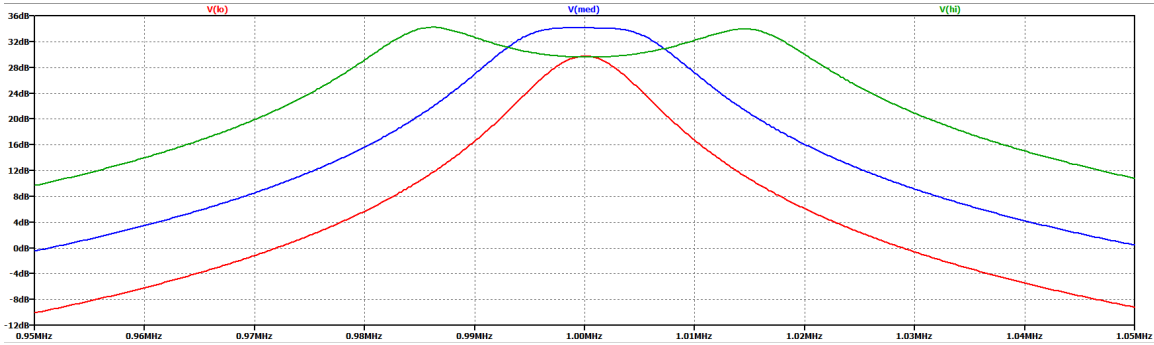


Figure 3.6: Double-tuned transformer response variations

off frequency will produce more signal in the receiver, but selectivity will not be as good.

To analyze this accurately, a lot must be known about all of the components, including those in the radio, but that's not usually the case. See the appendix for a bit more detail on double-tuned resonant transformer circuits.

The big take-away is that the critical coupling factor – where voltage into the receiver is maximized – occurs where

$$k = k_c = \frac{1}{\sqrt{Q_p Q_s}}$$

The term in the denominator is the geometric mean of the external loop Q and the internal ferrite antenna Q. The actual voltage gain at critical coupling is the geometric mean of the two Q values:

$$\frac{1}{k_c} = \sqrt{Q_p Q_s}$$

Because the portable receiver's antenna is treated as part of a transformer here, it's effective height is no longer of interest...assuming the additional signal imparted through the external loop is a lot bigger than that picked up directly by the internal antenna. Under this assumption, the total effective height of the dual-loop setup with critical coupling will be the external loop's non-resonant h_e , multiplied by the geometric mean of the two loop Q values.

Typical Coupling Factors

With an LCR meter it's possible to measure some typical values of k with a typical internal ferrite antenna magnetically coupled to an air or ferrite core loop. Some sample measurements are shown here for three different situations.

- Two ferrite rod antennas separated by 3/4 of an inch.

- A four-foot air core loop and ferrite rod antenna with the ferrite on the inside of the loop, one inch from the windings.
- The same four-foot loop, but with the ferrite rod on the outside of the air core loop, one inch from the windings.

Here's a summary of measured coupling factors for the three setups.

Situation	Coupling Factor	Relative Loss
Two ferrite rods	0.11	0dB
Inside 4-foot loop	0.036	9.7dB
Outside 4-foot loop	0.022	14dB

Some Good News

It is not a coincidence that external MW loop Qs are often designed to be of the same order of magnitude as a portable radio's tuned internal antenna, in the range from 50-100 or so. That's a consequence of the bandwidth of AM broadcast signals. This means the critical coupling factor is in the neighborhood of 0.01 to 0.02, and we see from the preceding section that it is often possible to slightly exceed the critical value with typical geometries encountered in the real world. This seems like just plain good luck.

If a radio with a numeric RSSI display is used, that makes it possible to carefully adjust the spacing between radio and external loop for the highest RSSI reading which would indicate critical coupling.

Comparing External Loops

As stated above, the total effective height for the dual-loop configuration is going to be

$$h_e = h_{ext} \sqrt{Q_{ext} Q_{int}}$$

where h_{ext} is the *non-resonant* effective height of the external loop.

We may wish to compare different external loops with the same portable radio. Assuming that critical coupling can be achieved with each external loop, the ratio of overall effective heights for two different external loops is

$$\frac{h_{e1}}{h_{e2}} = \frac{h_{ext1}}{h_{ext2}} \sqrt{\frac{Q_{ext1}}{Q_{ext2}}}$$

From this it is clear that to predict the *relative* performance of two external loops critically coupled to the same radio, knowledge of the two external loop Q values is necessary. However, knowledge of the Q of the radio's tuned ferrite loop is not required.

Effect of External Loop Q on Overall Q

Although this result has already been developed, it is worth repeating. The overall effective height of the coupled design is equal to the non-resonant h_e of the external loop, multiplied by the geometric mean of the resonant Q's of internal and external loops.

$$h_e = h_{ext} \sqrt{Q_{ext} Q_{int}} = \sqrt{Q_{ext}} \left(h_{ext} \sqrt{Q_{int}} \right)$$

The terms have been grouped to show that the overall effective height varies only with the square-root of the external loop's resonant Q. For a given radio and non-resonant height, doubling the external loop's Q (6dB) will only increase the overall height by about 41% (3dB).

Chapter 4

Noise

The minimum signal that can produce a useful output from a radio receiver is determined by the overall signal-to-noise ratio. This ratio is set by the external noise entering the receiver via the antenna and by the internal noise generated in the antenna and in the front end of the receiver. It's important therefore to briefly review sources of noise generation and single out those which are most objectionable at LF and MF.

Noise Sources	
Externally Generated	Internally Generated
Atmospheric (electrical storms)	Antenna ohmic resistance (thermal)
Cosmic (extra-terrestrial radiation)	Coupling circuit resistance (thermal)
Man-made static	Receiver front end
Precipitation static	Ferrite losses (thermal)
Radiation resistance (thermal)	

External Noise Sources

An important source for data on external noise sources is the ITU recommendation on radio noise [ITU-R]. Considering first external generators, the following noise sources are typically not important in MF and LF applications:

- Cosmic (or galactic) noise plays no important role below 2-3MHz. See figure 2 in the ITU recommendation.
- Thermal noise related to the radiation resistance of antennas to be considered in this report will be miniscule by comparison with other resistive components as a direct consequence of restricting this article to electrically small antennas.

- Precipitation static is caused by the discharge of charged particles in the immediate vicinity of the antenna. Accumulation of the charged particles can be caused by raindrops, hailstones, snow or dust clouds. This type of noise is of particular importance in aircraft receiving antennas, and will not be considered here.

That leaves two normally dominant noise sources:

- Atmospheric (electrical storms)
- Man-made

These two sources generate noise signals which are fundamentally different. The former gives rise to propagating electromagnetic waves in which the electric and magnetic field intensities are related by the characteristic impedance of free space (about 377Ω).

The latter on the other hand is a near-field phenomenon for which the E-field and H-field intensities are related by a factor which is a function of frequency and which is far greater than 377Ω for frequencies below 1500kHz. At the frequencies of interest for this report, man-made disturbances are primarily electric field phenomena.

Summing up these points, it is noted that atmospheric noise and the signals of interest both propagate via radiation fields and, in its passband, an omni-directional antenna cannot distinguish one from the other. In this respect, then, one antenna is superior to another only if its directivity is higher. An ideal loop antenna has a figure-eight pattern in the horizontal plane compared to the uniform pattern of a vertical open antenna, so this is a benefit.

Electrostatic disturbances can be effectively discriminated against by antennas that respond only to magnetic fields. This attribute is one of the chief advantages of the magnetic loop antenna. E-field noise can however generate common mode noise (capacitively coupled to the loop), and there may be identical noise signals on both antenna connections. Receivers must provide reasonable common-mode rejection performance when this occurs, or the loop must be shielded.

ITU Estimates of Atmospheric Noise

ITU recommendation ITU-R P.372-13 [ITU-R] provides estimates of atmospheric noise at any point on the Earth as a function of time of day (4-hour segments) and season. Noise levels are provided in the form of an *external noise factor*, F_a in decibels. It is the ratio between noise power produced by a lossless antenna to thermal noise at room temperature. A formula is provided to convert this value to an equivalent E-field magnitude.

Examples of the ITU data are shown in figures 4.1 and 4.2. Estimating noise is a two-step process. First, there is a set of six maps which show countours of F_a values

at 1MHz across the globe, one map for each 4-hour segment of a 24-hour day. There are separate map sets for the four seasons, Winter, Spring, Summer and Autumn. A second chart which allows determination of noise levels at other frequencies based on the 1MHz level.

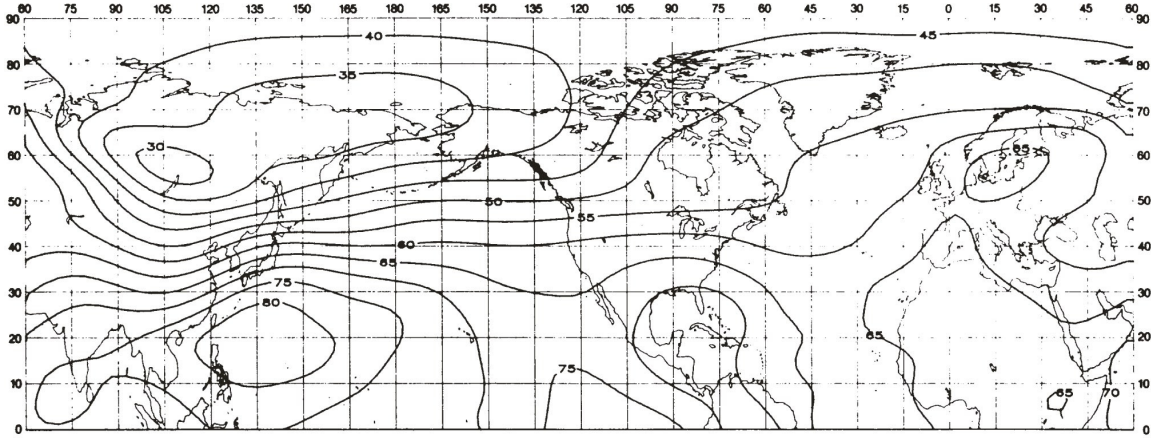


Figure 4.1: ITU atmospheric noise map at 1MHz in winter, 04:00 to 08:00 local time

Figure 4.1 (figure 16a in [ITU-R]), shows that 1MHz levels are around $F_a = 60\text{dB}$ over most of the contiguous US. Say we are interested in an antenna for receiving WWVB at 60kHz. Figure 4.2 (figure 16b in [ITU-R]) shows that for a 60dB level at 1MHz, F_a will be about 115dB at 60kHz. Equation (7) in the ITU document provides a conversion from F_a to electric field strength for electrically small antennas:

$$\bar{E} = F_a + 20 \log_{10}(f_{\text{MHz}}) + 10 \log_{10} B - 95.5 \text{ dB}\mu\text{V/m}$$

Where f is frequency in MHz and B is equivalent noise bandwidth in Hz, and The result is in units of $\text{dB}\mu\text{V/m}$. The mixed units of Hz and MHz in this equation may be a bit confusing for some, so this can also be written with all values in Hz:

$$\bar{E} = F_a + 20 \log_{10}(f) + 10 \log_{10} B - 215.5 \text{ dB}\mu\text{V/m} \quad (4.1)$$

For the example F_a value of 115dB at 60kHz and target bandwidth of 500Hz,

$$\bar{E} = 115 + 20 \log_{10}(60,000) + 10 \log_{10}(500) - 215.5 \approx 22.1 \text{ dB}\mu\text{V/m} \approx 13 \mu\text{V/m}$$

These equations are only valid for narrow bandwidths where the value of F_a is relatively constant. They would not accurately predict voltage levels produced by a broadband loop.

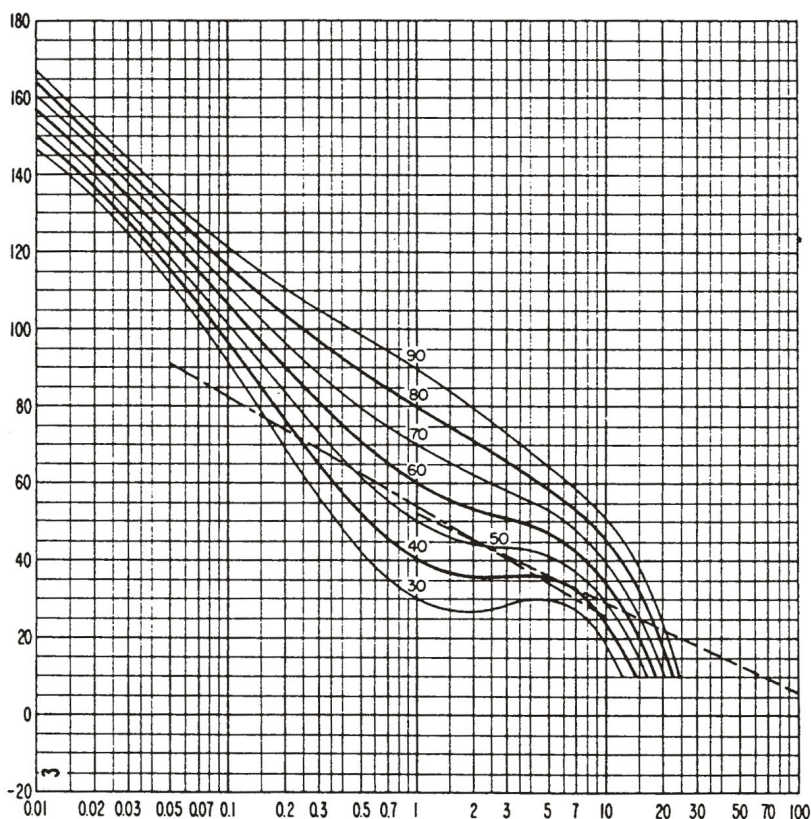


Figure 4.2: ITU atmospheric noise levels in winter, 04:00 to 08:00 local time

Parallel vs Series Resonance

Since atmospheric noise is highly frequency dependent, it is of interest to investigate its interaction with parallel and series resonant loop configurations. Gain plots for external signals shown in figure 3.3 have been added to manually digitized data from ITU figure 30b, with $F_a=70\text{dB}$ at 1MHz. This is a typical level of noise for much of the US Midwest on Summer afternoons from 1200 to 1600 local time. This is shown in figure 4.3 for antennas tuned to 60kHz and 1MHz, with three different values of Q . At 1MHz in particular, the series resonant configuration does a better job of rejecting atmospheric noise below resonance.

Ultimately, total atmospheric noise voltage at the receiver's input is obtained by integrating the power in these curves over linear frequency. Thus it is useful to plot this data linearly as in figures 4.4 and 4.5 for the two example resonant frequencies. For the 60kHz antenna and all but the lowest value of Q , both configurations do a reasonable job of rejection out of band, low frequency sferics (down to 10kHz, anyway).

This is not the case for the 1MHz antenna, where the series configuration may make a noticeable difference. This only considers filtering provided by the resonant

loop. In addition to this, unwanted atmospheric noise may also be reduced by further filtering in the receiver, as long circuitry prior to the filtering does not become overloaded.

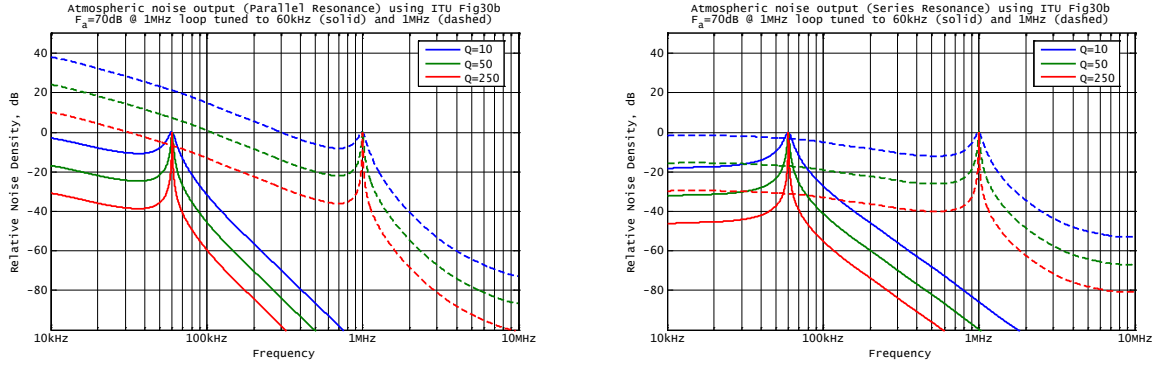


Figure 4.3

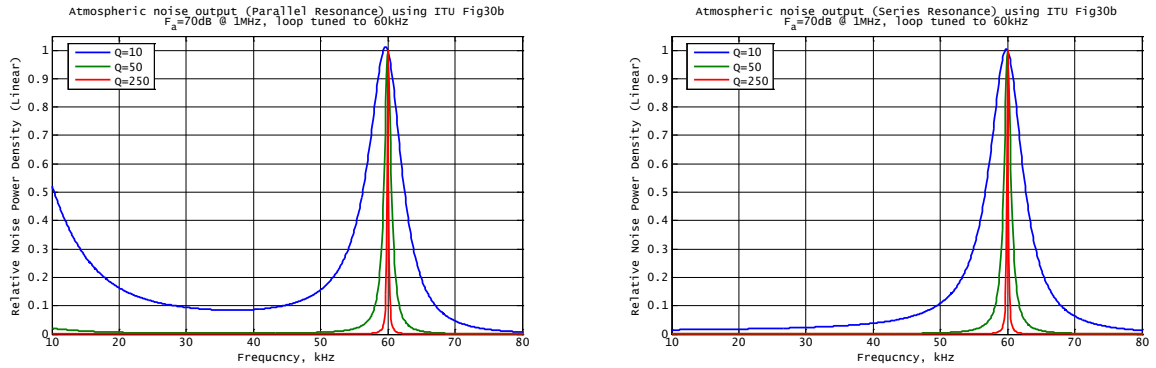


Figure 4.4

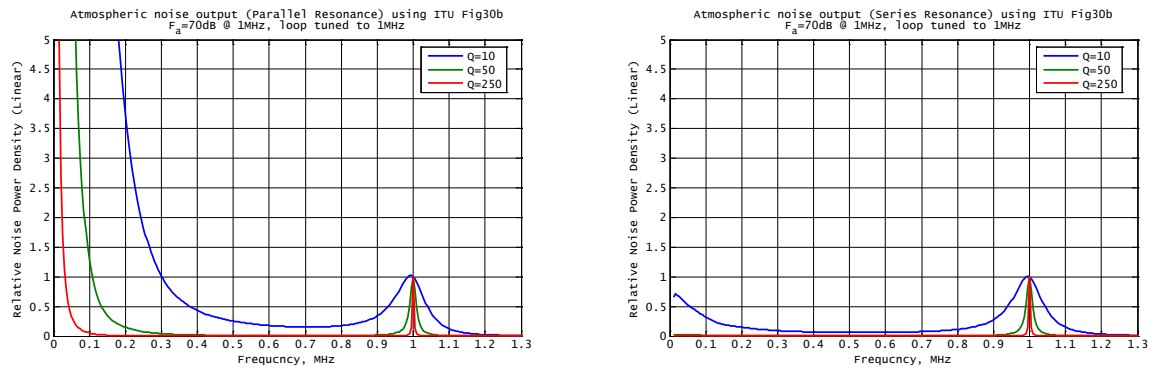


Figure 4.5

Signal to Atmospheric Noise Ratio

The total amount of atmospheric noise within the loop bandwidth is determined by the tuned frequency, resonant Q and the value of F_a . Tuned frequency and F_a are generally given as specifications, so the only loop design parameter available to control the noise level is resonant Q . Thus, it's useful to examine the computation of atmospheric noise E-field levels as a function of loop noise bandwidth (f in Hertz).

Recall that 3dB bandwidth is resonant frequency divided by Q , and noise bandwidth is that multiplied by $\pi/2$, or $\pi f/(2Q)$. We also make use of the fact that $10 \log_{10}(\pi/2) \approx 2.0$. Finally, atmospheric noise density is explicitly shown as a function of frequency, $F_a(f)$, to emphasize that it's the value from one of the ITU charts (e.g. figure 4.2)) at the loop's operating frequency.

$$\begin{aligned} E_{atm} &= F_a(f) + 20 \log_{10} f + 10 \log_{10} \frac{f}{Q} + 10 \log_{10} \frac{\pi}{2} - 215.5 \\ &\approx F_a(f) + 30 \log_{10} f - 10 \log_{10} Q + 2 - 215.5 \text{ dB}\mu\text{V/m} \end{aligned}$$

$$E_{atm} \approx F_a(f) + 30 \log_{10} f - 10 \log_{10} Q - 213.5 \text{ dB}\mu\text{V/m} \quad (4.2)$$

Based on a range of practical resonant Q values, we can easily determine the range of atmospheric noise levels that will be present for the tuned loop. For a loop receiving a narrow band signal (e.g. WWVB at 60kHz), the largest practical Q will be limited to perhaps around 200-300 or so. For a MW loop, Q may be limited by the signal bandwidth if the spectrum of a received AM signal is to be preserved.

This shows that practically speaking, there is limited control over atmospheric noise through varying resonant Q . Doubling the Q only reduces the noise level by 3dB. The equations presented above are mostly useful then for determining how much atmospheric noise will have to be dealt with.

Atmospheric noise can be further reduced by more narrow filtering in the receiver's block diagram (e.g. in the IF or baseband stages), but for that to be practical, noise must be held to some reasonable level at the receiver input to avoid overloading the input stages.

MW Sensitivity

Knowing what to expect from atmospheric noise levels can help in understanding what actual signal levels would be reasonable to design a loop antenna to receive. These guesses can be strengthened through consideration of FCC broadcast rules for MW in the United States.

Radiative external noise sources (e.g. lightning) create a lower limit for sensitivity to radio signals. Even in a quiet rural environment with little man-made noise, atmospheric noise is still present. This suggests a signal level beyond which additional sensitivity may be of minimal use. To get a better idea of what might be reasonable, there are some FCC regulations which can be compared with predicted atmospheric noise levels.

- The outer edge of the *fringe* area for AM broadcasting is defined by an E-field signal strength of $150\mu\text{V}/\text{m}$.
- The emissions limit in the AM broadcast band for intentional radiators and for low power college/university stations is $24,000/f \mu\text{V}/\text{m}$ at a distance of 30 meters, where f is in kHz. This translates to $45\mu\text{V}/\text{m}$ at 530kHz and $14\mu\text{V}/\text{m}$ at 1700kHz.
- FCC rules (CFR 73.37) do not permit a new station from overlapping with an existing station's signal as follows.
 - Where the existing station is $100\mu\text{V}/\text{m}$, a new station may not exceed $5\mu\text{V}/\text{m}$.
 - A new station may not exceed $25\mu\text{V}/\text{m}$ where existing station is $500\mu\text{V}/\text{m}$.

These regulations suggest that a decent AM receiver/antenna system is at least capable of detecting signals at $25\mu\text{V}/\text{m}$ and perhaps even at $5\mu\text{V}/\text{m}$. Given expected atmospheric noise of $1\mu\text{V}/\text{m}$ at 1MHz, one could infer that serious DXing might require a sensitivity somewhere in the range of 1-10 $\mu\text{V}/\text{m}$.

Sferics

It's said that much of the noise encountered at LF/VLF frequencies is caused by atmospheric lightning discharges (*sferics*, for short). This can be seen by comparing ITU maps for Winter in North America, where there is little lightning, to conditions during Summer.

Compare the previous ITU map for Winter at night to figure 4.6 below for afternoon in the Summer. While much of the U.S. is fairly quiet in Winter with F_a values around 60dB throughout much of the midwest, the story changes completely in the Summer. Noise levels in the midwest rise dramatically, to around $F_a = 75\text{dB}$ on afternoons in the Summer. However, there's not much change in conditions for the West coast of the U.S., as there are few lightning storms in this area at any time of year.

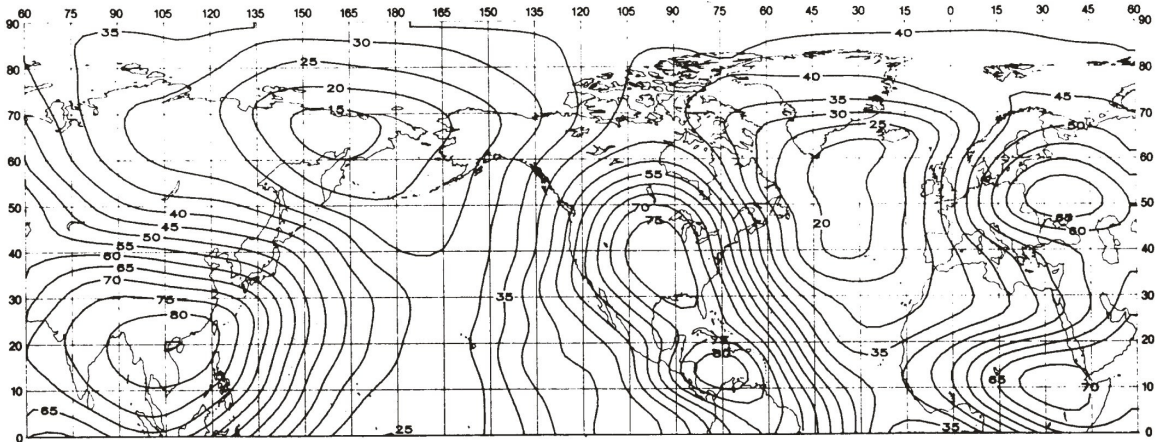


Figure 4.6: ITU noise map at 1MHz in Summer, 12:00 to 16:00 local time

Internal Noise Sources

- Thermal noise due to:
 - Antenna copper resistance
 - Resistance added to reduce resonant Q
 - Ferrite losses
- Receiver input noise

Copper wire resistance can be significant, especially when skin and proximity effects come into play, and must often be considered as part of the noise budget. It is usually undesirable to add resistance to intentionally lower the Q of the loop, but sometimes this is done.

It is generally accepted that receiver input noise at MF and LF can be made negligibly small by comparison with other unavoidable noise sources by proper design.

Any coupling circuits and their resistance as well as transmission lines used must also be considered. Typically, transmission lines are not used between a small loop antenna and the receiver. If an appreciable distance exists between loop and receiver, a pre-amplifier is typically located at the antenna, and a low-impedance amplified signal is sent over a transmission line to the receiver.

Thermal Noise

This is the Johnson-Nyquist noise due to the resistance R discussed above. Ferrite core losses also produce thermal noise and this can all be lumped into thermal noise from a single resistance. The total noise voltage over a given bandwidth is

$$e_n = \sqrt{4kTBR} \quad (4.3)$$

where

e_n is RMS noise voltage in volts,

k is the Boltzmann constant (about 1.38×10^{-23} Joules per Kelvin),

T is absolute temperature in degrees Kelvin,

B is bandwidth in Hertz, and

R is the resistance producing noise in ohms.

At room temperature (300K),

$$\sqrt{4kT} \approx 129\text{pV}/\sqrt{\Omega \text{ Hz}}$$

For example, with a 10-ohm resistor and 1kHz noise equivalent bandwidth we have

$$e_n \approx 129\text{pV}\sqrt{10 \times 1000} = 12.9\text{nV}$$

R is a lumped combination of several different contributions, and we must either assume all physical contributors (i.e. coil wire and ferrite core) are at the same temperature, or handle each one separately. Here, a uniform temperature of 300K is assumed.

Equivalent Noise Bandwidth

In evaluating equation (4.3), the bandwidth term is the system's *equivalent noise bandwidth*. This is usually not the same as the 3dB bandwidth of the system in question. For the single-tuned resonant circuit in figure 2.1, noise bandwidth is approximately given by

$$B_{noise} = \frac{\pi}{2} B_{3dB}$$

See the appendices for a derivation and analysis of the errors in this approximation.

Sensitivity with Excess Noise

One important situation to consider is where the receiver input RF gains are limited by one noise source, such as atmospheric noise. Signal and thermal noise levels will be some amount less than this. In other words, receiver AGC will set the gains such that the desired signal is not at the optimum level for demodulation.

Subsequent stages in the receiver may apply more narrow IF or baseband filtering, reducing the noise level to the point where the signal becomes dominant. Depending

on the design, it may not be possible to get the downstream signal up to the desired level without overloading the RF gain stages. It's useful to be aware of this issue, but it is really about the topic of receiver architecture which is beyond our scope.

Chapter 5

Air Core Loops

Figure 5.1 shows an air core loop being excited by a TEM plane wave. The magnetic field vector is aligned with the axis of the loop. In this case the dot product between loop axis and H-field may be replaced with a multiplication of field magnitudes. This is assumed in all that follows.

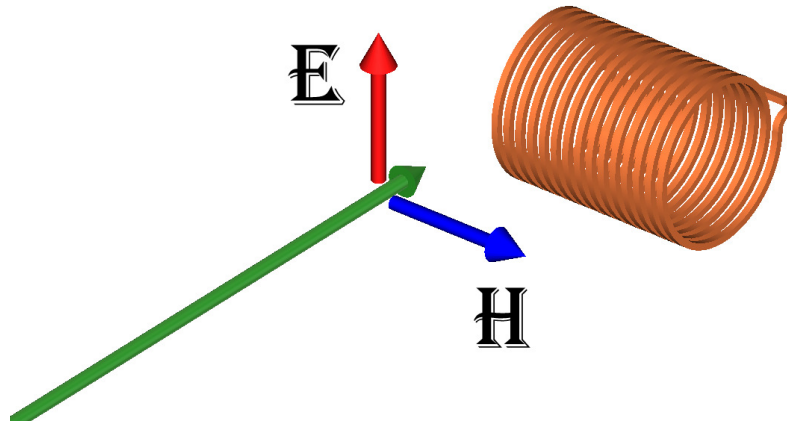


Figure 5.1: Air core loop excited by TEM plane wave

The open circuit voltage developed in a single turn, electrically small loop is given by (5-39) in [Balanis], and may be modified for an n -turn loop by multiplying by the number of turns:

$$V_{oc} = \omega A n \mu_o H$$

where A is the area inside the loop and H is magnetic field intensity. This expression is valid for electrically small loops – where the length of wire in the loop is not a significant fraction a wavelength.

This equation is often written with the term $\mu_o H$ replaced with the B-field value (in free space the two are equivalent). This formula assumes we know the H-field strength, but by convention, it's more common to work with E-field values. This

does not present a problem, because the signal is propagating in free space, and the ratio of E-to-H field magnitudes is given by

$$\frac{E}{H} = \sqrt{\frac{\mu_o}{\epsilon_o}} \approx 377 ,$$

and the induced voltage can be expressed in terms of applied E-field magnitude using the definition of β in (2.1).

$$V_{oc} = E \mu_o \omega A n \sqrt{\frac{\epsilon_o}{\mu_o}} = E (\omega \sqrt{\mu_o \epsilon_o}) A n = E \beta A n$$

The combined term multiplying E here is in units of meters and is known as the effective height of the antenna. For the air core loop then,

$$h_e = \beta A n \quad (5.1)$$

Inductance

Inductance may be calculated with a decent level of accuracy using one of Wheeler's formulas. This first one (published in 1928) is good for coils whose winding length is at least 80% of the radius.

$$L \approx \frac{10\pi\mu_o n^2 r^2}{9r + 10l} \quad (5.2)$$

where n is the turn count, r the radius and l the length of the winding. The radius and length are in inches for this formula. This is *not* a typical geometry for an air-core loop, and this can be in error by 25% or more for typical loop geometries. A better formula (published in 1982) and further optimized by Knight in 2016 is claimed accurate to ± 265 ppm for any geometry.

$$L = \mu_o r n^2 \left[\ln \left(1 + \frac{\pi}{2(l/d)} \right) + \frac{1}{2.3004 + 3.2219(l/d) + 1.7793(l/d)^2} \right] \quad (5.3)$$

where d is the diameter ($d = 2r$), and (l/d) is the coil's aspect ratio – length divided by diameter.

Algorithms instead of formulas

We prefer to use a computer-implemented algorithm for the computation of inductance and have had very good results with it. Typically, measured inductances come out with much less than 1% error when measured on a Hewlett-Packard LCR meter

with allowance for lead inductance. [Weaver] provides several algorithms for this purpose, and we have been using his `Lcoil()` function (see [Weaver-1]) with excellent results on typical air-core loop geometries.

Resistance

Given resistivity of wire used in the loop (including skin and proximity effects) of ρ ohms per meter, a coil of radius r and n turns has a total wire resistance of

$$R = 2\pi r n \rho$$

As defined here, ρ is a function of the wire diameter, material (copper), frequency, winding pitch and number of turns.

The resistivity includes skin effect, which can be accurately computed from the exact formula using modern computer applications such as Matlab and Octave. Proximity effect will further increase resistivity and is more difficult to estimate.

Skin Effect

The exact formula for the increase in resistance due to skin effect contains Kelvin functions, which are Bessel functions evaluated with specific arguments. These are difficult to evaluate using a hand operated calculator, and much effort has been expended to derive approximations that are more easily evaluated. See for example [Knight-1], and his equation (3.1) for the exact expression for resistance including skin effect.

Current computer applications such as Matlab and Octave can accurately evaluate the Kelvin functions, so it is easier to implement the exact solution rather than one of the approximations. Matlab/Octave scripts attached to this PDF document include functions to evaluate skin effect.

Proximity Effect

This section applies to solid and stranded copper wire. Although Litz wire is capable of achieving much higher Q, the amount of wire used in air core loops may make that option cost prohibitive.

Accurate proximity effect calculations for solid and stranded copper wire are difficult in some cases. The method suggested here uses data published by R. G. Medhurst in 1947 ([Medhurst-1], [Medhurst-2]). This data was developed for situations where the wire diameter is at least ten times the skin depth, and for coils having at least 30 turns.

Attempts to correct these estimates for greater skin depths, and smaller turn counts have been suggested [Knight-2] and do seem to produce more accurate estimates in many cases. However, the accuracy of these corrections over the full range

of loop geometries is unknown, and we've seen cases where these estimates have been in error by as much as 20-30%.

When wire diameter is small in terms of skin depth, both skin and proximity effects become negligible. Straight wire with a diameter of 2-½ skin depths has a resistance increase only 5% higher than at DC, and two skin depths is a 2% increase. These could be taken as two possible boundary conditions for the absence of skin and proximity effects. However, experiments seem to indicate that proximity effects for close-wound coils begin to appear with wire diameters as small as one to 1-½ skin depths¹.

For the purpose of estimating proximity effects, three regions may be defined:

- Wire diameter is at least ten times the skin depth, with 30 or more turns. Medhurst's data is valid.
- Wire diameter is less than 1 (or 1-½) skin depths. Skin and proximity effects may be ignored.
- Wire diameter is between 1 (or 1-½) and 10 skin depths, and/or turn count is less than 30. Proximity effects can be significant, and Medhurst's data is not valid in this region. The accuracy of Medhurst's estimates will be unknown.

Figure 5.2 shows the wire size limitations as a function of frequency. The green boundary line for the *No Effect* region is based on one skin depth, and the blue boundary line is for 1-½ skin depths. For convenience, wire diameter is shown as AWG wire size. The range of wire sizes where proximity effect estimates can be less accurate is labeled as an area of patchy fog and poor visibility. Except in the *No Effect* region, turn count is assumed to be 30 or more in this depiction.

The range of problematic wire sizes for LF and MF loop designs encompasses many of the wire sizes typically used to build such loops. For example, at 60kHz, wires sizes from 10 AWG through 26 or 30 AWG are inside this foggy zone.

Finally, don't get the idea that these wire sizes should be avoided; we're not saying that. It's just that predictions of AC resistance may be less accurate, and trial and error may be required to achieve the desired performance.

Dowell's Estimate

According to [Nan], a widely known method by [Dowell] gives answers with about 5% error at lower frequencies, but at higher frequencies can underestimate the effect by as much as 60%. However, these analyses apply to multi-layer windings, so it is not clear how much error there may be in using Dowell for single layer coils.

Earlier versions of this document included formulas for this estimate, but that's been removed as this method does not seem to be accurate for typical air core loops.

¹Earlier versions of this report stated this limit to be 2 to 2-½ skin depths. Recent experiments suggest this was incorrect.

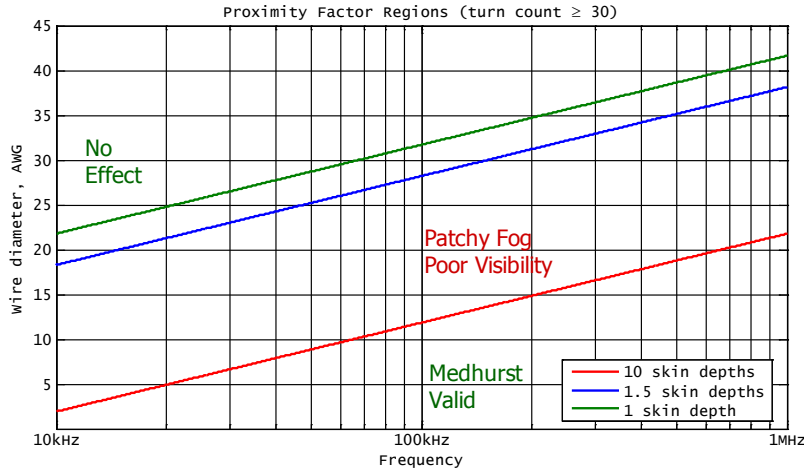
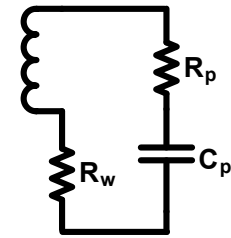


Figure 5.2: Regions of validity for proximity effect estimates

Dielectric Losses

To a first order, dielectric losses may be modeled as a resistance in series with the parallel capacitance associated with self resonance.² This causes a reduction in Q at the SRF. This model (shown to the right) suggests that dielectric losses have little effect on overall loop Q at frequencies well below self-resonance. A quick estimate is that the maximum frequency at which Q is not significantly degraded by dielectric loss is



$$f_{max} \approx f_{SRF} \sqrt{R_{SRF}/R_p}$$

where R_{srf} is the loop's AC resistance at the self-resonance frequency, f_{SRF} . Since both R_w and R_p vary with frequency, this is only an approximate value. If the operating frequency is close to the SRF, it's best to run some mathematical calculations or SPICE models to get a more accurate answer.

In summary, as long as SRF is large enough compared to the loop operating frequency, forms made of high-loss dielectric materials (e.g. PVC) can often be used without a significant impact on overall Q . Several experiments with loops wound on high-loss PVC forms seem to bear this out.

This is perhaps stating the obvious, but measurement of loop Q at SRF is necessary to determine the equivalent circuit values, and the frequency limit.

²A more accurate model might have another resistor connected across the top and bottom nodes, but this is usually a very large value and has been omitted for the purposes here.

Reality Checks

Three loops have been built for which in-situ measurements of resonant Q were made. Predicted Q values using Medhurst compare favorably with the measurements. Being measured in operation, there aren't any issues about LCR meter accuracy.

Resonant Q was determined by exciting the loop with a magnetic field over a range of frequencies and fitting the measured response to an ideal RLC circuit. These are all 60kHz designs and used polypropylene dielectric resonating capacitors. Figure 5.3 describes the three sample loops.

Form	Diameter	Pitch	Wire AWG	Insulation	Turns
6-inch PVC Pipe	170mm	1.27mm	22	PVC	83
40-inch Spokes	1016mm	3.18mm	20	PVC	24
33-inch Spokes	838mm	2.76mm	16	enameled	30

Figure 5.3: Three Sample Loops

In figure 5.4, the measured Q of each sample loop is shown along with the estimates of Q made using Medhurst data with corrections for turn count and frequency. Predicted Q values include loading of the loop as configured for measurement.

Loop	Wire Dia	Q	
	Skin Depths	Measured	Estimated
6-inch	2.4	151	140
40-inch	3.0	140	152
33-inch	4.8	238	263

Figure 5.4: Measured and predicted Q of sample loops

Optimum Winding Pitch

Performance of resonant loops depends strongly on the quality factor, Q . Within certain limits, it is may be desirable to have the highest possible value for Q . Sometimes, minimum limits on loop bandwidth will make high Q designs undesirable, such as with AM broadcast reception. Other times, such as with 60 or 75kHz designs for WWVB or DCF reception, maximizing Q may be desirable.

By incorporating most of the relevant factors, such as resonating capacitor losses and receiver input impedance, it's possible to examine the variation of Q with winding pitch, and it's generally found that there is an optimum value.

Figure 5.5 is an example of scanning a design for the optimum pitch. This can be accomplished using the `AnalyzeAirCoreLoops` Matlab/Octave script. It incorporates variable coil AC resistance due to skin and proximity effects, as well as variable capacitor ESR as a function of frequency according to dissipation factor (DF).

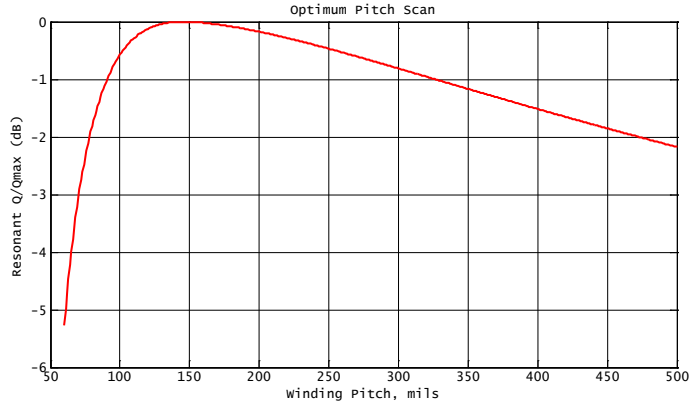


Figure 5.5: Loop Q versus Winding Pitch

High-Q Designs

High Q loops must be operated in the clear – away from objects such as walls, floors, furniture and metals. The higher the designed Q, the more spacing is required. This should be thought of in terms of loop diameters. Larger loops require more spacing. Distances of 1-3 loop diameters may be required to attain the highest Q.

Antenna Thermal Noise

Thermal noise from an air core loop is dominated by effective wire resistance. Radiation resistance for electrically small loops is so small as to be irrelevant.

$$e_n = \sqrt{4kTBR} = \sqrt{8\pi kTBrn\rho}$$

Above, the wire's resistivity multiplied by its length has been substituted for the total wire resistance. Note that ρ is not the resistivity of copper, but the resistance of the wire being used, in ohms per meter.

We are interested in how this noise level will compare to the voltage induced in the loop by an external electric field. The external E-field might represent a radio signal or atmospheric noise levels. If the effective height of the antenna is known, this noise level may be referred back to an E-field strength by dividing by the loop's effective height.

$$E_n = \frac{\sqrt{8\pi kTBrn\rho}}{h_e}$$

Self Resonance

One upper limit on the amount of wire used in a loop antenna is determined by self resonance. In general, the loop SRF should be significantly higher than any tuned receive frequency to allow for accurate and stable tuning.

Estimating SRF is a complex topic and the subject of another report. As a rule of thumb, if total wire length is limited to no more than 10-20% of the wavelength at the highest frequency of operation problems won't arise from an SRF that is too low. If the boundaries are to be pushed to achieve larger effective heights, then one must delve more deeply into this topic and that's beyond the scope of this report.

Shape

All the loops examined so far have been circular, but they don't have to take that shape. A circular loop maximizes the area for a given circumference which is often the reason for using that shape.

A square loop may be easier to build in some cases. The area of a circular loop made with 2π meters of wire is π square meters. A square loop made with the same length of wire has an area of $(\pi/2)^2$ square meters, so the ratio of areas is:

$$\frac{\pi^2/4}{\pi} = \frac{\pi}{4} \approx 78\%$$

The reduction in area (and effective height) is about 2.1dB.

Both circular and square loops take up a lot of planar space, and a lot of volume if they are to be rotated in use. One solution to this problem is to change the shape to a rectangle with a high aspect ratio (e.g. 3:1 or 4:1). A rectangle with aspect ratio r has sides of length 1 and r , thus the area is r with circumference $2(r+1)$. A rectangle with aspect ratio r and circumference 2π meters will have sides of length $\pi/(r+1)$ and $\pi r/(r+1)$. Its area is then $\pi^2 r/(r+1)^2$, and relative to a circle with the same circumference it is;

$$\pi \frac{r}{(r+1)^2}$$

For example, a rectangle with aspect ratio of 4:1 would have $4\pi/25 \approx 50\%$ of the area of a circle with the same circumference. This represents about a 6dB reduction in area and effective height. This effect is graphed in figure 5.6.

In exchange for the loss of effective height, a high-aspect ratio loop will require considerably less space when it is rotated. A four foot circular loop essentially requires a cube of space four feet on a side (64 cubic feet) in which to operate. However, a rectangular loop with the same circumference, 15 inches by 5 feet mounted with the long edge vertical requires considerably less room for operation, but suffers a 6dB

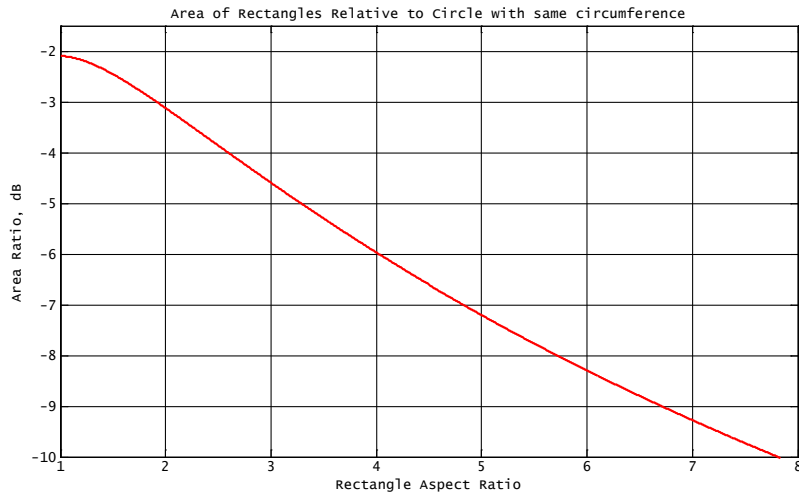


Figure 5.6: Loss of Area in Rectangular Loops

reduction in effective height. This loop could be operated in a 15x15x60 inch cube of space (about 8 cubic feet) – one eighth of the volume required by the circular loop.

As long as the loop’s thickness (winding pitch times turn count) or pitch is not too large, the radiation pattern won’t be any different than that of a circular loop. This might not be the case for thick loops, but most situations where a high aspect rectangle is desirable will involve small turn counts and the resulting loop will not be all that thick.

Analysis Tools

A set of Matlab/Octave scripts are included in the zip file attached to this PDF document containing tools to analyze air core loop performance. The analysis includes the ability to calculate inductance, and resistive loop losses. With input of information about capacitor losses and load impedance, accurate estimates of resonant Q and effective height are possible. This permits scans of design parameters such as diameter, turn count and winding pitch as an aid to finding the best loop design for a particular application.

Construction Notes

One loop was built for 60kHz which demonstrates an unexpected behavior having to do with wire pitch. The usual winding technique places each turn of wire a constant distance from the previous turn, and each turn is wound on an identical diameter.

An octagon loop was built with 33-inch equivalent diameter with 16 AWG wire on a pitch of two wire diameters. There were eight spokes used as wire supports to

form the octagon. A wire support with evenly spaced notches was attached to the end of each spoke. Wire was unsupported in between the supports.

The initial build had very uneven wire spacing between supports as the relatively stiff magnet wire inevitably had small deviations from being straight. In places adjacent turns were touching and in others the spacing was much more than the average. This led to concerns that the AC resistance might be unduly raised by the uneven spacing.

In an attempt to prevent wire spacing less than the average, two wire loom spacers were inserted in between each of the eight main supports (16 total looms). This was done in such a way that even turns were forced inwards on one side of the loom, and odd turns outward on the other side. Radial spacing between adjacent turns was four wire diameters. Even and odd turns were spaced radially an average of four wire diameters apart. This ensured that adjacent turns were never closer than one wire diameter. Photos of the loop are shown in figure 5.7.

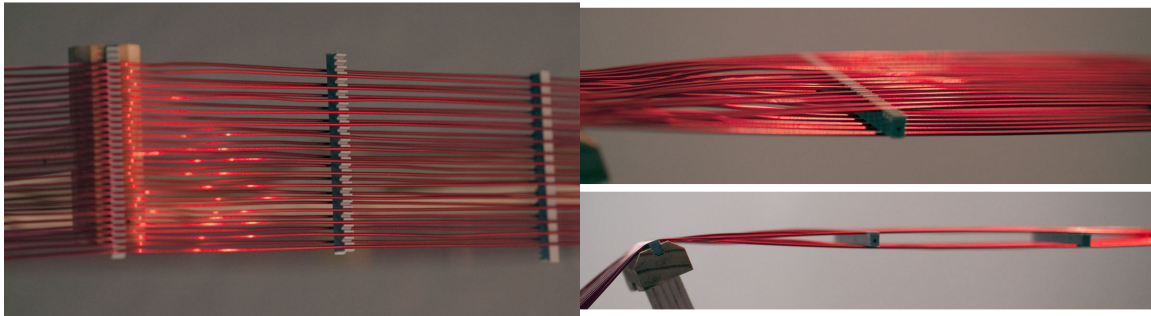


Figure 5.7: Wire spacing technique used in octagon loop antenna

This configuration has the same average axial pitch as before, but now there is a significant radial spacing between adjacent turns. The surprise was that this did not alter the inductance much at all, reducing it from $1570\mu\text{H}$ to $1520\mu\text{H}$. Furthermore, the AC resistance did not change much either and that was perhaps the bigger surprise.

Analysis

We discovered that methods suggested in [Weaver] provide accurate estimates of inductance when alternate coil turns have different radii. The method used in Weaver's `Lcoil` function is to sum the mutual inductance between every pair of turns in the coil, using Maxwell's formula for the inductance between two circular loops. This algorithm allows for each loop turn to have a different radius.

The `Lcoil` function can be modified for the case where each turn has a distinct radius. In fact, it can be modified for each turn having a different wire size, as well as for each turn having a non-uniform spacing from previous turns. It can therefore

be used to investigate the effect that random axial spacing of turns would have on inductance (each turn having the same radius).

A Monte-Carlo analysis was done for a 30-turn loop with random turn spacing, using 16 AWG wire, average pitch of 100 mils and minimum pitch of 1.1 times the wire diameter. Turn spacing was uniformly distributed and scaled to meet the minimum and average pitch values. A sample of five such random spacing sets is depicted to the right.

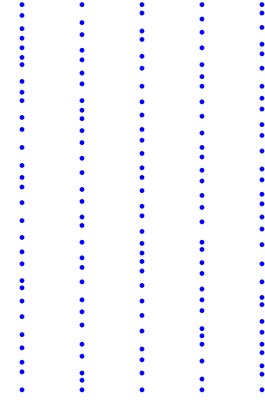


Figure 5.8 shows the cumulative distribution function for inductance computed from this simulation, using 10,000 sets of random spacings. The result is, not surprisingly, a good fit to a normal (Gaussian) distribution, with standard deviation being 0.5% of the average.

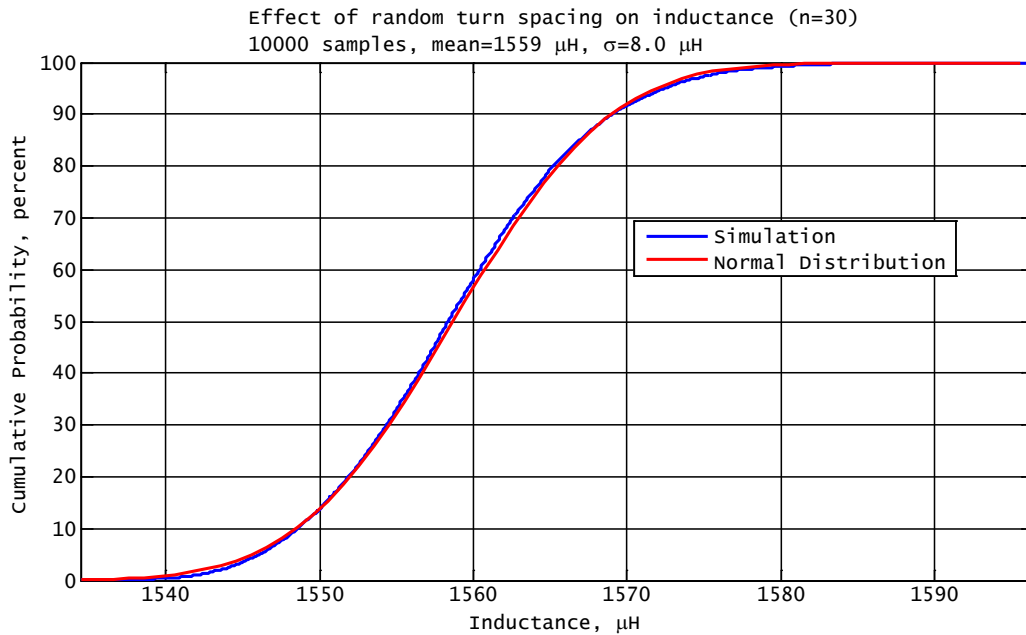


Figure 5.8: CDF of inductance with random turn spacing

The following conclusions regarding coil winding techniques are suggested:

- Average axial wire spacing is the most important parameter. Offsetting every other turn radially by 5 wire diameters had little effect on inductance and AC resistance.
- Uneven wire pitch has seems to have little effect on inductance and AC resistance.

Chapter 6

Permeability

To get an intuitive understanding of ferrite core loops, a review of permeability is in order.

What is Permeability?

We'll start with the the fields H and B and their relationship to each other. These fields are really vector fields (or tensors, but that's way beyond the scope here), but for simplicity they will be carefully treated as scalars.

B symbolizes the total magnetic field magnitude at any point in space. H is also a field and represents only that portion of B caused by free currents (e.g. those flowing in a coil)¹. The total field at any point is the sum of that caused by free currents and magnetization of the materials in the field. In free space, there is no magnetization, so the relationship is trivial

$$B = \mu_o H$$

In CGS units, it is even simpler, ($B = H$) but this article will stick with MKS units. In general however, there will be magnetized materials such as ferrites present and then

$$B = \mu_o(H + M), \text{ or } H = \frac{B}{\mu_o} - M$$

where M is magnetization (e.g. associated with ferrite domains). We are only concerned with currents and fields which have a sinusoidal variation in time – not static ones. In other words, there's no such thing as a 1MHz permanent magnet. So, any magnetization must be induced by free currents somewhere. Note that M can be quite a bit larger than the H that induced it.

¹ H does not include portions of B caused by bound currents such as magnetic moments associated with magnetized domains in ferrite

It's worth restating that the H field doesn't really exist. It cannot be measured directly² – only the B field is directly measurable. H is none the less a useful concept because it permits total induced fields to be easily calculated.

In materials where magnetization is approximately proportional to H , such as soft ferrites operated below saturation levels, the constant of proportionality is called magnetic susceptibility and usually denoted as χ . Thus we have $(H + M) = (H + \chi H)$ which yields

$$B = \mu_o(H + \chi H) = (1 + \chi)\mu_o H \equiv \mu_r \mu_o H$$

This bit about B and H is intended mostly as background material, and we won't concern ourselves with susceptibility χ or magnetization M going forward. The important points to keep in mind are

- Free currents induce the H field which is unaffected by the permeability of the medium in which it exists.
- B is the sum of H and any magnetization produced by H . The amount of field enhancement due to magnetization determines the relative permeability.

This knowledge will help a lot in understanding how the ferrite rod works, both as an antenna and an inductor.

Intrinsic Permeability

Passing current through a coil of wire wrapped around a ferrite toroid creates an H -field. The toroid forms a closed magnetic circuit, and nearly all of the field from the coil remains inside the ferrite. Under these conditions, the ratio between B and H fields in the ferrite is known as the intrinsic permeability, μ_i . This is an inherent characteristic of the material and has little to do with the size or exact shape of the toroid.

A toroidal inductor makes a poor antenna because the magnetic circuit is closed and flux can't get in or out very easily. For antennas, open magnetic circuits are required, and different measures of permeability have been defined to deal with them.

Variations on the Theme

There are two very different H field configurations in which the behavior of the ferrite rod is of interest.

1. The rod is placed into a uniform H field – specifically one that is part of a propagating radio signal (TEM wave).

²except in free space where there's no magnetization

2. The rod forms the core of a coil in which a current has been established (free current).

These scenarios are quite different. We feel that many treatments of ferrite rod antennas do not give adequate attention to the differences, and explanations of why they are important. These two scenarios are discussed in detail below.

Permeability in a Uniform Applied Field

Consider a propagating radio signal oriented as shown in figure 6.1. The rod is perpendicular to the direction of propagation and the H-field is parallel to the long axis of the rod.

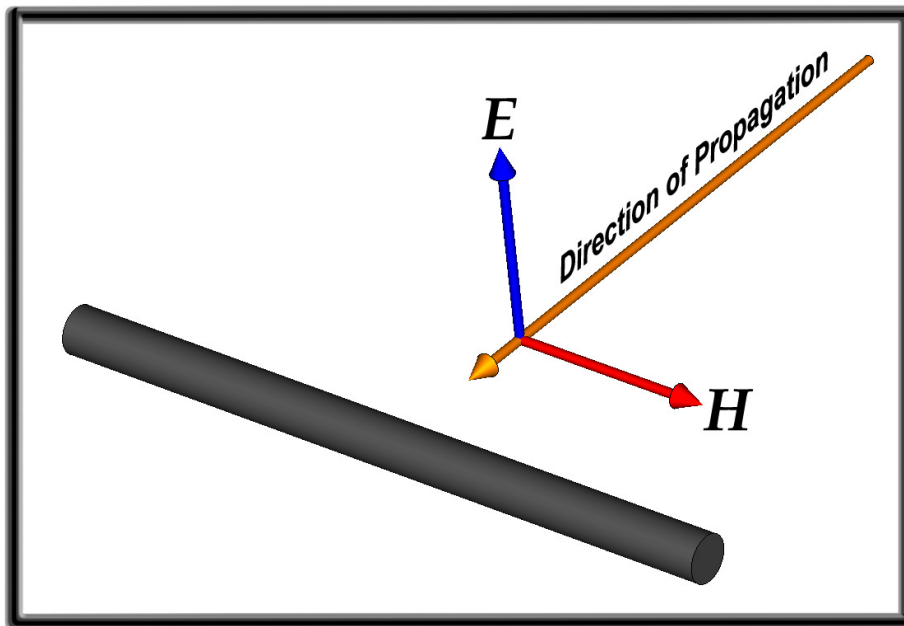


Figure 6.1: Ferrite Rod Orientation

The plane wave and associated H field was generated by free currents in a transmitting antenna (miles distant, presumably). This means that the electric and magnetic fields are quite uniform. We assume either that there is no coil of wire on the rod yet, or that any coil is open-circuited and nowhere near self-resonance. The TEM wave's H field will induce magnetization in the rod and that in turn will add to the B field in and around the ferrite rod.

This is a crucial point: the ferrite core does not distort the H field – by definition. The only free currents in this picture are those back at the transmitting antenna. As a result, H is still uniform everywhere around the rod, including inside and in the vicinity of it. It is only the B field that is modified by the rod's presence.

The amount of magnetization (and therefore the B field) is not uniform throughout the rod (see figure 6.2). It is strongest in the center. If a coil of wire is wrapped around the rod, the total B field inside the coil will induce a voltage in the coil – not just the H field. And because the B field has been enhanced by magnetization of the ferrite there's a larger induced voltage than there would be without the rod.

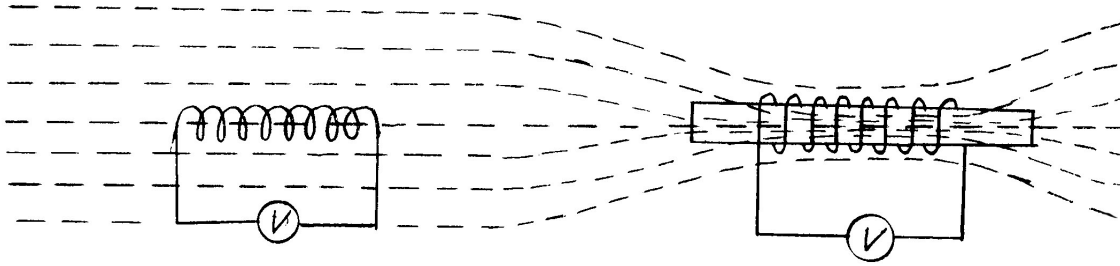


Figure 6.2: Illustration of μ_{ext}

Figure 6.2 shows a rough idea of the difference in B-field with and without the ferrite core. The air-core loop on the left has no effect on the B field, but the ferrite core produces a larger B field in its vicinity. This drawing from [CIA] in 1957 is in fact pretty accurate; figure 6.3 shows a typical B-field computed by modern E-M simulation software (the scaling on the plot is highly logarithmic for clarity, and the field falls off much faster away from the rod that the image tends to imply).

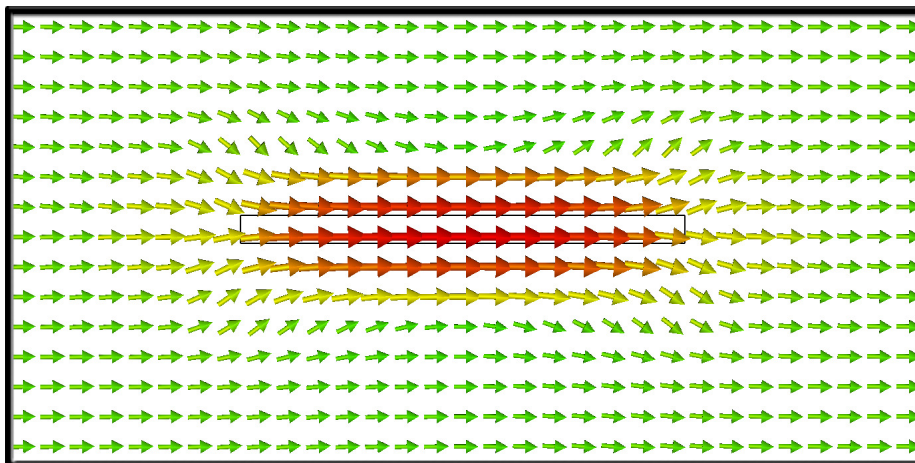


Figure 6.3: Simulated B-field around ferrite rod ($\mu_i = 300$) in uniform H-field

The B field is not uniform throughout the interior of the rod, even though the H -field is. In other words, the apparent relative permeability is not constant inside the rod; it is a function of position. No one number can describe this situation. As a result, two different measures of relative permeability have been defined in an attempt to quantify these variations. Even two numbers cannot completely describe this, but it's better than only one.

Apparent Permeability

After intrinsic permeability, the next variant of permeability we run into has to do with the current situation – a ferrite core immersed in a uniform magnetic field. Apparent permeability is known by at least two different names, μ_a and μ_{rod} . It is the ratio of the axial B field at the center of the rod to the externally applied H field.

This value is most directly applicable to a very short receiving coil located at the center of the rod. It varies as a function of the ferrite's permeability in a closed magnetic circuit (μ_i) and the rod's length-to-diameter ratio. Being based on a very short receiving coil, this is not always directly useful, but it serves as a starting point for determining additional measures of permeability. So far, this only considers the B and H -fields, there's no talk of coils or voltages here.

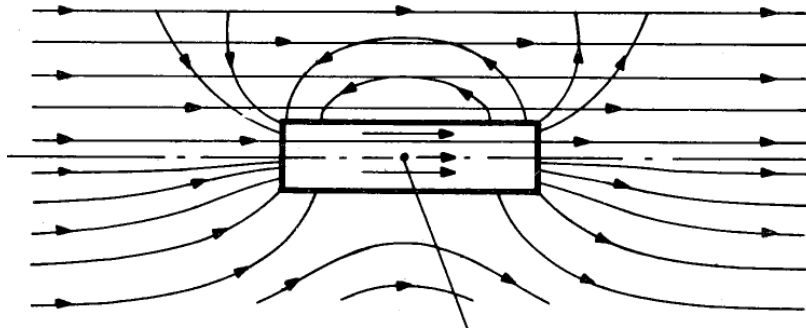


Figure 6.4: Separating the field components

To help visualize what's happening, figure 4.7(d) from [Snelling] is reproduced in figure 6.4. The upper half of the drawing shows three separate sets of magnetic field lines, the uniform plane wave, the enhanced field inside the core, and the field external to the core created by the enhanced field – these are the flux return lines that complete the magnetic circuit. The bottom half shows the resultant field which is the vector sum of the three separate fields.

The net effect is a reduction in the field outside the core along its axis. The shorter the core, the more concentrated these return lines become and the field at the core's midpoint, just outside the core can become severely attenuated with very short, high permeability cores. In the next section, we discuss how this attenuation can be estimated.

A Funny Thing Happens

For the sake of curiosity, we look here at how the B-field varies in the close vicinity of a ferrite rod.

There will be much more later about how μ_{rod} depends on the length-to-diameter ratio of a ferrite rod. For now let's just note that for long skinny rods, μ_{rod} is fairly large and can be 50% or more of the intrinsic permeability, μ_i . For short, squat rods μ_{rod} can be surprisingly small.

Consider a rod with $\mu_i = 350$ and $\mu_{rod} = 120$ immersed in the magnetic field of a plane wave (at say, 1 A/m). At the center of the rod in the ferrite, the B-field will be 120 times stronger than the H-field (i.e. 120A/m – because that's what μ_{rod} means.)

This is where things get a bit odd. Far away from the ferrite, the B-field is 1A/m because the relative permeability of free space is one³. However, the B-field near the center of the rod, in the air just outside the ferrite is only about 0.34A/m. This is caused by the flux return lines shown in figure 6.4 reducing the ambient B-field.

Here's the surprising (or maybe not so surprising) observation about this reduction in B-field. If you take the B-field at the middle of the rod, just at the outer edge of the ferrite and divide it by the *intrinsic* permeability ($\mu_i = 350$), you get the exact value of the B-field just outside the ferrite. So the 120A/m inside divided by 350 gives us the 0.34A/m that actually exists.

Example B-Fields

To provide an example, the previously discussed rod with $\mu_i = 350$ and $l/d = 20$ which has $\mu_{rod} = 120$ was simulated. A couple of plots show how the B-field varies through the rod and outside it in figure 6.6. Both of these plots only depict the axial component of the B-field because that's what is linked by an antenna coil and will produce an output voltage. Colored arrows in figure 6.5 shows the lines along which the B-fields are sampled in the two plots.

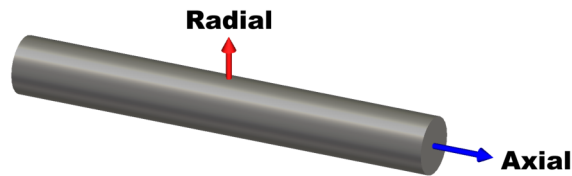


Figure 6.5: B-field directions sampled in figure 6.6

The plot on the left shows field magnitudes along the red radial line in figure 6.5. Distance is normalized so the rod's radius is one, and the applied H-field magnitude (TEM wave) has magnitude of 1.0 A/m in free space. Inside the rod, B-field is running at 120A/m as expected, but just outside the rod (where B and H fields are the same), the field is reduced substantially to a value of about 0.35A/m.

³See comments on units below

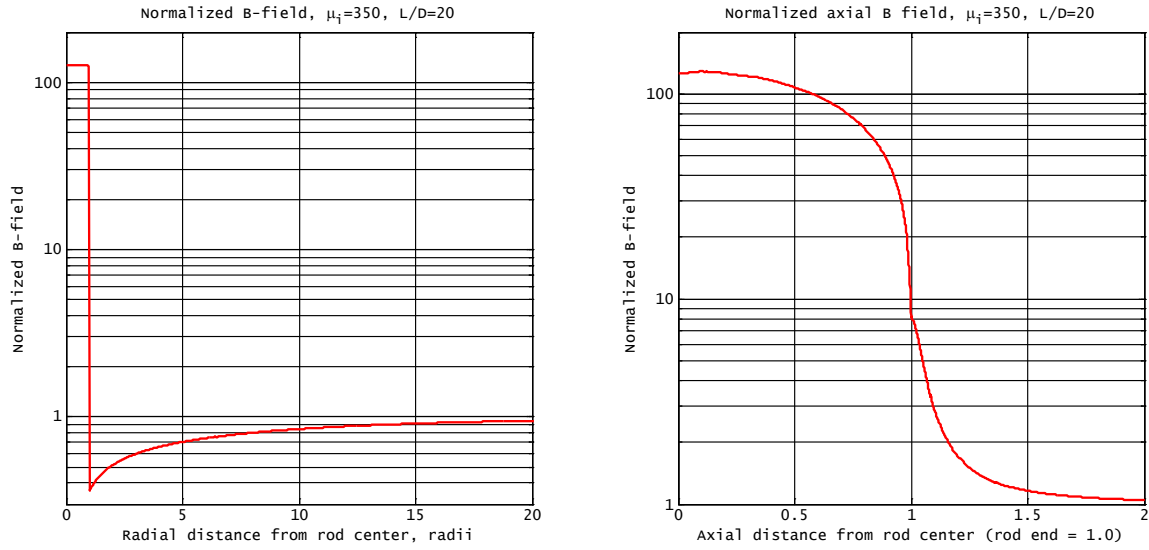


Figure 6.6: B-fields in and around a ferrite rod

The right-side plot shows the field along the axis of the rod, with the rod length scaled so the end of the rod is one. Again, the field is maximum at rod center (120A/m), and drops quickly to the ambient value of 1.0A/m past the end of the rod.

Units

We need to be a bit careful with units when discussing B and H fields as they are related by $B = \mu_o \mu_i H$, where μ_o is the permeability of free space and μ_i is the intrinsic (relative) permeability of the medium. In CGS units, $\mu_o = 1$ so we can numerically compare B and H fields in free space or air without worrying too much (except we shouldn't forget which one we're talking about – B or H). In MKS units however, $\mu_o = 4\pi \times 10^{-7} \text{H/m}$ and B and H fields are numerically quite different, even in free space.

So above, in discussing B and H field values there's an assumption that the μ_o conversion constant is silently allowed for, and we may speak of B fields in units of A/m even though that's not a valid unit for B.

Interactions Between Rods

As illustrated in figures 6.4 and 6.6, a ferrite rod in a uniform H-field, such as that which is part of an E-M plane wave, will alter the B-field in it's vicinity. In figure 6.7, transparent cylinders have been placed around two ferrite rods, hinting at the size of the affected volume. In reality, there is no sharp edge to the affected volume, but that's shown here to illustrate the point.

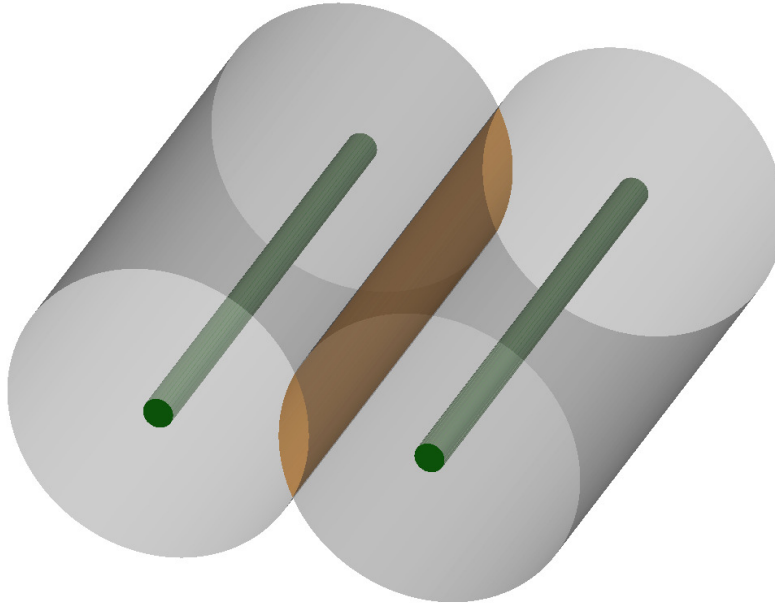


Figure 6.7: Ferrite rods affect H-fields in their vicinity

Inside the affected volume and outside the rod, the resultant magnetic field is reduced, and any additional antennas placed with this volume will have less overall B-field to work with.

Since μ_{rod} is an indication of how much flux intensity is increased by the rod's presence, it could be thought of as gathering the flux from an area larger than the rod's cross section, and concentrating that flux within the rod. Under this analogy, the radius from which flux is collected would be $\sqrt{\mu_{rod}}$ times the rod's radius. This isn't exactly correct but it helps to provide an intuitive grasp on the effect.

In figure 6.7, the two rods are spaced such that their affected volumes overlap (shaded as brown in the image), with the result that antenna coils wound on either rod will pickup less signal voltage in the presence of the other rod.

Simulations were run with three parallel rods, and figure 6.8 presents the results for two values of spacing. The spacings are relative to rod radius, so for a half-inch diameter rod with $\mu_{rod} = 122$, a spacing of $(2r\sqrt{\mu_{rod}})$ would be $0.25 \times \sqrt{122} \approx 5.5$ inches.

μ_i	l/d	μ_{rod}	dB loss at rod spacing	
			$\sqrt{\mu_{rod}}$	$2\sqrt{\mu_{rod}}$
350	20	122	1.6	0.6
125	15	62	1.8	0.7
2000	15	103	2.3	0.7

Figure 6.8: Flux loss in middle rod of three parallel rods

External Permeability

Of primary interest for antenna designs, another definition of relative permeability relates the voltage induced in a coil (not necessarily a short one) wound around the rod by a uniform external H field. This will be symbolized here as μ_{ext} .

This permeability is determined by the total amount of B field flux linked by the coil along its length, and it depends on the length of the coil and where the coil is located on the rod. Referring back to right side of figure 6.6, its easy to see that placing a coil at the end of the rod will link less flux than in the middle.

μ_{ext} is defined as the ratio of voltage induced in the coil with and without the ferrite rod. This is often expressed as the product of apparent permeability and a factor which is partially dependent on the coil geometry.

$$\mu_{ext} = \mu_{rod} F_{ext} = \mu_a F_{ext} \quad (6.1)$$

Too Many Names

Published literature on ferrite rods provides a plethora of names for various measures of permeability. In some places, μ_{rod} will be referred to as the *fluxmetric* permeability, and it's measured at the center of the rod.

Permeabilities are also measured which involve an average of flux levels over the entire volume of a ferrite rod. These are variously called *magnetometric* or *ballistic*. Subscripts such as $\mu_{a,f}$ and $\mu_{a,m}$ are sometimes used to distinguish apparent fluxmetric and magnetometric permeabilities. This report considers fluxmetric values almost exclusively and we define $\mu_{rod} \equiv \mu_a \equiv \mu_{a,f}$. Whenever possible, only μ_{rod} will be used in this article.

The moniker “ballistic” is a reference to permeability measurement techniques. A device known as a ballistic galvanometer is sometimes used to measure bulk (i.e. average) properties of ferro-magnetic materials.

Permeability in a Coil-Generated Field

Above, apparent permeability was defined in the context of immersing the ferrite rod in a uniform magnetic field (i.e. a radio signal). The motivation was to be able to predict how much voltage would be induced in the receiving coil.

Here, we'll look at the fields induced by currents flowing in the receiving coil. The motivation is different – we wish to predict the self-inductance of the receiving coil. This is another very important design parameter for the antenna.

With no radio signal present, consider the magnetic field generated by alternating currents in the coil, as in figure 6.9 (copied from [CIA]). On the left is a coil with air core, and a ferrite core is shown on the right side of the figure. There, a closed flux path is setup by the coil, part of which is in ferrite and part in air. Once again, the B

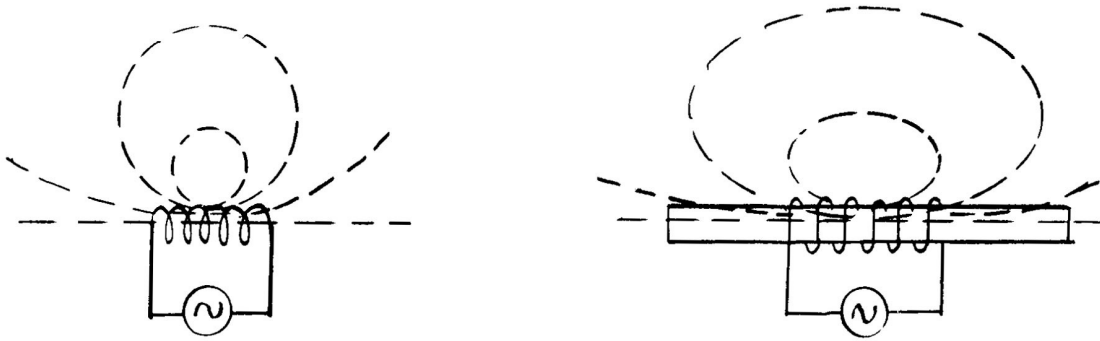


Figure 6.9: Illustration of μ_{int}

field in the rod will not be uniform, and depends on both the coil and rod geometries. Figure 6.10 shows the B-field from an E-M simulation of a coil on a ferrite rod; the coil is centered on the rod and half the rod's length (red shaded area). Notice that this field looks nothing like that in figure 6.3. The rough drawing in figure 6.9 from [CIA] is pretty accurate.

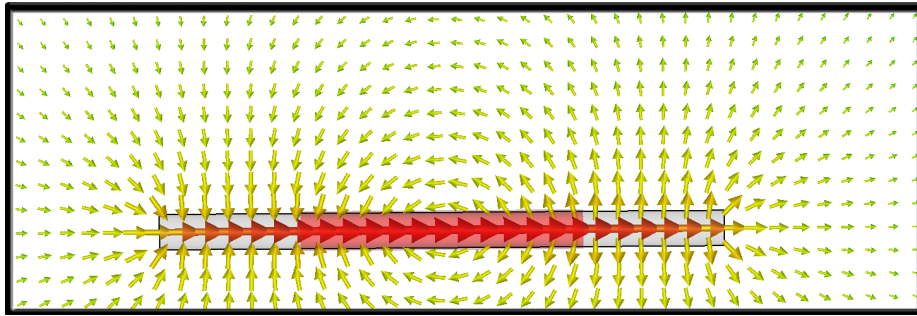


Figure 6.10: Simulation of B-Field generated by coil on ferrite core

The specific geometry of the air and ferrite portions of the path, and the ferrite material's μ_i all factor into the electrical inductance of the coil. The ratio of inductance with and w/o the ferrite core defines another measure of permeability, μ_{int} . It is often expressed as the apparent permeability (μ_a) multiplied by a factor F_{int} .

$$\mu_{int} = \mu_a F_{int} \quad (6.2)$$

In general $\mu_{int} \neq \mu_{ext}$.

Losses in Ferrite Materials

Rods with large aspect ratios (for example, $l/d \geq 10$) are often used in antenna designs. In this case, ferrite losses can end up limiting the maximum achievable Q

for the loop antenna. Losses are usually specified as the imaginary part of a complex permeability, and/or the associated loss tangent:

$$\mu = \mu' - j\mu'', \quad \tan \delta = \frac{\mu'}{\mu''}$$

This is a function of frequency and manufacturer data sheets should contain graphs of the real and imaginary parts of the permeability, as in figure 6.11. One may think of the loss tangent as being approximately equal to the Q of the ferrite material.

Why is Permeability Complex?

Somewhere in the calculation of inductance, permeability is going to appear as a multiplicative term, yielding a complex value of inductance: $L = a - jb$ (the imaginary part of permeability is always negative). When working with complex frequency, $s = j\omega$, the calculation of complex impedance for an ideal inductor is $Z = sL = j\omega L$. When inductance is complex, the result is this:

$$Z = j\omega L = j\omega(a + jb) = j\omega a + \omega b = \text{ideal inductance} + \text{loss resistance}$$

This automatically incorporates a frequency dependent loss resistance in series with the inductor to represent ferrite losses. It's now apparent why the imaginary part of the permeability (b in the above equation) is negative – it makes the loss resistance positive. See [Snelling] section 2.2.1 for more on this.

For resonant ferrite rod antennas in the AM broadcast band (up to 1710 kHz), 61 Material ($\mu_i = 125$) is one of the few currently available materials that makes any sense. We have tested some rods of unknown materials removed from AM broadcast receivers which appear to have $\mu_i \approx 200$. There don't seem to be any rods with μ_i in this range currently available in the U.S. from reputable manufacturers, so it's not known what material they might be made from.

All materials with higher values of initial permeability have too much loss at AM broadcast frequencies. There are materials with less loss than 61 Material but with substantially lower permeability.

Figure 6.11 is reproduced from an Amidon specification sheet about the material. The ratio between real permeability μ'_s and imaginary permeability μ''_s is the maximum Q achievable. At 2MHz and below that value is greater than 100, probably several hundred, although the curve dives off the bottom of the graph there, so it's value is unknown.

More detail on ferrite losses is presented in the next chapter. Loss may be much less of an issue in the case of Ferrite Sleeve Loop antennas because of the tiny aspect ratios they typically have. See the chapter on FSL designs for more on that topic.

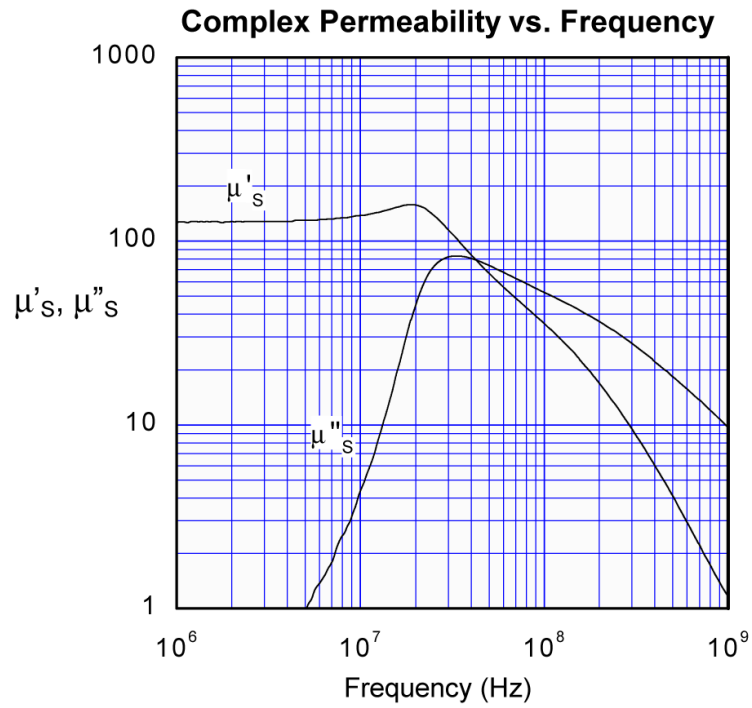


Figure 6.11: Complex permeability of 61 material

Summary

The worst is over now. If you've got a fair understanding of the material in this chapter, the rest of this will seem pretty simple and make a lot of sense.

Chapter 7

Ferrite Core Loops

This chapter presents a method for accurately estimating the effective height of ferrite core loops. Readers may find it helpful to refer back to the chapter on permeability while reading this chapter.

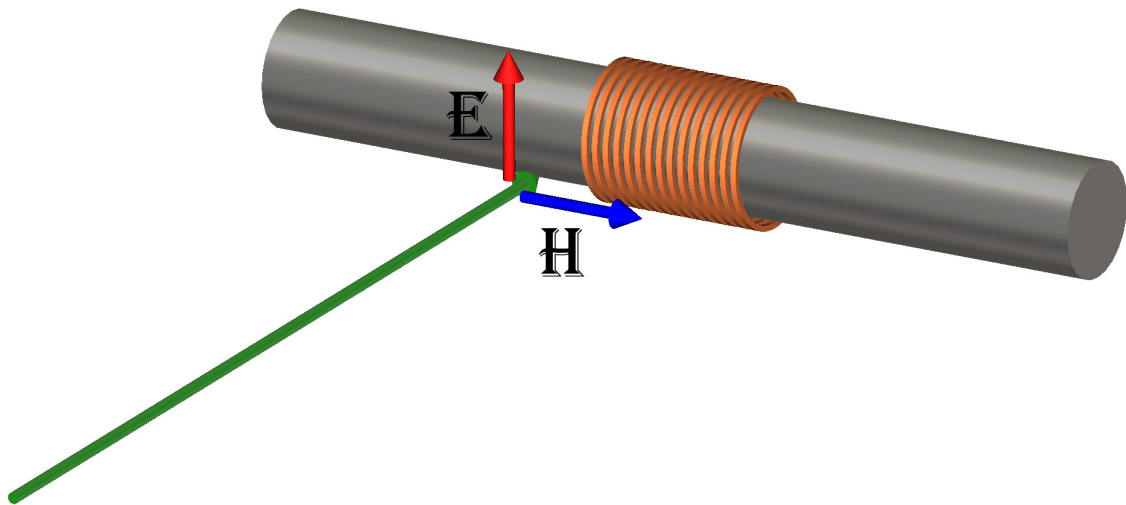


Figure 7.1: Ferrite core antenna receiving TEM plane wave

Empirical Approach

Although the cylindrical rod is a simple geometric shape, it's still complex enough that no closed form solutions exist to calculate the magnetic fields induced by TEM plane waves. The same can be said about predicting the self inductance of coils wound around such rods.

What is typically found in literature are attempts to approximate the cylindrical shape with other shapes (for which solutions are known), or curve fits to empirical

data. For example, an ellipsoidal spheroid, when highly elliptical starts to look like a cylindrical rod, as in figure 7.2.

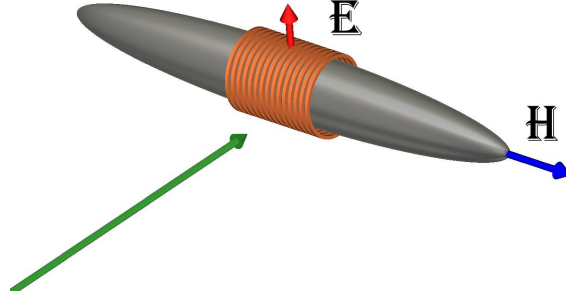


Figure 7.2: Approximating a cylindrical rod with an ellipsoidal spheroid

This article takes an empirical approach to the problem. Electromagnetic simulations were run over a range of reasonable rod and coil geometries. Data sets have been generated covering a multi-dimensional grid of design parameters which may be interpolated to estimate the performance of a given design. The data and equations provided here are based on literally thousands of simulations.

The range and sampling density of research involving physical experiments is necessarily limited by time and resources. A wide range of geometric parameters can be more densely sampled with the simulation approach used here. This would be a prohibitive task experimentally, but with simulations, it just requires more computer time.

The simulated data can either be directly interpolated, or replaced with low order polynomial fits. Both techniques are used here. Scripts for Matlab/Octave are provided which perform this interpolation, or can serve as examples for writing code in other computer languages. Polynomial coefficients and data sets are provided in Matlab/Octave-format data files.

Induced Voltage

The same equivalent circuit is used for the ferrite core antenna as was used for air core loops. The voltage induced by a vertically polarized TEM wave propagating is

$$e_f = (\mu_{ext}\beta A_f n)E \quad (7.1)$$

and E is the electric field intensity. The ferrite core antenna's effective height is the combined multiplier on the electric field intensity.

$$h_e = \mu_{ext}\beta A_f n$$

As with air core loops, this assumes the magnetic field vector is aligned parallel with the coil's (and rod's) axis as shown in figure 7.1. A subscript is included on the

area term (A_f) to emphasize that it is the area of the ferrite core, not the area inside the coil. The coil diameter is often slightly larger due to the presence of insulation or a coil form. That suffix may be dropped at times, but when dealing with ferrite core loops, it's always assumed that A refers to the ferrite core area, not the coil area. The case of a coil wound with a much larger diameter around a ferrite rod is not considered here.

Determination of μ_{ext}

This would be a much shorter chapter if it weren't for the presence of the external permeability multiplier in the effective height formula. The concept of μ_{ext} was introduced in the chapter on permeability, and it will be expanded on here.

To review, the value of, μ_{ext} is the factor by which the effective height of the antenna is increased by inserting the ferrite rod. It is a function of several factors.

- The ferrite material's intrinsic permeability, μ_i .
- The ferrite rod's length-to-diameter ratio, a.k.a. *aspect ratio*.
- The length and placement of the coil on the rod.

For analysis, μ_{ext} is broken down into two components, μ_{rod} and F_{ext} :

$$h_e = \mu_{rod} F_{ext} \beta A_f n \quad (7.2)$$

Equation (7.2) is the money equation for ferrite core loops, as (5.1) is for air core loops. The primary focus of this chapter is to provide the means for accurately estimating the first two terms on the right hand side, μ_{rod} and F_{ext} .

The first term, μ_{rod} is the amount by which the ambient magnetic flux level is increased at the middle of the ferrite rod. This is also known as the apparent permeability or fluxmetric permeability.

The F_{ext} term is necessary because magnetic flux inside the ferrite is not constant everywhere. It varies along the length of the rod, and also radially between center and outside radius. When a coil of finite length is wrapped around the rod, Ampere's law tells us that the total amount of flux within each turn of the coil contributes to the overall induced voltage. Because each turn of the coil encircles a different amount of flux, the total induced voltage becomes an average of the flux levels from one end of the coil to the other.

Flux in a cylindrical ferrite rod is generally greatest at the center of the rod, and falls off towards the ends (see figure 6.6). To get the largest induced voltage then, the coil should be centered. For the same reason, centered short coils will have a higher induced voltage per turn than long ones since they will only be sampling the higher flux levels near the center of the rod.

Most of the remainder of this chapter will be concerned with accurately predicting the values of μ_{rod} and F_{ext} . There are published formulas for this purpose and some of them are presented.

We found that existing formulas have some accuracy issues, and in some cases there is a lot of variation between published research data and theory. Alternative methods for estimation presented here are based on extensive E-M simulations of bare ferrite rods, and ferrite cored coils excited by TEM plane waves. To the extent these simulations are inaccurate, so are the estimating functions published here. No hard comparisons between simulations and real-world measurements have been made, and the reader should keep that in mind. That said, we believe the simulations are reasonably accurate.

Apparent Permeability

Some published approximations define a demagnetization factor N , and apparent permeability is derived from that as follows.

$$\mu_{rod} = \frac{\mu_i}{1 + N(\mu_i - 1)} \quad (7.3)$$

Solving for μ_i ,

$$\begin{aligned} \mu_i(1 - \mu_{rod}N) &= \mu_{rod}(1 - N) \\ \mu_i &= \frac{\mu_{rod}(1 - N)}{1 - \mu_{rod}N} \end{aligned} \quad (7.4)$$

and for N ,

$$\begin{aligned} \mu_{rod} + N\mu_{rod}(\mu_i - 1) &= \mu_i \\ N &= \frac{\mu_i - \mu_{rod}}{\mu_{rod}(\mu_i - 1)} \end{aligned} \quad (7.5)$$

Approximations from [Bolton-1]

These are formulas that Bolton collected from various sources. Below are two different estimates for either μ_{rod} directly, or indirectly through the demagnetization factor. This article will provide estimates for μ_{rod} based on simulation data, so these approximations are included only for purposes of comparison.

The first approximation is said to be less accurate for l/d ratios below 10; above 10, it may be most accurate to use both equations and average the result.

$$\mu_{rod} \approx \frac{\mu_i [(l/d)^{5/3} + 2.5]}{\mu_i + [(l/d)^{5/3} + 2.5]} \Big|_{(l/d) > 10} \quad (7.6)$$

$$N \approx 0.37(l/d)^{-1.44} \Big|_{2 \leq (l/d) < 20} \quad (7.7)$$

More complex equations, claimed to produce accurate results over the entire range of l/d ratios are shown in (7.8) and (7.9). They are found in [Bolton-1], and originally come from [Cross]. The formula also requires the spheriodal demagnetization factor N_{ell} as presented in figure 4.3 in [Bolton-1]. We fit a polynomial visually to that graph and it is included below as equations (7.10) through (7.12).

$$N = \frac{k_c N_{ell}}{1.2 + 0.05 [0.3 + (\log_{10}(l/d) - 0.7)^2]^{-1}} \quad (7.8)$$

$$k_c = \left(1 + \left[\frac{l/d}{1.178769 \mu_i^{5/7}} \right]^{4/3} \right)^{-1/2} \quad (7.9)$$

$$x = \log_{10}(l/d) \quad (7.10)$$

$$\begin{aligned} \beta = & 0.01851729x^4 - 0.01515424x^3 - 0.37379092x^2 \\ & - 0.79188605x - 0.50881135 \end{aligned} \quad (7.11)$$

$$N_{ell} \approx 10^\beta \quad (7.12)$$

A graph based on equations (7.3) and (7.8) through (7.12) for several common values of initial permeability is shown in figure 7.4. This chart, or something very close to it may be found on many different ferrite manufacturers' web sites.

Approximations from Simulations

A large number of E-M simulations were run of ferrite rods with a 1-turn centered coil, excited by a TEM plane wave. The simulated ferrite material had no losses and no dispersion. The longest rod simulated was 0.0056 wavelengths long at the simulation frequency. A one-turn coil was used to sample the flux in the center of the rod as shown in figure 7.3. As such, $F_{ext} = 1$ by definition.

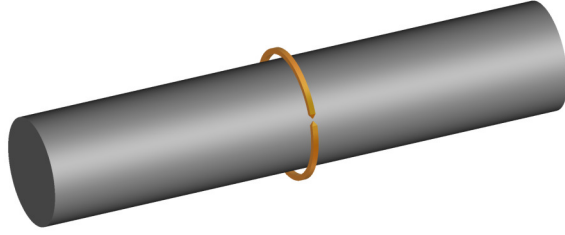


Figure 7.3: Simulation setup for estimating μ_{rod}

Based on the voltage induced in each simulation, and the formula for induced voltage (7.1), the value of μ_{rod} was determined. The f subscript is added to rod geometry parameters (e.g. l_f , A_f) to indicate they apply to the ferrite rod and not the coil. Once μ_{rod} was determined, the demagnetization factor N could be computed using (7.5). The last equality in the formula below includes the substitutions $E = 1\text{V/m}$, $F_{ext} = 1$ and $n = 1$.

$$\mu_{rod} = \frac{V_{oc}}{EF_{ext}\beta A_f n} = \frac{V_{oc}}{\beta A_f} \Big|_{n=1, F_{ext}=1, E=1}$$

Using this technique, simulations were run with values of μ_i from 63 through 4000, and aspect ratios from about 0.37 up through 33. This gave a 2-dimensional table of μ_{rod} versus both μ_i and aspect ratio. The best choice of independent variables for interpolation seems to be the logarithms of μ_i and aspect ratio, and logarithm of μ_{rod} for the dependent variable. Thus, the following function is suggested for interpolation:

$$M \equiv \ln N = f \left(\ln \mu_i, \ln \frac{l_f}{d_f} \right) \text{ and then } \hat{N} = e^M$$

Figure 7.4 is based on equations from Cross, because it covers a very wide range of aspect ratios – including ridiculously large ones which will probably never be encountered in the real world. This is done to show asymptotic behavior of the function with different values of μ_i . Our simulations did not cover this wide range of aspect ratios and it would not be appropriate to extrapolate the results that far.

Graphs over a practical range of aspect ratios based on simulation data are shown in figure 7.5 and for very small ratios in figure 7.6. The small aspect chart is referred to in the analysis of ferrite sleeve loop antennas in a following chapter. It can be seen that for smaller aspect ratios, the value of μ_i has a smaller effect on μ_{rod} , and for $l/d < 5$, the initial permeability has very little effect.

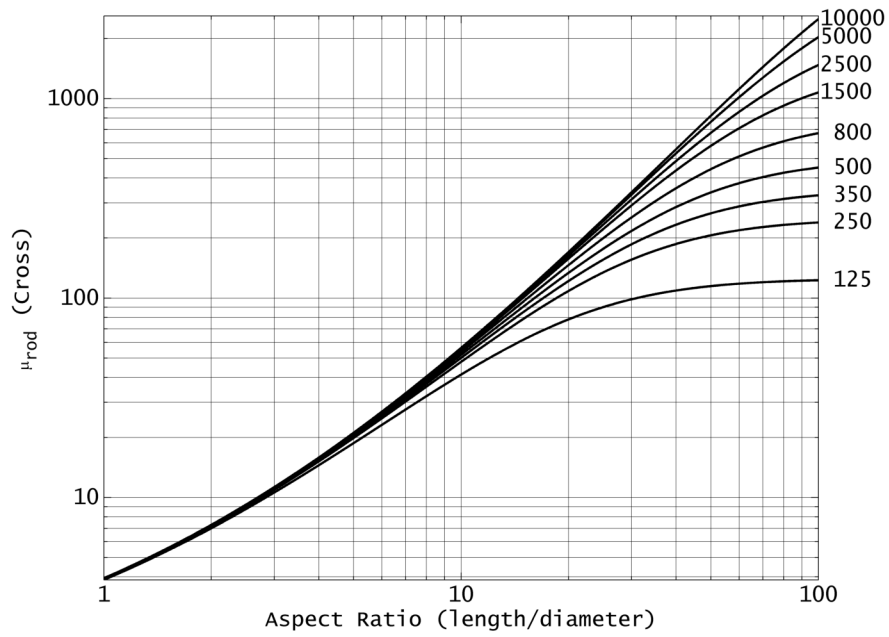


Figure 7.4: Apparent permeability over a wide range of aspect ratios

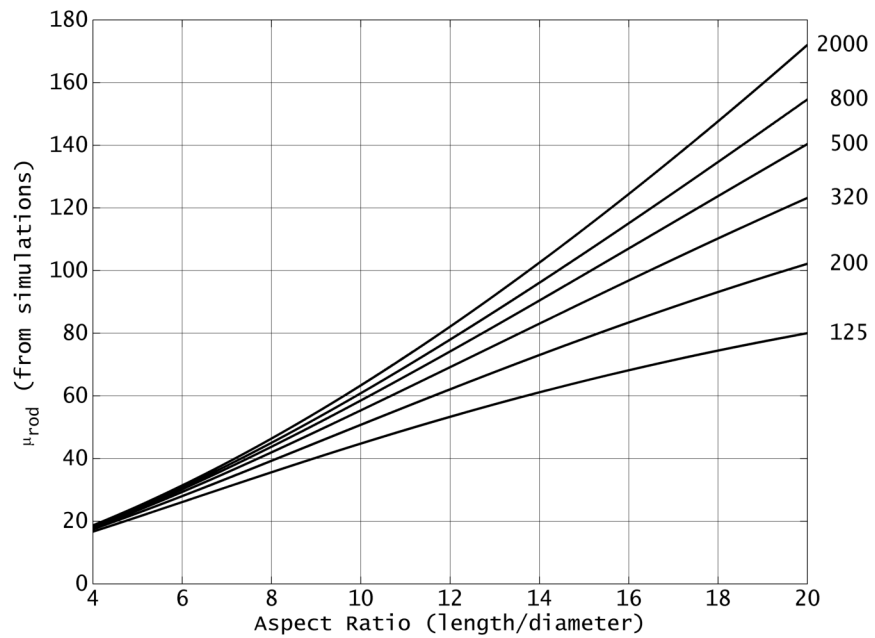


Figure 7.5: Apparent permeability for practical aspect ratios

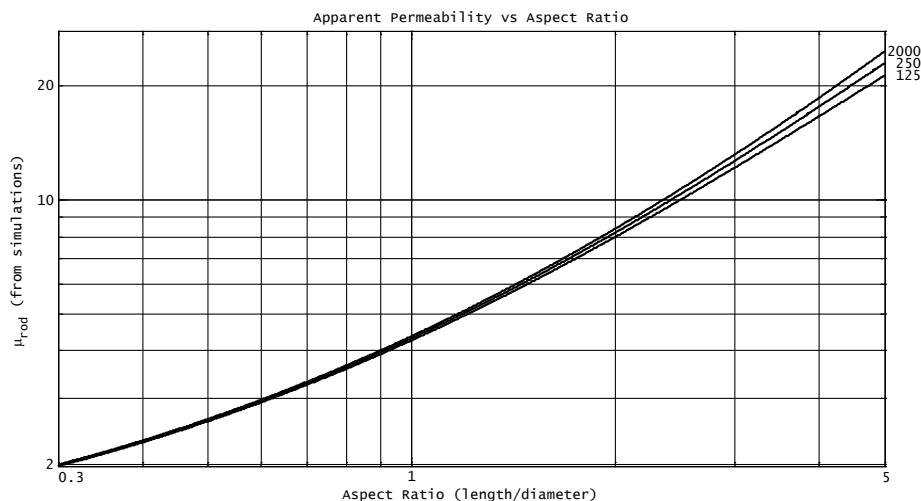


Figure 7.6: Apparent permeability for very small aspect ratios

Comparing Estimates

The differences between computing μ_{rod} with equations (7.8) through (7.12) and simulation data are shown in figures 7.7 and 7.8.

Formula-based values are in red, while simulation-based data is in black. The formulas consistently under-estimate simulated μ_{rod} values for aspect ratios in the range $\{1..10\}$ or so, and agree pretty well from about 20 to 40. Our simulations did not examine ratios above 33, but the graphed fits have been extrapolated out to ratios of 100:1 just out of curiosity. Curves for five different values of intrinsic permeability are shown for both formula and simulation-based data: 125, 250, 500, 1000 and 2000.

In figure 7.8, the differences between the two sets of data in decibels are shown as a 3-D surface plot. The formulas come out as much as 1.5dB higher than simulations at all values of μ_i , and the largest differences occur over a range of aspect ratios from about 1 to 10.

These E-M simulations have not been verified against any real world measurements, so there's no claim of any specific level of accuracy. This is due to the fact we have no way to accurately measure the intrinsic permeability of any of our test rods.

It's felt that the simulations are reasonably accurate and that's about the best assurance that can be offered. The best alternative for those who don't trust the simulation data is to use equations (7.8) through (7.12) to get N instead.

The F_{ext} function

If the magnetic flux in the rod were constant along its length, there would be no need for this function. However because it does vary, the coil essentially takes an average of the flux in the rod over its length. Although equations exist to approximate this

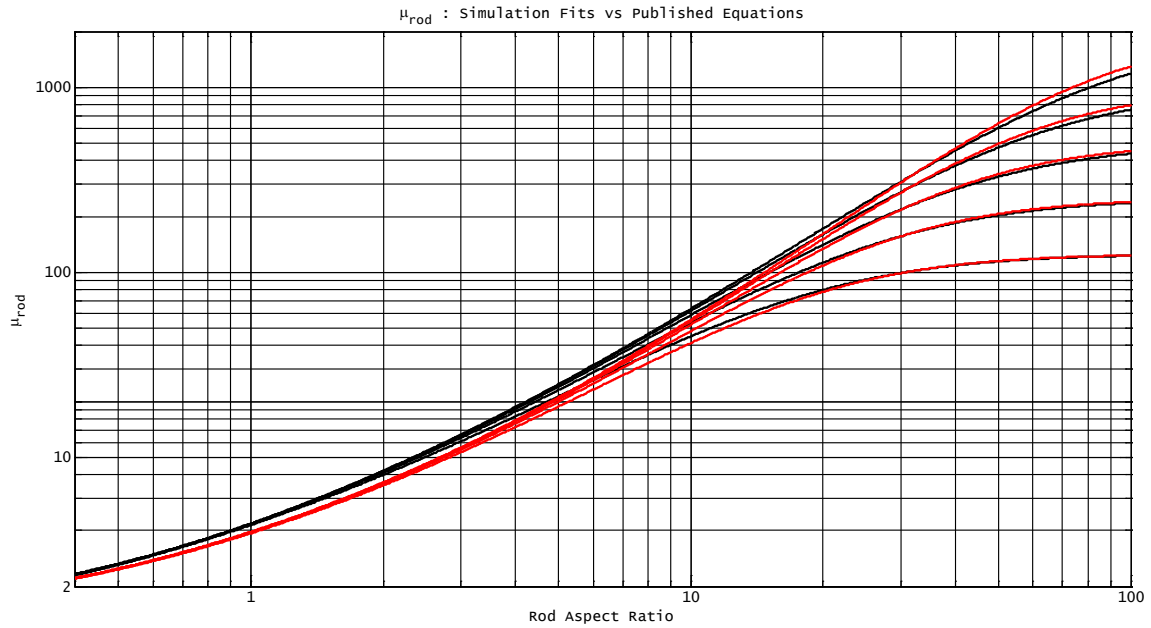


Figure 7.7: Comparing μ_{rod} equations to simulation polynomial fits

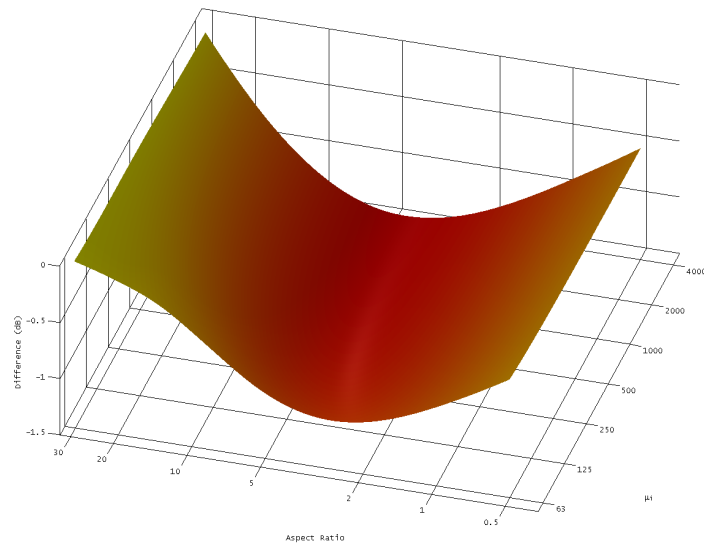


Figure 7.8: Difference between μ_{rod} equations and simulations in dB

average for coils centered on the rod, a more general approach is to have approximations for the flux variations along the rod. These approximations can then be averaged over the physical range of the coil. This method can easily handle off-center coils.

The paper by Bolton [Bolton-1] contains a graph and some functional approximations for centered coils as a function of the coil length. One question not addressed by Bolton is whether this function depends at all on the rod’s l/d ratio, or the initial permeability of the ferrite. Using an l/d ratio of 10:1, we first verified that our simulations matched figure 4.8 in [Bolton-1], which is reproduced here as figure 7.9. That data is almost identical to the curve labeled “Smith 2007”.

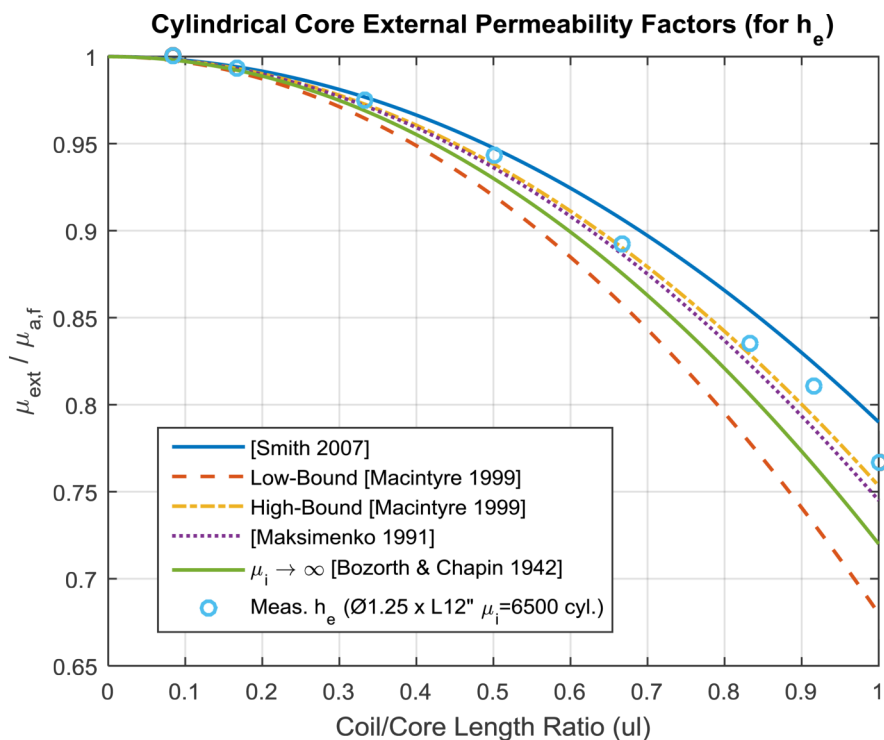


Figure 7.9: Bolton’s figure 4.8

Further simulations with other aspect ratios however show that F_{ext} does depend on both the aspect ratio and initial permeability, μ_i .

Simulation-based F_{ext}

Simulations were run over a wide range of permeability and aspect ratios. Data on axial magnetic field variations across the rod were used generate polynomial curve fits to the axial field variations. A total of 42 fits were generated for combinations of seven different permeability values from 63 to 4000, and six different aspect ratios from 5 to 28.

Because the magnetic field varies not only along the axis of the rod, but radially as well, each simulation examined the field not only along the rod’s axis, but along two additional parallel lines. One was half-way between center and edge radially, and the other just in from the outer radius of the rod. These three field values were

averaged go get the value to which curve fits were generated. Figure 7.10 depicts the three paths along which the fields were evaluated inside the ferrite.

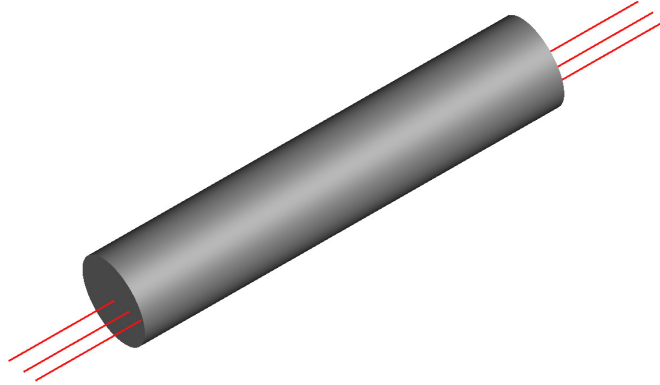


Figure 7.10: Axial paths for magnetic field evaluation

The resulting fits may be evaluated to get reasonably accurate approximations to axial field variations through the rod. These fits may then be averaged (i.e. integrated) across the coil position and compared to the field at the center of the rod to generate the F_{ext} value.

For combinations of μ_i and aspect ratio that are not tabulated, our suggestion is to integrate *all* of the tabulated polynomials over the coil position using one of (7.13) through (7.15). This will result in a set of F_{ext} values over a 2-dimensional grid of μ_i and aspect ratios. Then a 2-D interpolation may be used to get the desired estimate. Matlab/Octave scripts are attached to this document which perform these operations.

Using the axial field approximations

These are polynomials in x , where x represents a position between center of the rod and the end. The rod's center is at ($x = 0$), and at the end, ($x = 1$). The B field magnitude at the center has been normalized to one, so averaging across the coil position will directly give the value for F_{ext} . For a coil occupying a position between x_1 and x_2 ,

$$F_{ext} = \frac{1}{x_2 - x_1} \int_{x_1}^{x_2} P(x) dx \quad (7.13)$$

This assumes the coil lies solely on one side of center. For a coil which spans the rod's center, and is not centered, two integrals must be evaluated, one from center to one end of the coil, and one from center to the other end. Let $\{x'_1, x'_2\}$ represent the ends of the coil as the distance from the rod's center (relative to half the length of the rod).

$$F_{ext} = \frac{1}{x'_1 + x'_2} \left(\int_0^{x'_1} P(x) dx + \int_0^{x'_2} P(x) dx \right) \quad (7.14)$$

In the special case of a centered coil of length $2x$, both integrals yield identical results and this can be simplified

$$F_{ext} = \frac{1}{x} \int_0^x P(x) dx \quad (7.15)$$

Since the integrands are polynomials, the definite integrals may be explicitly written:

$$\int_{x_1}^{x_2} P(x) dx = \int_{x_1}^{x_2} \sum_{k=0}^N c_k x^k dx = \sum_{k=1}^{N+1} \frac{c_{k-1}}{k} x^k \Big|_{x_1}^{x_2} \quad (7.16)$$

Coefficients for the polynomial fits are available in the appendix, and are encoded as part of the attached Matlab/Octave scripts.

Inductance

This is a large topic in itself and is beyond the scope of this article. A separate article [osengr-1] from Open Source Hardware Engineering deals with the topic of estimating inductance of coils wound on ferrite rod cores.

Stacking Rods

Ferrite rods may be stacked end-to-end to achieve a larger aspect ratio. Air gaps must be kept small, and some simulations with stacking two identical rods with $l/d = 5$ per rod to achieve a combined $l/d = 10$ yielded the following curve fit for estimating decibels of lost permeability as a function of gap length relative to rod diameter, where g is the gap length:

$$\text{Loss(dB)} = -19.034 \left(\frac{g}{d} \right)^{2/3} + 0.074 \Big|_{l/d=10, \mu_i=125}$$

Only a few simulations were performed, and it's known that the sensitivity to gap length is different for different values of μ_{rod} and or l/d . However this gives a hint that if the gap can be kept to less than about 0.02 rod diameters either for materials with low permeability or combined aspect ratios less than 10, the loss won't be more than one decibel.

Additional experiments with $\mu_i = 2000$ and stacked $l/d = 30$ show that gaps must be kept to less than 0.004 rod diameters to avoid more than one decibel or so of loss.

For example, with half-inch diameter rods, the maximum gap would be 2 mils. A gap of 6 mils would result in about a 2dB loss. The curve fit for this case is

$$\text{Loss(dB)} = -39.84 \left(\frac{g}{d} \right)^{2/3} + 0.010 \Big|_{l/d=30, \mu_i=2000}$$

Physical experiments with stacking two rods having estimated $\mu_i = 350$ and $l/d = 7.56$ (per rod) seem to back this up. The ends of the two rods were manually flattened with sandpaper, and when joined the resulting inductance was about 1dB less than predicted by simulation for a solid rod. Adding a 4-mil gap to the simulation matches the measured inductance.

Ferrite-Imposed Limitations on Q

In various literature, the maximum attainable Q for the open magnetic configuration of a ferrite cored inductor is claimed equal to the Q of a closed circuit multiplied by the ratio $(\mu_i - 1)/(\mu_{rod} - 1)$. The other possibility is that using μ_{int} might be more accurate, but as explained below, this provides less accurate estimates. This is described in [Ferroxcube], and it requires treating the ferrite rod inductor as a air-gapped magnetic circuit. This upper limit considers losses in the ferrite material only and does not consider wire resistance, so the actual Q obtained will always be less.

Q in a closed-circuit is given by the ratio of real to complex permeability, usually denoted μ'/μ'' , or sometimes referred to as the loss tangent, $\tan \delta$. These values are frequency dependent and must be taken from manufacturer specifications. This is the expression for maximum attainable Q based on ferrite losses alone.

$$Q_{max} \approx \frac{\mu'}{\mu''} \frac{\mu_i - 1}{\mu_{rod} - 1}$$

For reasons explained in [osengr-1], using μ_{int} in this formula instead of μ_{rod} , as is sometimes done, does not make much sense.

$$Q_{max} \neq \frac{\mu'}{\mu''} \frac{\mu_i - 1}{\mu_{int} - 1},$$

The second term in the equation for Q_{max} reveals another engineering trade-off. Maximizing μ_{rod} by using a high permeability material and a very large L/D ratio, increases μ_{rod} , which reduces the second term in the above expression for Q_{max} . If the ferrite material's inherent Q value is not large enough for the loop design, it will place an upper limit on the L/D ratio, and this is at odds with the goal of maximizing the effective height.

To work an example, consider a rod of 61 material with L/D=15, wound with an 80% full-length coil. For this we find $\mu' = 118.54$, $\mu'' = 0.76$, $\mu_i = 125$, $\mu_{rod} = 64$, so a guess for maximum attainable Q at 2MHz is:

$$Q_{max} = \frac{118.5}{0.76} \frac{125 - 1}{64 - 1} \approx 295$$

Consider what happens if we now double the rod length so that $L/D=30$, but we keep the coil winding length unchanged. Now $\mu_{rod} = 99$ which lowers Q_{max} to about 190. The situation would be worse if using 52 Material which has a lower inherent Q value.

For example, in [Tongue] we have an example of such data, with a 61 Material rod. Using the 'B' coil in his data table, air core inductance is $19.3\mu\text{H}$ while it rises to $248\mu\text{H}$ with the ferrite rod inserted. This provides a direct calculation of $\mu_{int} = 248/19.3 = 12.85$. For the 61 Material, $\mu_i = 125$ and at 500kHz, $\mu' = 117.95$, $\mu'' = 0.48$, so

$$Q_{max} = \frac{117.95}{0.48} \frac{125}{12.85} \approx 2390$$

The overall Q is limited by the coil in this case, and doesn't provide much help confirming any of this.

Self Resonance

Antenna coils will resonate at an often much lower frequency when wound on a ferrite rod. How much lower depends partly on how much space there is between the rod and coil. Larger diameter coils can result in a many-fold increase in SRF compared to minimum diameter coils. This can permit many more turns in the coil and the concomitant increase in effective height.

Unlike air core coils, the Q factor can plummet precipitously around the self resonant frequency (SRF). We have been unable to find a definitive explanation for the cause of this behavior. Antenna coils are rarely operated near self resonance and this might explain the lack of published research on the topic.

Coils wound with Litz wire also show this drop in Q factor, which suggests the cause may be something other than proximity effect.

An Accurate Circuit Model

When very high values of Q (e.g. more than 100-200) are desired, an accurate model of the coil's self resonance may be necessary. The schematic model shown in figure 7.11 provides an excellent match to the measured impedance below and near SRF of one test coil wound with Litz wire on a 77-material ferrite rod.

In this model, the large value of resistance (400Ω) in series with the capacitor is responsible for the degradation of Q over a wide range of frequencies near SRF. This makes achieving a high Q (e.g. several hundred) impossible anywhere above about 10% of SRF or so.

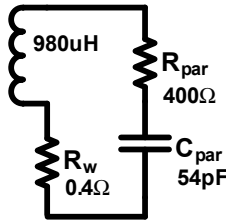


Figure 7.11: Model matching impedance near SRF

It is tempting to associate the loss of Q at resonance with some kind of loss (possibly dielectric loss) in the ferrite. The dielectric loss tangent of some ferrite materials can be very large in support of this idea. There is additional support for this idea in section 5.7.4 of [Snelling]. If this idea is correct, and for it to be useful, a method for computing the loss resistance would be required and that's beyond the scope here.

Coil Diameter Experiment

The coil in question was wound directly onto the rod with no former. We wondered if the capacitance between ferrite and coil provided coupling into a the high-loss dielectric material (ferrite) at SRF. To explore this, more experiments were performed with different coil diameters on the same 77-material rod. The hoped-for result was that the loss of Q near resonance would be vastly reduced with the larger diameter coil. That's not what was found, but the results are still useful.

One coil was wound directly on the $\frac{1}{2}$ -inch diameter rod, and the other on a 1-inch diameter form (a clear acrylic tube). Both coils had approximately the same turn count (184 for one and 189 for the other), and inductance was about the same for both. Figure 7.12 shows approximate models generated to match the measured impedance of each coil. These were not as good a match to measured data as was found in the case of figure 7.11, so another parallel resistor was added to the model to get a better match (as suggested in [Green]).

The large diameter coil's SRF was 5.7 times larger than the smaller coil (2MHz vs 350kHz). The Q at resonance of both coils is quite low. The main effect of a larger diameter coil was to drastically increase the SRF. This allows high Q to be maintained to higher frequencies, or for much larger turn counts to be used without loss of Q .

These models were based on impedance measurements at discrete frequencies. We did not have a means to directly measure the bandwidth of the coil at resonance, which would have been preferable.

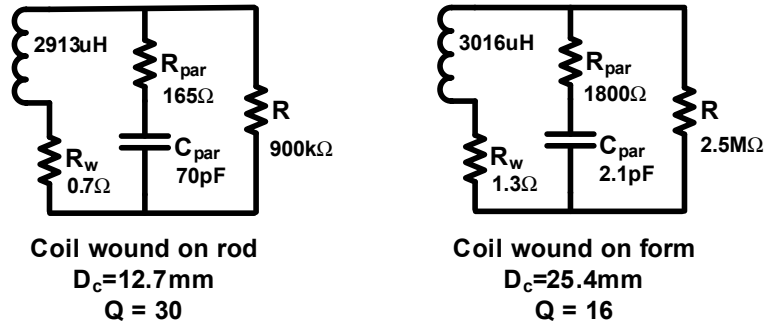


Figure 7.12: Models for different coil diameters, and Q at SRF

Musings On Mechanisms

Based on these results, it might be that at resonance, losses in the ferrite are excited by magnetic fields generated by the coil. If these losses were excited by capacitive coupling to the coil, one would expect them to be reduced a lot with a larger diameter coil – and that did not happen. The advantage of using a larger coil diameter is solely due to the increase in SRF – not from any reduction in actual losses at SRF. It’s possible the increase in SRF is a capacitive issue involving the ferrite, but losses at SRF don’t appear to be.

That said, it’s worth noting that self resonance is an electromagnetic phenomenon – not an electric or magnetic one. As such, our attempts above to associate observed behaviors with capacitive or inductive phenomena should be taken with a grain of salt. Lacking more evidence, we will avoid the temptation to attribute this behavior to any particular cause, and close this section with the conclusion that when SRF rears its ugly head, using larger diameter coils may solve the problem.

Don’t Forget the Capacitors

If high Q (e.g. a couple hundred or more) is the goal, be sure to take into account losses in the capacitors used to resonate the loop. A very high Q ferrite design can be ruined by using lossy capacitors. Even low-loss capacitors such as those constructed with polypropylene film dielectric may still have a measurable effect on the overall Q of the tuned antenna.

Wire Losses

Over at least some range of frequencies, losses computed for air-core coils wound with solid wire may be used with ferrite core designs to estimate copper losses. According to [Payne] however, at higher frequencies additional losses may appear and they can

be significant.

We built one antenna using 77-Material with $\mu_i = 2000$, and the measured Q at 60kHz was much smaller than even predicted by Payne. This left us at somewhat of a loss for accurate estimates. All we can suggest is that the actual Q may be lower than expected.

This topic is not explored further and the reader is referred to the referenced article for more information. Scripts attached to this document do not take into account the possibility of these higher losses.

$$R_{ac} = \pi \frac{d_c}{l_c} \frac{\rho}{\delta} N^2 \frac{p}{d_w}$$

The last term accounts for the fact that the coil is not solid copper and it's the inverse of the fraction of the coil's length made of copper, not air.

$$\begin{aligned} R_{ac} &= 32\pi \frac{\rho}{\delta} N^2 \frac{d_w}{p} \frac{d_f^2}{4d_f^2 + l_c^2} \left(\frac{l_e}{l_c}\right)^2 \frac{d_c}{2l_c} \left(\frac{d_c}{d_f}\right)^2 \left(\frac{L_f}{L_{air}}\right)^2 \\ &= \frac{16\pi}{l_c} \frac{\rho}{\delta} N^2 \frac{d_w}{p} \frac{d_c^3}{4d_f^2 + l_c^2} \left(\frac{l_e}{l_c}\right)^2 \left(\frac{L_f}{L_{air}}\right)^2 \end{aligned}$$

The task of estimating wire losses for coils wound with Litz wire is not attempted here.

Temperature Dependence of μ_i

The permeability of ferrite varies with temperature, and the characteristic can be quite different for various materials. In fix-tuned antenna applications with high Q, this must be taken into account to prevent the resonant frequency from straying too far in operation at different temperatures.

The inductance of a ferrite-cored antenna coil is given by

$$A_L n^2$$

and therefore varies directly with the inductance factor A_L . The resonant frequency varies with the square root of inductance, so for small relative changes in inductance, resonant frequency will move by half as much. This is because

$$\sqrt{1+x} \approx 1 + \frac{x}{2} \Big|_{x \ll 1}$$

The temperature dependence of A_L may be explored if a table or graph of μ_i versus temperature is available from the ferrite manufacturer. If a table is not provided, then

a published graph may be converted by eye into a table of temperature-permeability pairs. Once this is done, each permeability in the table can be converted into an A_L value for the proposed antenna design, and then plotted versus temperature. Determination of inductance factor requires specification of coil length in addition to ferrite rod μ_i and dimensions. See [osengr-1] for details on calculating A_L .

Eyeballing the graph provides a clue as to how linear the behavior is over temperature. An example of manually digitizing graph data, using the Amidon data sheet for their 77 material is shown in figure 7.13.

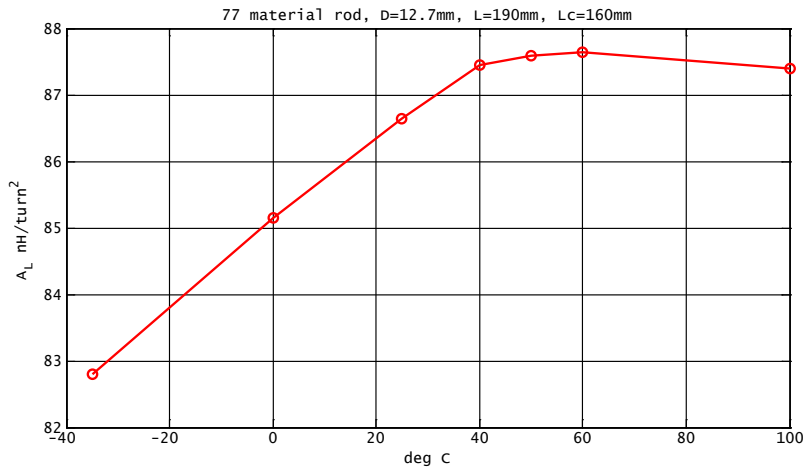


Figure 7.13

For further analysis, the temperature dependence of A_L may be linearized around a some temperature of interest, T_o . The graph of A_L versus temperature gives an idea over what range of temperatures the linearized approximation might be valid. In figure 7.13, it appears that A_L is fairly linear with temperature from -35C to +40C.

Working with μ_i specifications

Sometimes the manufacturer will specify a maximum temperature coefficient for μ_i over some range of temperatures. A small amount of differential calculus will show how this specification may be used. The specified value (e.g. 0.7%/deg C) is the partial derivative w.r.t. temperature, relative to the value at any temperature within the specified range. Here we assume the value is in percent but it can be done unit-less as well.

$$\frac{100}{A_L(T_o)} \frac{\partial A_L}{\partial T}$$

We consider two different estimates of the inductance factor, A_L now, one of which is very common:

$$A_L = \mu_o \mu_{rod} \frac{A_f}{l_f}$$

Here, the only thing that changes significantly with temperature is μ_{rod} because it depends on μ_i :

$$\mu_{rod} = \mu_{rod}(\mu_i(T, \dots))$$

In fact, μ_i depends on other parameters as well, such as frequency and applied DC magnetic fields. We assume those other parameters are constant and will not indicate them in subsequent formulas. With these assumptions, the relative variation of inductance factor in percent per degree C at temperature T can be estimated by using the chain rule. This will be denoted by $\alpha_{rod}(T)$ here:

$$\alpha_{rod}(T_o) = \frac{100}{\mu_{rod}} \frac{\partial \mu_{rod}}{\partial \mu_i} \frac{\partial \mu_i}{\partial T} \Big|_{T=T_o}$$

An alternate way to proceed is to use the estimates of A_L developed in [osengr-1]. Here, the formula for inductance factor is

$$A_L = \mu_o \mu_L \sqrt{l_f d_f}$$

The only thing that varies significantly with temperature here is the inductive permeability, μ_L and we may define a temperature coefficient as above:

$$\alpha_L(T_o) = \frac{100}{\mu_L} \frac{\partial \mu_L}{\partial \mu_i} \frac{\partial \mu_i}{\partial T} \Big|_{T=T_o}$$

Although using the inductive permeability can give significantly better estimates of inductance compared with μ_{rod} , for the purposes here it doesn't matter too much which one is used. That will be demonstrated below.

The partial derivatives of μ_{rod} or μ_L can be estimated by computing their changes over small changes in μ_i . The amount of change depends on how linear the temperature dependence is, but in general it's probably okay to use roughly a 1% change in μ_i or μ_L for estimation. There may be exceptions for highly non-linear materials but we have not seen one that would require that. For example, with 61 Material and nominal $\mu_i = 125$ at 25C, a change in μ_i of ± 1 would work:

$$\frac{\partial \mu_L}{\partial \mu_i} \approx \frac{\mu_L(126, \dots) - \mu_L(124, \dots)}{126 - 124}$$

Note that μ_L is a function of more than just μ_i , the other parameters being indicated by ellipses in the formula are identical in both invocations of the μ_L function. The ellipses will be omitted in subsequent formulas.

Specifications of μ_i

The temperature sensitivity (aka temperature coefficient) of μ_i is usually specified as a relative value in percent:

$$\alpha_i = \frac{100}{\mu_i} \frac{\partial \mu_i}{\partial T}$$

so the slope is

$$\frac{\partial \mu_i}{\partial T} = \frac{\alpha_i}{100} \mu_i$$

As an example, the coefficient for 77 material from 20 to 70C is specified as being no more than 0.7%/deg C. At 25C, μ_i is specified as being 2000, so the slope there can be expected to be no more than

$$\frac{0.7 \times 2000}{100} = 14 \left|_{20 \leq T \leq 70C}\right.$$

This is in units of per deg C since relative permeability is unit-less.

Final Result

Comparison of the temperature coefficients computed using μ_{rod} versus μ_L are shown here. For the example of 77 material, if the rod has an aspect ratio of 15:1, then the approximate derivative of μ_L or μ_{rod} versus μ_i at 25C may be found by computing μ_L or μ_{rod} for μ_i values of (for example) 1990 and 2010 as suggested above. Values shown here for μ_{rod} use the Matlab/Octave scripts attached to the PDF file for computing μ_{rod} , but similar results will be obtained using formulas found in [Bolton].

$$\frac{\partial \mu_{rod}}{\partial \mu_i} \approx \frac{\mu_{rod}(2010) - \mu_{rod}(1990)}{2010 - 1990} = \frac{113.3158 - 113.2601}{20} \approx 0.00278 \left|_{T=25C}\right.$$

$$\alpha_{rod}(25C) = 14 \frac{100}{\mu_{rod}(2000)} \frac{\partial \mu_{rod}}{\partial \mu_i(T)} \approx \frac{1400}{113.2881} \times 0.00278 \approx 0.0344\%/C$$

The same calculation using inductive permeability looks like this:

$$\frac{\partial \mu_L}{\partial \mu_i(T)} \approx \frac{603 \times 10^{-6}}{20} \approx 30.2 \times 10^{-6}$$

$$T_L(25) = 14 \frac{100}{\mu_L(2000)} \frac{\partial \mu_L}{\partial \mu_i(T)} \approx \frac{100}{1.305} \times 30.2 \times 10^{-6} \approx 0.0324\%/C$$

Methods published in [osengr-1] have been used for computing μ_L above. There's only a 6% difference in the coefficients determined by these two methods and in most cases it won't matter which method is used.

Temperature Limits

A reasonable requirement would be to limit the resonant drift to no more than one-half of the 3dB resonant bandwidth, which is the frequency divided by Q . The maximum relative drift in frequency would be $1/(2Q)$ or $\pm 1/(4Q)$. The relative drift in inductance would be limited to twice this much then, or $\pm 1/(2Q)$.

Continuing the example, If the resonant Q is 200, the inductance, and therefore μ_{rod} or A_L should not drift by more than $1/400 = 0.0025 = \pm 0.25\%$. Given the known temperature coefficient of μ_{rod} , the maximum temperature change to achieve this goal based on μ_{rod} is

$$\Delta_T = \frac{0.25\%}{0.0344\%/C} \approx \pm 7.3C$$

and using μ_L it is

$$\Delta_T = \frac{0.25\%}{0.0322\%/C} \approx \pm 7.8C$$

Collecting Terms

To summarize all of these formulas, there are three computations. First determine the slope of μ_i at a temperature of interest, T_o , given the permeability at that temperature, and a relative temperature coefficient in percent per deg C there:

$$\left. \frac{\partial \mu_i}{\partial T} = \frac{T_c \mu_i}{100} \right|_{T=T_o}$$

Second, estimate the slope (partial derivative) of μ_L or μ_{rod} for the value of μ_i at a temperature of interest; often that will be room temperature. Below, μ_L is shown, but μ_{rod} may be substituted.

$$\frac{\partial \mu_L}{\partial \mu_i} \approx \frac{\mu_L(\mu_i(T_o) + \delta) - \mu_L(\mu_i(T_o) - \delta)}{2\delta}$$

where δ is a small number such as $0.01\mu_i(T_o)$ as suggested above. Then get the relative temperature coefficient in percent per deg C by combining the two results above which are shown in brackets below:

$$\alpha_L(T) \approx \frac{100}{\mu_L(\mu_i(T))} \left[\frac{\partial \mu_L}{\partial \mu_i(T)} \right] \left[\frac{\partial \mu_i(T)}{\partial T} \right]$$

where μ_{rod} may be substituted for μ_L if desired.

More Examples

Let's modify the above example to use Amidon 61-Material with $\mu_i = 125$ at room temperature and $\alpha_i = 0.1\%/C$, keeping the rod dimensions the same. Skipping the details (an exercise left to the reader), we find that

$$\alpha_L = 0.0431\%/C$$

Even though the ferrite temperature coefficient is less by a factor of 7:1, after reducing μ_i from 2000 to 125, the coefficient is still larger than in the previous example.

If the rod aspect ratio is reduced from 15:1 to 8:1, keeping everything else the same, the coefficient drops to

$$\alpha_L = 0.0231\%/C$$

Big Picture

The above examples demonstrate that two things in particular drive the temperature sensitivity higher: lower values of μ_i and larger rod aspect ratios. But of course, for best performance the desire is usually for large aspect ratios, and the choice of μ_i is often pushed lower than we'd otherwise like by ferrite losses. Understanding this issue helps in making the best trade offs for fix-tuned designs.

Overall Tuning Accuracy

So far, the analysis has ignored some additional important factors which must also be considered in a practical design.

- Ferrite permeability and capacitance values will not be exact and some additional allowance for component tolerances is necessary. For high-Q designs, hand tuning of each loop may be necessary.
- Coil windings may have variability from coil to coil and should be considered.
- Temperature dependence of capacitors used to resonate the loop must be considered. In many cases this will not be a significant issue.

For variable tuned designs, these considerations do not come into play as long as means are provided for tuning the loop to resonance at each frequency of interest.

Materials for AM Broadcast

For the frequency range from 500 to 1700kHz, the ferrite materials which have the highest initial permeability *and* acceptable levels of loss up to about 2MHz are the 61 ($\mu_i = 125$) and 52 ($\mu_i = 600$) materials, both of NiZn composition. Only rods made from 61 Material seem to be readily available in 2019. Estimated maximum Q values are plotted for three different L/D ratios for both materials in figures 7.14 and 7.15. These plots reflect only ferrite losses.

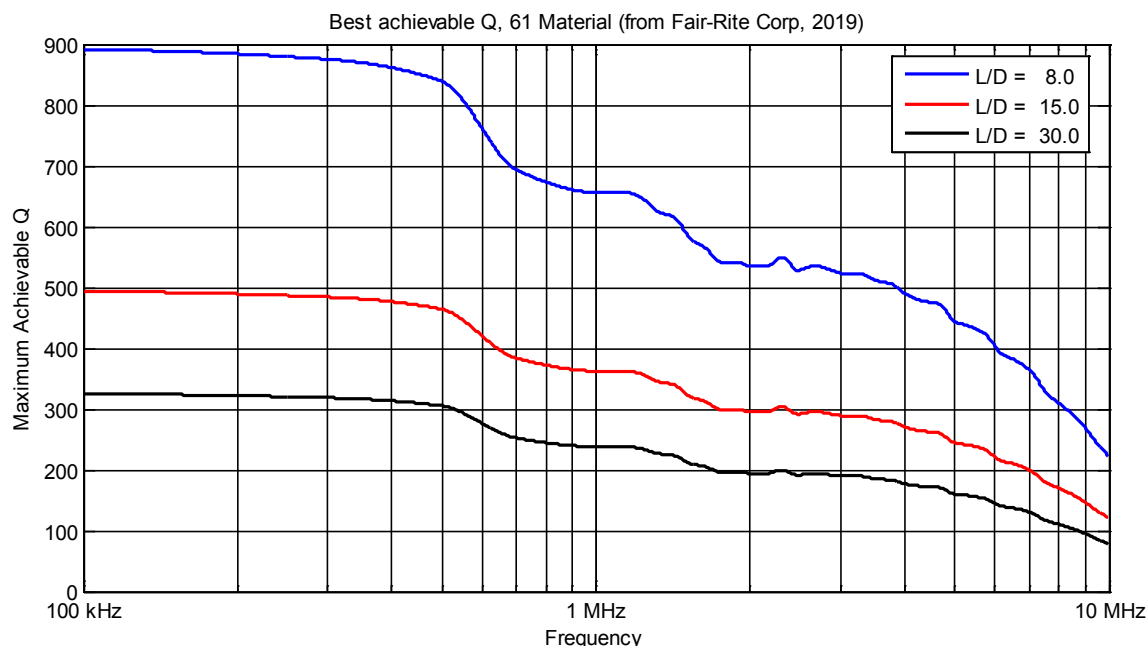


Figure 7.14: Ferrite 61 Material Q factor

The other effect of varying μ_{rod} is on effective height. The largest commonly available rods are about one-half inch in diameter (12mm). The longest such rods reasonably priced are 7.5 inches long (L/D=15). One vendor offers a 7.5-inch rod for \$24US in 2019. They are also the only vendor which seems to offer a 12-inch rod (L/D=24) for about \$100, which represents a large increase in the cost per linear inch.

As the L/D ratio is increased without limit, μ_{rod} will eventually become equal to μ_i . Since in the end, antenna effective height varies linearly with μ_{rod} , it is useful to plot the ratio μ_{rod}/μ_i in decibels.

Figure 7.16 gives a good feeling for the point of diminishing returns as L/D ratio is increased with 61 material. L/D ratios of commonly available rods, or series combinations thereof are marked on the X-axis. Compare for example the difference between half-inch diameter rods with lengths of four and 7.5 inches – it is about 5dB and this is a significant difference. Likewise, compare one 7.5 inch rod to two of them joined

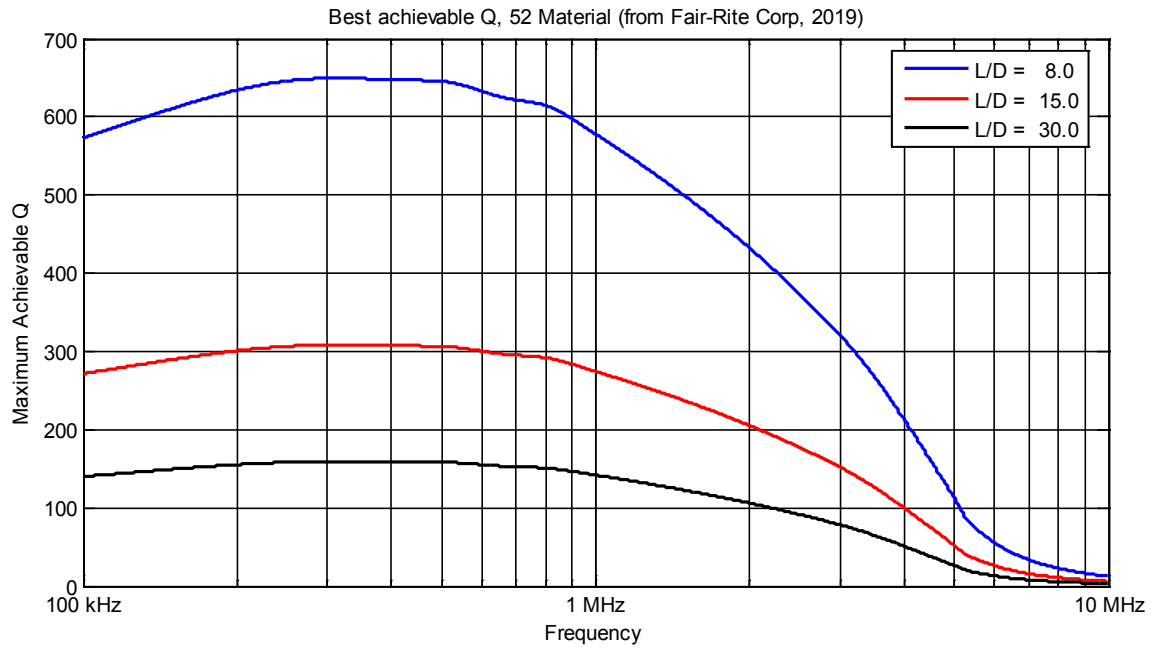


Figure 7.15: Ferrite 52 Material Q factor

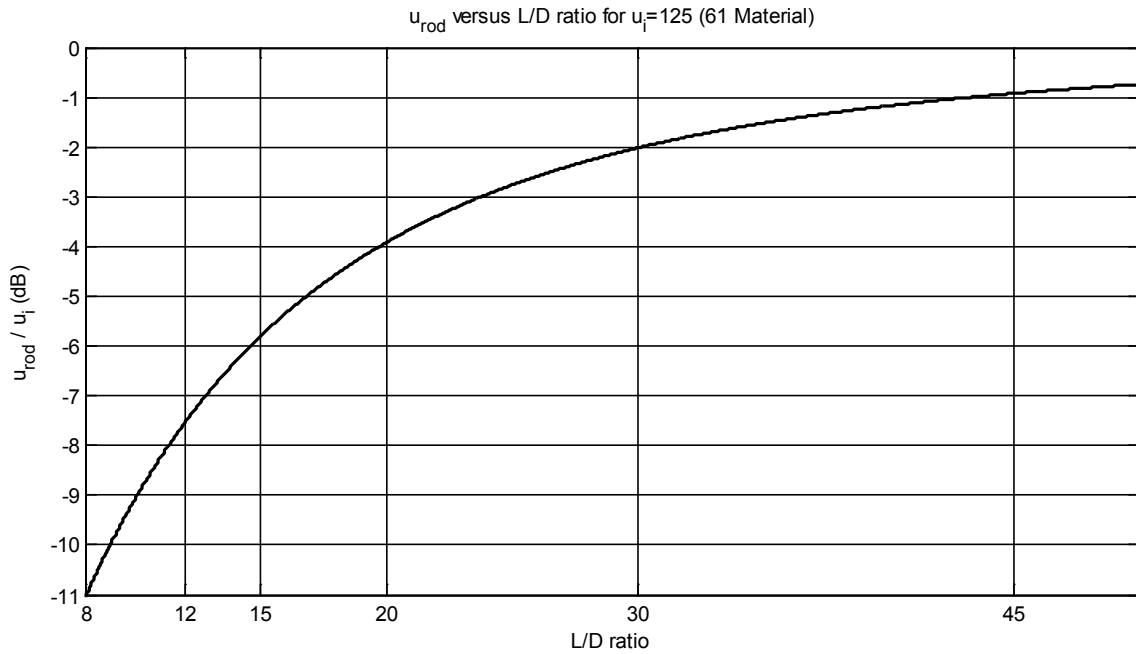


Figure 7.16: Ferrite 61 Material effect of L/D ratio

tightly in series (L/D ratios of 15 versus 30). This is almost a 4dB difference and also significant. However, stacking three rods in series (L/D 45) only yields another

1dB improvement in the limit. These benefits come at the cost of reduced Q-factor and that may in some cases be the limiting factor.

If ferrite losses are low enough, it may be desirable to design an antenna with two long ferrite rods stacked in series. This can end up being quite long – e.g. about 15 inches for half-inch diameter rods, but the alternative is going to be an air core loop of perhaps an 8-inch diameter.

To get the most out of stacking rods, the ends must be in intimate contact with each other to minimize any air gaps. Even a slight gap, just a fraction of a millimeter must be avoided. Experiments have not been performed on methods to implement this idea. It may be necessary to lap rod ends for a perfect fit, and it is not known whether attempting to bond them together with some sort of glue would create an unacceptable gap.

Optimum Aspect Ratio

A useful question to answer is this: Given a fixed volume of ferrite to be fashioned into a rod, what aspect ratio will give the largest effective height? It is assumed that the coil will be wound to obtain a fixed target inductance.

A simulation was run for this scenario, with the volume of ferrite defined as that within a 12 x 700mm rod. Diameters between 12 and 25mm were examined to determine the resulting non-resonant effective height of a ferrite rod antenna. For each diameter, the number of wire turns required for a $350\mu\text{H}$ inductance (with a 1.8mm winding pitch) was determined, and used to compute h_e .

The most interesting result is that the largest value of h_e is achieved with the smallest diameter rod, and highest aspect ratio.

One conclusion is that given a small number of ferrite rods (e.g. 3-5), how best to arrange them for effective height? The answer seems to be stacking them in series, rather than forming a larger diameter bundle. This goes with earlier caveats that effectively stacking rods may require very small gaps between rods, especially where higher permeability is concerned.

The simulation in this case had to consider aspect ratios as large as 58:1, and that's really out of the valid range for some of the calculations, so for aspect ratios more than 30-40, take this with a grain of salt.

Optimum Coil Length

Effective height is improved by a larger turn count, but at some point the inductance becomes too large, or SRF too small. Often the largest manageable inductance value is chosen to maximize sensitivity.

In these cases, maximizing the coil length by increasing the winding pitch may result in a slight gain in effective height. Longer coils will need more turns to achieve

the same inductance, and that has a positive effect on h_e . However, longer coils also have a smaller value of F_{ext} and this lowers the resulting effective height. The net result however is that the added turn count usually wins out over reduced F_{ext} values so there's a slight advantage to longer coils.

There is one caveat however. Increased turn count required for longer coils will increase wire resistance and since we're comparing coils with a constant inductance, the Q will be smaller. This will not be a problem if the Q is higher than necessary, as it will need to be lowered anyway. A good example is an antenna for AM broadcast. The largest usable Q may be in the range of 50-200 due to the bandwidth of AM signals. Here, a coil tight-wound with Litz wire may have a Q of 500 or more, and a longer coil still provides adequate Q.

As a case in point, consider a 10mm diameter by 200mm long ferrite rod with $\mu_i = 250$. Taking a target inductance of $350\mu\text{H}$, we computed the turn counts required to achieve this inductance for a number of coil lengths between 40 and 190mm. The value of F_{ext} was also computed for each coil length. Based on the equation for effective height,

$$h_e = \beta An\mu_{rod}F_{ext} ,$$

and the fact that β and rod area are constant for each design, the performance different choices of coil length can be compared by examining the product of turn count and F_{ext} . The answer varies depending on the specific antenna design.

Applications which need to maximize Q may not benefit from increased coil length. Here, the output voltage when the loop is resonated will drop if Q is lowered. A good example is a 60kHz antenna for WWVB which has a very narrow bandwidth. Higher Q in this case results in larger output voltage from the loop, up to a limit determined by receiver input impedance. In this situation, a longer coil with more turns has three effects, more output due to more turns, and reduced output due to both F_{ext} and Q dropping. Now the two declining tendencies will typically win out against the increased turn count and a longer coil may not be helpful.

Estimating the Q of ferrite core loops is beyond the scope of this article, and test coils may need to be built to quantify the trade-offs presented here.

In summary, there can be some benefit to longer coils, depending on requirements, ferrite material and antenna geometry. Where Q must be limited, this benefit is more significant with lower permeability ferrite materials, and larger rod aspect ratios. At best, the improvement will be 2dB or so, but each case needs to be examined to determine the exact numbers.

Chapter 8

Ferrite Sleeve Loops



Figure 8.1: Example of Ferrite Sleeve Loop Antenna for MW band

A relatively new and popular antenna design uses a large number of ferrite rods arranged as shown in figure 8.1. These are often called *ferrite sleeve loops* or FSLs for short. A lot of qualitative praise is given to such antenna designs, but there is a dearth of quantitative measurement, or theoretical analysis on the topic.

This chapter develops methods to predict effective heights, and validates these methods with comparative measurements of air core and FSL antennas.

The chapter on loop antenna output coupling is relevant here, as many FSL designs use magnetic coupling to the internal antenna of a portable receiver and the result is a double-tuned transformer.

Analysis

FSL antennas are mostly air-cored with a relatively thin ferrite sleeve upon which the coil is wound. The theory and formulas presented so far apply to solid ferrite rods and that will be a good place to start. To make things a bit simpler at first, it's assumed there are no gaps between individual ferrite rods and that they form a solid sleeve.

Replacing the sleeve with a solid ferrite rod having the same outside dimensions would be expected to improve the performance. Figure 8.2 shows the difference between a solid rod and the ferrite sleeve. This is a useful first step in the analysis as methods have already been developed to estimate the effective height of the antenna using a solid rod.

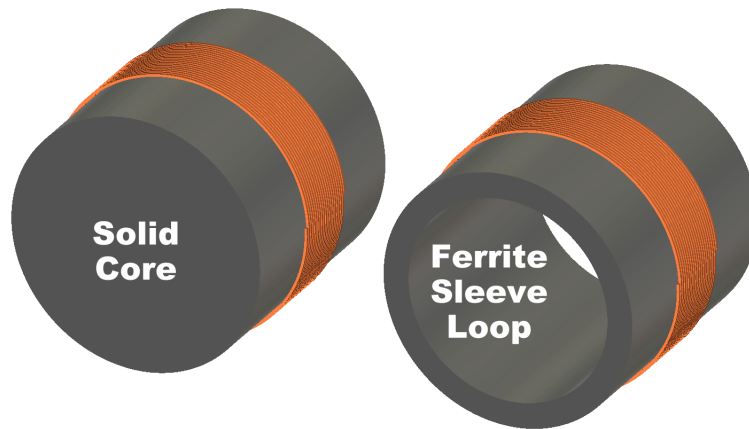


Figure 8.2: Solid rod versus ferrite sleeve

The example design considered here (figure 8.1) uses 36 rods, each with a 10x11mm rectangular cross section and 140mm long. The outside diameter of the sleeve is 147mm, and the rods have a specified permeability of $\mu_i = 800$. The sleeve is inserted into a 20-turn coil wound on a 168mm diameter form.

Consider an antenna using a solid ferrite rod with the same outer dimensions as the sleeve – 147mm in diameter and 140mm long. This is a big, fat, stubby rod, and its aspect ratio is tiny, $140/147 \approx 0.95$.

The value of μ_{rod} can be obtained from figure 7.4, but will be easier using figure 7.6, which is another view of figure 7.4, zoomed in on small aspect ratios. In this case, with a ratio of 0.95, the graph reveals that initial permeability, μ_i , has little effect on μ_{rod} .

For the solid rod version of the antenna in figure 8.1, we've determined that $\mu_{rod} \approx 4.2$, but what exactly does this mean? It's time for a....

Reality Check

Wait. Hold the iPhone. We're talking about μ_{rod} values of a whopping 4.2 here. A typical single rod design for MW would have a μ_{rod} value of 50 or more. This bears repeating.

Using a solid 5-3/4-inch diameter, 5-1/2 inch long ferrite core to build a loop antenna will only increase the output voltage by a factor of 4.2 (about 12dB), compared to an air core.

And the true benefit isn't even really *that* big. Without the ferrite core it would require more turns in the coil to get the same inductance, and that would reduce the effective benefit. On top of that, the coil is often wound on a form that's significantly larger in diameter than the ferrite sleeve, so the air core version picks up a bit more signal due to the increase diameter as well.

For the antenna in figure 8.1, it was necessary to increase the turn count 50% to get the same inductance with the sleeve removed, and the coil form is 168mm diameter compared to the sleeve diameter of 147mm. In total, there is a 50% increase in effective height due to added coil turns, plus a 31% gain in area from the increased diameter, $(168/147)^2 \approx 1.31$. This is a total gain of $1.31 \times 1.50 \approx 2.0$ or 6dB, so the net difference between the FSL and air core antennas is $4.2/2.0$, roughly a 2:1 difference.

The Root Cause

While the ferrite sleeve does increase the effective height, the actual improvement seems small, and you may be wondering why the benefit isn't larger. Well, it's the ferrite rod's aspect ratio (l/d) of 0.95 that kills the effective permeability – go back and have a look at figure 7.6.

In a typical, ferrite core MW antenna, the aspect ratio is usually at least 8-10 or so, and here it is only 0.95. To increase μ_{rod} from 3.9 up to a more respectable 25, we would need $l/d = 5$ so that solid ferrite core would need to be 29 inches long.

With the solid rod, computations for the non-resonant effective height at 1MHz look like this:

$$h_e = \beta An \mu_{ext} = \frac{2\pi \times 10^6}{3 \times 10^8} \frac{\pi}{4} \times 0.147^2 \times 20 \times 4.2 \approx 0.030\text{m}$$

With the ferrite sleeve removed, and a 30-turn coil on the 168mm coil form,

$$h_e = \beta An = \frac{2\pi \times 10^6}{3 \times 10^8} \frac{\pi}{4} \times 0.168^2 \times 30 \approx 0.014\text{m}$$

The effective height of 30mm is roughly twice the 14mm height that would result from removing the solid core and adding ten more turns to the coil.

From Rod to Sleeve

So in reality it's not quite as bad as all that. Solid 147mm diameter ferrite rods aren't available, and they wouldn't be affordable even if you could find one. Not to mention that it would weigh about 24 pounds. So, let's hollow out the center of the rod, leaving behind only a thin sleeve. This can be approximated by a plethora of small rods laid out in a circular pattern, as in figures 8.1 and 8.5.

Removing material from the center of the solid ferrite core would be expected to reduce μ_{rod} , but the question is: by how much? This was investigated with several E-M computer simulations. The reduction in μ_{rod} resulting from removal of some percentage of the ferrite core area depends on both the l/d ratio and the value of μ_{rod} for the solid rod. In general we find that the lower μ_{rod} is with a solid core, the more material can be removed without reducing the permeability too much.

Figure 8.3 below shows this effect in two different ways. The x-axis on the two graphs is the percentage of original core area remaining after we hog out the middle. This is based on simulations for ferrite with $\mu_i = 125$. Because this effect depends on the solid core's aspect ratio, there are separate curves plotted for cores with l/d ratios of 0.8, 1, 2, 4 and 10.

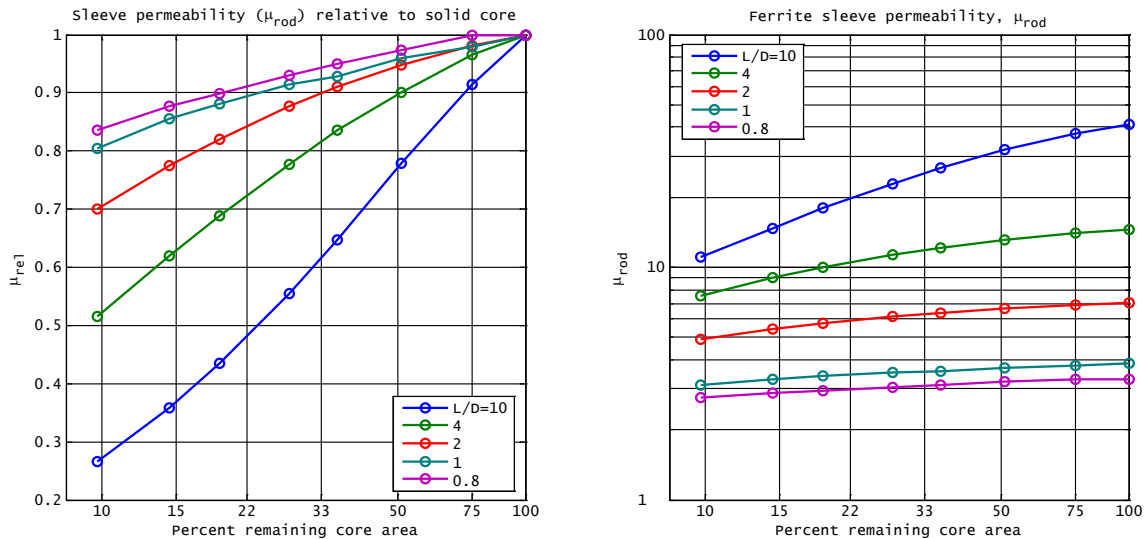


Figure 8.3: Ferrite Sleeve Permeability

The left side of figure 8.3, shows the reduction in permeability compared to a completely solid ferrite rod. The smaller the l/d ratio, the less effect there is if some of the core is hollowed out. This suggests that small l/d ratios are good.

However, the graph on the right side of figure 8.3, showing absolute permeability values reveals that small l/d ratios have smaller values of μ_{rod} to begin with. It's not as helpful that you can hollow out the rod without losing much more. You already gave away the farm by choosing a small l/d ratio.

For the example antenna, the percent of remaining core area works out to about 27%, which results in $\mu_{sleeve} \approx 3.9$ for an initial permeability of five hundred¹. This reduces the effective height from 30mm (solid rod) to 28mm (ferrite sleeve). Indeed, not much performance has been lost by removing 73% of the ferrite from the core of the solid rod.

Estimating μ_{rod} , aka μ_{sleeve}

The terms μ_{rod} and μ_{sleeve} are used interchangeably in this article, and μ_{sleeve} is sometimes used to make it clear that it refers to a sleeve, not a solid rod. However, μ_{rod} may be used to refer to a sleeve or solid rod depending on the context.

One way to estimate this value is to use figures 7.6 in combination with the left side of figure 8.3. The two values obtained from those charts would be multiplied together to come up with μ_{sleeve} . The other approach is to use the results of E-M simulations we ran, which are attached to this document along with Matlab/Octave scripts to interpolate them.

In both cases, the expression for the fraction of core material remaining in the sleeve compared to a solid rod of radius r and diameter d is given by

$$A_{rem} = \frac{r^2 - r_i^2}{r^2} = 1 - \left(\frac{r_i}{r}\right)^2 = 1 - \left(\frac{d_i}{d}\right)^2 \quad (8.1)$$

where r_i, d_i are the radius or diameter at the inside edge of the sleeve.

The value of μ_{rod} for the ferrite sleeve is a function of three variables: μ_i , the aspect ratio and A_{rem} . As with the prediction of μ_{rod} for solid rods, an empirical approach was taken and a large number of E-M simulations (about 2,200 in fact) were run to create a data set of apparent permeability (μ_{rod}) covering a 3-dimensional grid of values of μ_i , aspect ratio and A_{rem} . This data set may then be interpolated using various algorithms.

Similar to the situation with solid rods, it's felt the best set of independent variables for interpolation is the logarithms of μ_i , aspect ratio and A_{rem} , and the logarithm of μ_{rod} as the dependent variable. In other words, we take the natural logarithm of the output and all input variables and interpolate using that data, instead of the raw values.

$$M \equiv \ln \hat{\mu}_{sleeve} = f \left(\ln \mu_i, \ln \frac{l_f}{d_f}, \ln A_{rem} \right) \text{ and then } \hat{\mu}_{sleeve} = e^M$$

¹Although the ferrite used had a specified permeability of 800, we suspect it is actually lower due to shock and vibration in shipping, perhaps in the range of 300-500, and that value was used in this calculation.

Rod and Bar compensation

So far, it's been assumed the ferrite sleeve is solid. Typically, the sleeve is comprised of either small diameter rods, or flat bars arranged on a large diameter circle. Some allowance should be made for the fact that there's less ferrite in this kind of construction than there would be in a solid sleeve.

The appendix discusses this compensation in more detail. The gist of it is to assume a sleeve for estimating purposes which has the same average diameter as the actual construction, but the thickness is reduced so the cross sectional area of the solid sleeve and actual sleeve are the same.

What about F_{ext} ?

Axial field simulation data for solid rods is of unknown applicability to ferrite sleeves. It certainly won't be exactly correct and it's not known how much error would be introduced by using it. However, since F_{ext} is usually pretty close to one for rods with small aspect ratios, we can probably just set $F_{ext} = 1$ for typical ferrite sleeves. The bottom line however, is that this was not investigated with simulations, and any use of solid-rod data for estimating F_{ext} of ferrite sleeves would be pure guesswork.

Inductance

Fully characterizing the μ_L parameter that was defined for solid rods in [osengr-1] would require a huge number of simulations covering a 4-D parameter space: μ_i , sleeve aspect ratio, sleeve thickness and coil length. This has not been attempted.

The value of μ_{sleeve} computed for the sleeve antenna could be used as a starting point for predicting inductance, or computing a turn count. The accuracy of that is unknown, so just wind the coil and measure it. Then adjust the turn count and/or spacing as necessary to get the desired inductance.

In general, μ_L is significantly smaller for full length coils. Actual values of μ_L computed from inductance measurements on two test antennas ($\mu_{sleeve}=3.9$) are $\mu_L=2.3$ for a 110mm long coil, and $\mu_L=4.3$ for a 13mm long coil.

Optimum Coil Length

A few simulation runs show that even for aspect ratios as small as 0.6, the inductance factor can be half as much for a full length coil compared to a very short one. By that we mean the wire turns are spaced such that the coil occupies the entire length of the ferrite sleeve.

However, F_{ext} remains close to one for all coil lengths. This suggests that about 40% more turns of wire could be used if spaced out over the full length of the sleeve,

without adding more inductance. Because F_{ext} remains close to one, effective height would be improved by about 40% or 3dB by doing this.

The longer length of wire might result in reduced resonant Q which could cancel the gain due to more turns. However, this would only be the case if wire resistance is the determining factor for Q. Some experimentation would be required to figure this out.

Resonant Q

When loops are wound with solid (or stranded) wire, adding a ferrite sleeve may result in a large increase in resonant Q and therefore effective height. This difference seems to be much less or non-existent when loops are wound with Litz wire, and this reduces potential benefits of the FSL version of the antenna. A Litz wire upgrade probably costs less than the ferrite rods, and adds little weight to the design. There's still a gain due to the ferrite sleeve, but as discussed above, this can be offset with more turns on the air-core coil, and/or a somewhat larger diameter.

To determine the net benefit of higher Q, the effect of losses in resonating capacitors, and loading by the receiver must also be accounted for. Depending on these additional losses, the actual net benefit may be close to, or much less than the improvement in unloaded resonant Q.

Output Coupling

The preceding analysis assumes the output is directly coupled to a receiver. That's often not the case, and the FSL antenna is magnetically coupled to the internal ferrite antenna of a portable or tabletop radio. The chapter on output coupling deals with this scenario and it is fully applicable here, so refer to that chapter for more detail on magnetically coupled designs.

Designs which use magnetic coupling will see an improvement equal to the square root of the Q ratio. For example, quadrupling the Q of the tuned loop (keeping all else constant) will increase the signal strength seen by the receiver by a factor of $\sqrt{4} = 2$.

Analysis Procedure

To summarize the preceding material, here's a step-by-step procedure for estimating the non-resonant effective height of an FSL antenna design.

- If not known, assume a value for μ_i . 125 is a good choice for MW band ferrites. A higher value might be appropriate for LF and VLF designs. Otherwise, use the known value.

- Determine the true cross sectional area of the ferrite in the sleeve. Then, using the average diameter of the sleeve material, determine the thickness of a solid sleeve that would have the same cross sectional area. This gives the effective OD and ID of a solid sleeve for computational purposes.
- Compute the sleeve aspect ratio which is the length divided by the adjusted outside diameter from the previous step.
- Compute μ_{rod} (aka μ_{sleeve} for ferrite sleeves) by interpolating the simulation data set. The simulation data, and sample Matlab/Octave scripts attached to the PDF form of this document should be used.
- Dealer's choice. Either set F_{ext} to one, or use the estimate of μ_{rod} to compute F_{ext} using the simulation data for a solid rod. Neither of these is technically correct, but for small aspect ratios, using a value of one will not be too far off the mark.
- Compute effective height using the formula below.

$$h_e = \beta \frac{\pi}{4} d^2 n \mu_{rod} F_{ext}$$

An Aside

This section may be skipped without any loss of continuity. The computation of μ_{rod} using (7.3) and (7.8) through (7.12) can be a bit tiresome if a math-oriented computer application is not available. To save some effort and expose an interesting relationship, we can linearize the result of those equations for a single value of μ_i (e.g. $\mu_i = 125$). This approximation covers three different ranges of aspect ratio and results in no more than a 0.5dB error compared to the full equations.

$$\mu_{rod} \approx a \left(\frac{l}{d} \right) + b$$

$$\mu_{rod} \approx 2.7946(l/d) + 1.0903 \Big|_{0.1 \leq l/d \leq 1.4}$$

$$\mu_{rod} \approx 3.6139(l/d) - 0.1602 \Big|_{1.25 \leq l/d \leq 4}$$

$$\mu_{rod} \approx 3.0555(l/d) + 0.8535 \Big|_{0.4 \leq l/d \leq 2.2}$$

Ignoring the additional reduction in μ_i due to the sleeve being hollowed out², an interesting simplification results. Substituting this into the effective height equation above gives

²The reduction is minimal for small aspect ratios.

$$h_e = \mu_{rod} F_{ext} \beta \frac{\pi}{4} d^2 n \approx \beta \frac{\pi}{4} F_{ext} n (ald + bd^2)$$

Let's assume that F_{ext} doesn't vary much (it doesn't for small l/d) and set it to one. Also, keep the aspect ratio within the range of a single linear approximation.

$$h_e \approx \beta \frac{\pi}{4} n (ald + bd^2)$$

Furthermore, if we assume either that ($ald \gg bd^2$) or equivalently ($al \gg bd$), then

$$h_e \approx \beta \frac{\pi}{4} n (ald + bd^2) \approx \beta \frac{\pi}{4} n al \Big|_{al \gg bd}$$

Under all of these constraints, effective height is proportional to the product of the ferrite sleeve's length and diameter and the coil turn count. The reason this is worked out here is that one experimenter (DeBock) discovered this rough dependence on the length-diameter product, and invented a score for FSL designs which is the ferrite rod or bar length in mm multiplied by the outside diameter of the sleeve construction in inches. The score did not include coil turn count, and it's possible that variations in antenna diameters (the bd^2 term) was compensated for by smaller turn counts being required for larger diameters.

Air Core Equivalents

Based on the simulations we ran, the FSL design shown at the beginning of this chapter (figure 8.1) has a non-resonant effective height of 28mm at 1MHz and the coil form outside diameter is 168mm (6.6 inches).

The following air core designs compare favorably in non-resonant effective height. Heights listed below are computed at 1MHz, and the height ratio compared to the FSL design will be the same at other frequencies.

- A 254mm (10 inch) diameter loop with 29 turns of wire on 2.7mm pitch has $h_e = 31$ mm. Approximate inductance would be $300\mu\text{H}$ and an SRF in the range of 7-8MHz.
- A 220mm (8.7-inch) diameter loop with 38 turns of wire on 3.7mm pitch has $h_e = 30$ mm. It would have an inductance of about $290\mu\text{H}$ and SRF in the range of 3.5-4MHz. With the wide winding pitch, Litz wire might not be required.
- A 185mm (7.3-inch) diameter loop with 43 turns of wire on a 3.3mm pitch would have the same coil length as the original sleeve (140mm) and the same coil diameter. SRF is again in the 4-5MHz range. The inductance would be about $280\mu\text{H}$ with $h_e = 24.3$ mm – 1.2dB less than the FSL antenna.

This demonstrates that adding ferrite rods to the antenna as a sleeve does improve performance, but the small sleeve aspect ratios typically encountered limit these designs to a modest reduction in size over an equivalent air core coil.

Since μ_{rod} (for a solid rod) can be looked at as a gain term, we can generate a plot of best possible gain due to a ferrite sleeve versus its aspect ratio, as seen in figure 8.4. The vertical axis there is $20 \log_{10}(\mu_{rod})$. In published designs, the largest aspect ratio we see is about 2.3, but it's typically much smaller.

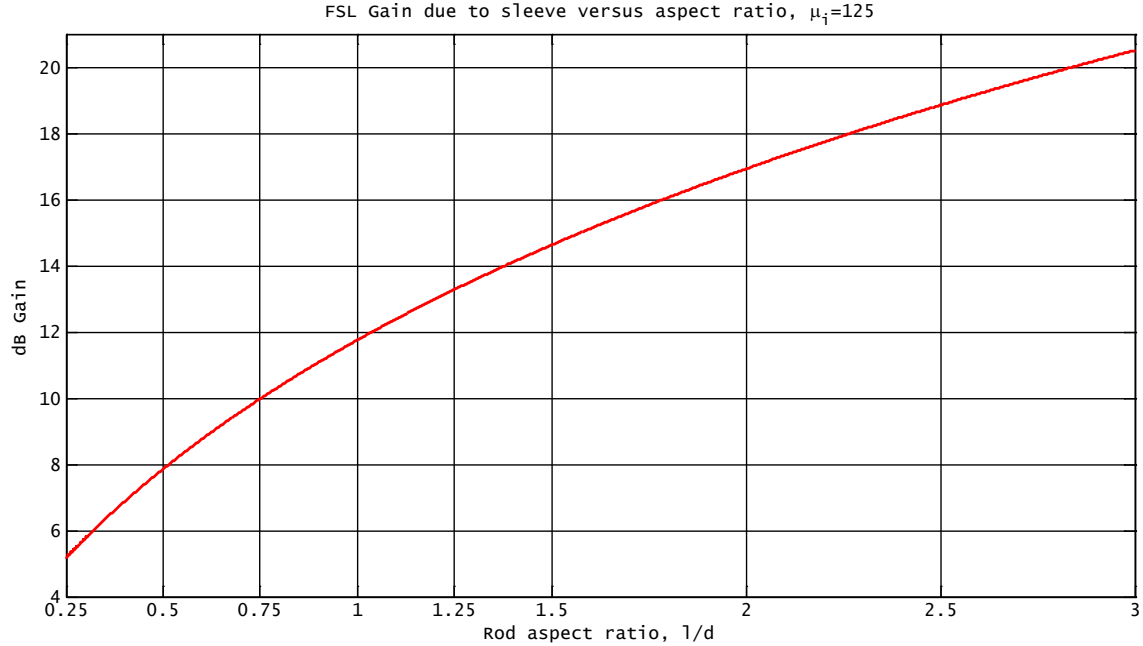


Figure 8.4: Effective sleeve gain vs aspect ratio

Comparisons Between Loops

Here is a proposed performance factor which may predict the relative performance of two different resonant external, magnetically coupled loops – assuming the receiver can be located for critical coupling with each loop.

$$\frac{h_{e1}}{h_{e2}} \sqrt{\frac{Q_1}{Q_2}}$$

The subscripts {1,2} refer to the two external loops being compared.

Experimental Verification

To test the validity of the above results, signal voltages produced by two FSL test antennas were measured and compared to voltages from several air core loops. Up until recently, the cost of purchasing enough ferrite rods for this purpose was prohibitive. After much searching, an affordable source of ferrite rods was found, which has allowed some experimental verification of predicted effective heights at 60kHz and 560kHz.

Tests performed at 60kHz used a custom receiver with a known input impedance. At 560kHz, antennas were connected directly to the input of the Si473x receiver IC in a Tecsun PL380 portable radio. These tests are less well controlled, since resistive losses at the receiver input are variable (managed by firmware in the radio IC) and unknown³. Steps were taken to mitigate this issue as described below.

The ferrite sleeve and the three test coils are depicted in figure 8.5. The two coils on the right side are wound on 6-inch PVC pipe sections in which the ferrite sleeve may be installed, while a third coil (air core only) is wound on a 10-inch (254mm) fiberglass form.

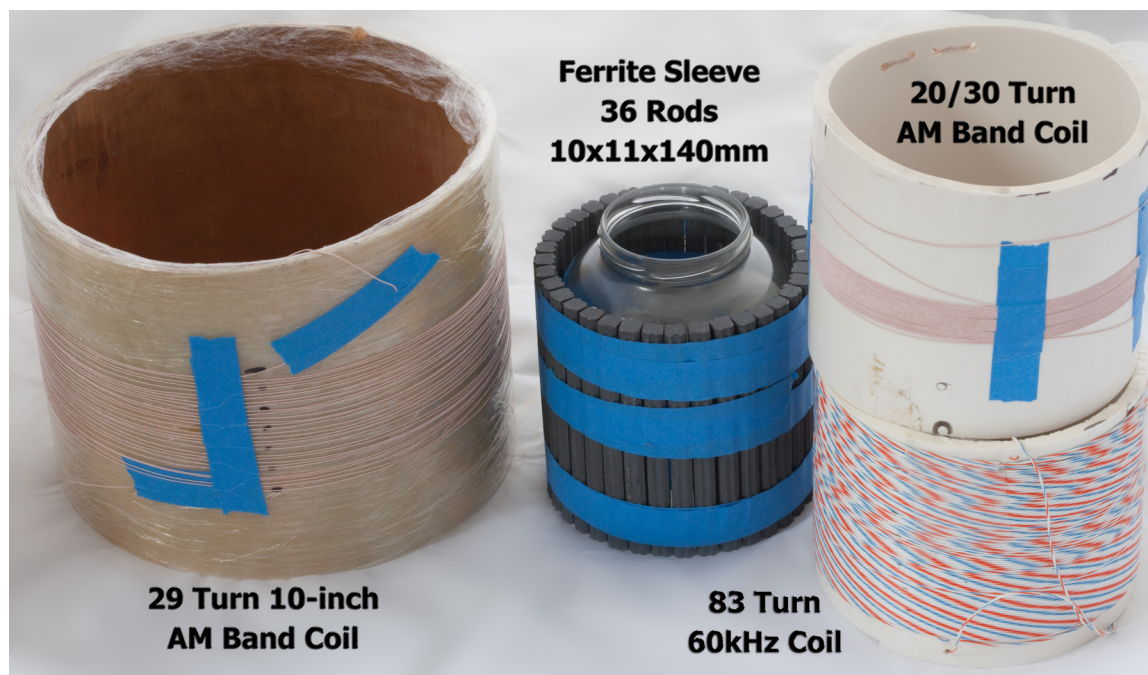


Figure 8.5: Ferrite sleeve and coils used in testing

³See the SiLabs Si473x datasheet for details on radio-managed input resistance.

The Ferrite Sleeve

A ferrite sleeve was constructed using 36 12x140mm rods. These were affixed on the outside of a glass jar, with a resulting outer diameter (147mm) that fits easily inside the 6-inch PVC pipe sections (152mm inside diameter) used as coil forms. This setup allows the ferrite to be easily inserted and removed during testing.

For computing μ_{sleeve} , the effective mean diameter of the sleeve was set equal to the physical mean diameter. The effective thickness was adjusted to account for the sleeve cross section not being fully filled with ferrite. That yielded an effective OD of 145.7mm and an ID of 126.3mm. Assuming $\mu_i=800$, we computed $\mu_{sleeve}=3.96$, and that was used in computing the effective height of the FSL antenna.

60kHz Tests

These tests used an 83-turn coil close wound on the 6-inch PVC pipe section, with PVC-insulated, stranded 22 AWG wire (lower right coil in figure 8.5).

The coil was resonated at 60kHz using low-loss polypropylene capacitors. Series resistance was added to each 60kHz antenna, lowering the loaded Q to 50; this makes resonance tuning less critical and eliminates differences in Q from the results. As a result, the difference in received signal strength should depend only on the ratio of non-resonant effective heights.

A large 32-inch octagonal loop with a resonant effective height of 4.33m was also compared; this antenna's resonant Q was not lowered 50, as it had been carefully tuned.

The custom receiver adjusts internal gains (AGC) to produce a fixed baseband output voltage, and is therefore an indication of received signal strength. Tests were performed at mid day, when the incoming signal from WWVB is fairly constant, with these results:

Parameter	Air Core	FSL	Large Octagon
Computed h_e	116mm	350mm	4330mm
Rx AGC Gain	40.78dB	31.28dB	10.28dB
FSL vs air core	$\Delta h_e = 9.53\text{dB}$	$\Delta \text{AGC} = 9.50\text{dB}$	
FSL vs octagon	$\Delta h_e = 21.92\text{dB}$	$\Delta \text{AGC} = 21.00\text{dB}$	

The difference between predicted and measured values is only 0.03dB comparing the coil with and w/o the sleeve, and 0.92dB comparing the FSL and large octagon antennas. The variable gain circuitry in the receiver has a typical linearity specification of $\pm 0.5\text{dB}$ ($\pm 2\text{dB}$ maximum). This test provides a reasonable confirmation of the theory presented above.

AM Broadcast Band Tests

Two different air-core antennas were compared to the FSL test antenna at 560kHz. Litz wire containing 47 strands of 40AWG enameled wire was used to wind a 20-turn coil directly adjacent to a 10-turn coil, which could be connected in series to form a 30-turn coil. This coil was wound on a 6-inch PVC pipe section, which allows the ferrite sleeve core to be inserted and removed, without otherwise disturbing the experimental setup. A second air core antenna was wound on a 10-inch form, designed to have the same non-resonant effective height as the FSL antenna. These three coils are pictured in figure 8.5.

- 20-turn loop on 168mm PVC form, with ferrite sleeve installed.
- 30-turn loop on 168mm PVC form, w/o sleeve.
- 29-turn loop on 254mm fiberglass form (air core).

Due to the unknown behavior of the receiver input impedance, a strategy likely to remove this uncontrolled parameter was devised. It was reasoned that if each antenna presented the same impedance to the receiver, and very strong signals were avoided, then the receiver would present the same tuned input impedance to each antenna.

Differences in Q were removed from the experiment by adding series resistors to bring all coils down to a Q of 100. The table below shows measured parameters for each of the three antennas, at the test frequency of 560kHz⁴. R_q is the series resistance which reduces the Q at 560kHz to 100. Thick film surface mount resistors (0805 size) were used.

Core	Coil Dia	Turns	L, μ H	Q	R_q, Ω	h_e
Air	168mm	30	297	381	7.9	7.8mm
Ferrite Sleeve	168mm	20	310	468	9.1	15.1mm
Air	254mm	29	300	324	7.5	17.2mm

Test Results

Receiving a local station of moderate strength at 560kHz yielded these results:

Parameter	FSL	6.6-inch air core	10-inch air core
RSSI	61dB	56dB	61 to 62dB
RSSI relative to FSL	0dB	-6dB	+0 to +1dB
h_e relative to FSL	0dB	-5.8dB	+1.1dB

This data agrees with predicted values of non-resonant h_e within ± 1 dB. The most convincing comparison is with the 10-inch air core loop. Not only does this antenna

⁴Measured with LCR meter from 10kHz to 2MHz in 1,2,4,10 sequence. The value at 560kHz is derived from an RLC model fit to the measured data

present the same impedance to the receiver, but it theoretically also presents the same signal voltage (within 1dB). So, even if the receiver is varying the input losses as a function of signal strength, that should not be a factor in comparing the FSL and 10-inch air core antennas.

Capacitive Noise Pickup

We attempted to ascertain the susceptibility to electrical noise of the FSL antenna and the 10-inch air-core equivalent. Both antennas were operated inside a building where electric noise from 120V 60Hz wiring is significant. Although in some cases, it seemed like the FSL antenna might be picking up less electric field noise, the results were far from conclusive and repeatable.

When operated outside, at least 30 feet away from electrical noise sources (e.g. buried power lines), there was no perceptible difference in noise levels between the two antennas.

Signal Nulling Capability

Another often discussed performance parameter is the depth of nulls in the antenna pattern. We attempted to compare the FSL and air core antennas in this respect, but were unable to reach a conclusion. The depth of nulls seems quite sensitive to the antenna's immediate surroundings, especially metallic objects. In a range of different situations, we found no consistency in which antenna had deeper nulls. Values ranging from 20-40dB were found with both antennas, as a function of antenna placement, and frequency.

FSL Test Summary

Tests at both 60kHz and at 560kHz showed that measured differences agreed with predicted values within ± 1 dB. This is reasonable evidence to conclude that the analysis presented in this chapter is correct.

Published Examples of FSL Antennas

DeBock published an article [DeBock-1] which compares the performance of eight different FSL antennas using magnetic coupling to a portable receiver. We added two more designs to the list, one 2-inch FSL made with flat ferrite bars, and a monster 17-inch design using 10x200mm rods.

Each antenna's effective height was both simulated and calculated using the procedures defined in this chapter. Figure 8.6 shows the results, and compares simulated to estimated heights as well as a modified DeBock score (see below). OD values are

in inches. Rod/bar dimensions and effective heights are in millimeters. This odd mix of units was chosen to match DeBock’s scoring algorithm.

FSL Design Name	Rod/Bar Size	Count	Sleeve		Coil		Effective Ht		Modified
			OD	Turns	Sim	Calc	Debock		
3-inch Micro	Rod 8 x 65	27	3.00	36	11.38	11.95	17.00		
3.5-inch Long John	Rod 10 x 200	23	3.50	27	28.81	29.64	24.77		
5-inch Short-rod	Rod 8 x 65	47	5.00	30	18.73	19.08	19.00		
5-inch Ultra Light	Rod 8 x 140	45	5.00	26	28.48	29.27	24.77		
7-inch AM-Band	Rod 8 x 140	64	7.00	20	32.61	33.24	29.08		
17-inch DXpedition	Rod 10 x 200	129	17.00	10	66.04	67.05	66.31		
3-inch Bar	Bar 3x20x100	10	3.25	42	18.93	21.19	19.00		
5-inch Bar	Bar 3x20x100	17	5.00	33	25.16	27.48	21.69		
7-inch Bar	Bar 3x20x100	25	7.00	23	27.39	29.39	24.77		
3-inch PL-380 Model	Bar 3x20x100	8	2.24	36	11.00	12.64	17.45		

Figure 8.6: Partial calculation data for rod-based FSLs.

DeBock in [DeBock-1] compared eight of these designs and proposed a score to rate their performance. If that score is divided by 65 and 14 is added to it, there’s a good correlation between that and the effective heights (both simulated and estimated). Figure 8.7 shows how the estimated heights, and modified DeBock scores compare to the simulated heights, which are shown in decibels relative to one millimeter.

Although not mentioned in his report, we believe there’s an unstated detail in DeBock’s comparisons that the coil turn count in each design was selected to give approximately the same self inductance. This places a further constraint on the test designs, and it would appear this aids in making those scores agree well with effective height values. Clearly, one could add or remove turns from the coil in any given design, changing the effective height but not the DeBock score, as that only depends on the ferrite sleeve’s length and diameter.

A Smaller FSL Design

The smaller 2-inch FSL that was analyzed above is shown in figure 8.8. It’s built with eight flat eight ferrite bars, 3mm thick and 100mm long arranged with a 50mm (2-inch) ID and 56.8mm OD.

\$1,000 FSL Design

The monster 17-inch design included in the analysis above is pictured in figure 8.9. The ferrite sleeve has an OD of 420mm, ID of 400mm, and uses 129 10x200mm ferrite rods.

This air-core design should be equivalent to 17-inch FSL monster: A 19-inch diameter loop with 19 turns spaced out to 150mm total length would occupy the same volume as the 17-inch FSL design and have a non-resonant effective height of 65mm – compared to 66mm for the FSL antenna. There would be a large savings in both weight and cost with the air core antenna.

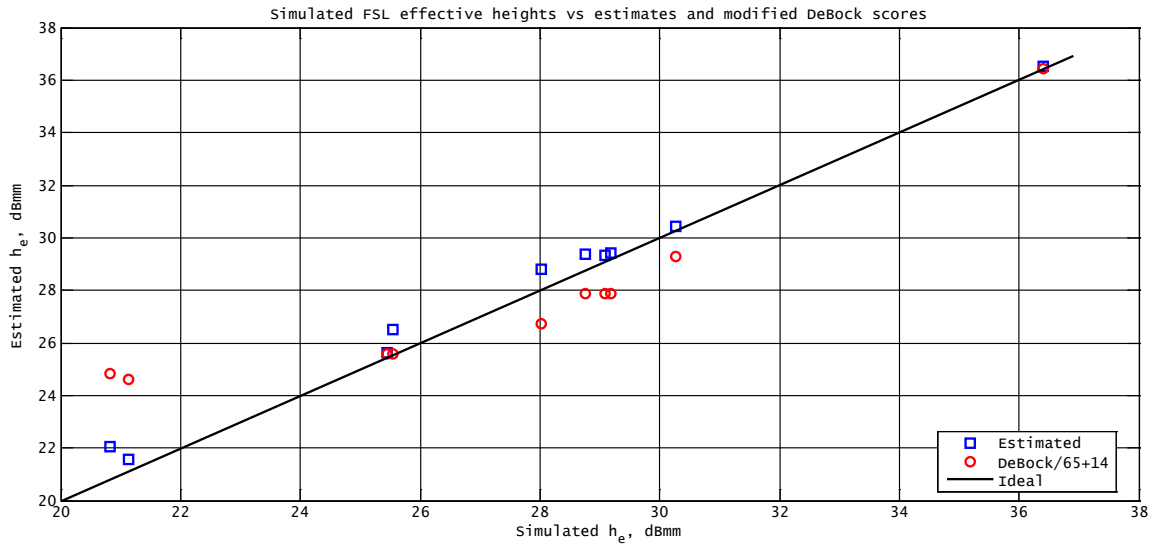


Figure 8.7: Simulated heights vs estimates and DeBock scores



Figure 8.8: 2-inch FSL using flat ferrite bars

FSL Simulation Details

The eight designs analyzed in [DeBock-1] are built with 660/46 Litz wire (OD of 56 mils) closely spaced. We didn't want to simulate the full turn count, but did want to get the coil lengths right, so simulations used 28-mil solid octagonal wire spaced 112 mils apart and half the number of turns. Simulated heights were then compensated by doubling the induced voltage, to make up for the difference in turn count.

A 100 mil gap was assumed between ferrite form and coil. The use of solid wire in the simulations will not effect the non-resonant effective height, but it would be important for AC resistance and Q estimates.

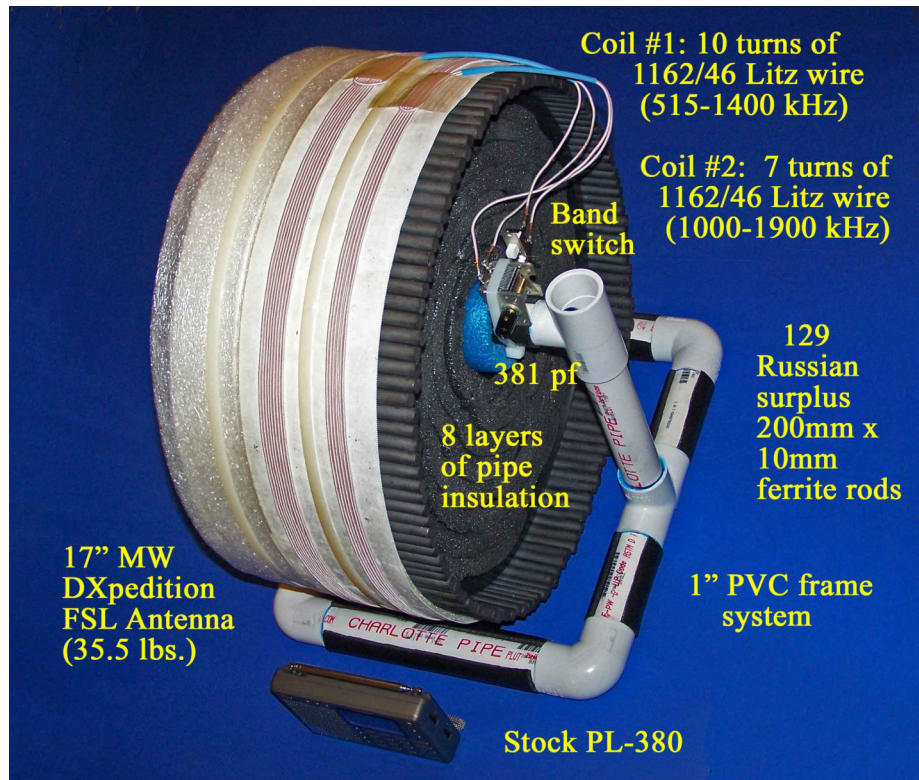


Figure 8.9: \$1000 FSL antenna

Unknowns

Although there is good correlation between estimated effective heights and most of DeBock's performance rankings, there are some uncontrolled experimental variables that add an unknown amount of uncertainty.

- Simulated and estimated values are non-resonant height comparisons.
- Experiments used double-tuned magnetic coupling, with an unknown coupling coefficient.
- The effective Q of each loop tested is unknown.
- It's not known if the FSL diameters listed in the report are actual OD values for the sleeve, approximate numbers, or measurement of some other value such as coil diameter. It is assumed they are sleeve OD values.

It can be claimed that the estimating techniques proposed herein compare well with simulation results. The same cannot be said for the apparent correlation between DeBock's results due to the uncertainties listed above.

Comments on Published FSL Performance

There are several published examples of good performance obtained using FSL antennas. One in particular that stands out are many reports of trips to some cliff-side pullouts off Highway 101 just north of Manzanita, Oregon. Apparently, this is a location where MW signals from New Zealand and the South Pacific area can be frequently received. There are many reports of FSL antennas being used with good results in this location. The problem is, there don't seem to be any reports of comparisons with different antennas (preferably air-core loops) with known design parameters. As such, it is very difficult to conclude anything about the performance of FSL antennas compared to air core loops from these trip reports.

There are also comments about FSL antennas being less noise sensitive, but there's so little quantitative information available about this that it's hard to say much about it here. Our experiments did not provide conclusive evidence of differences in electrical noise pickup between air core and FSL antennas.

If the issue is capacitive pickup of electric field noise, this might make some sense. A larger loop with more wire will have a larger capacitive coupling to such noise sources, unless the antenna is balanced and common mode rejection in the receiver is adequate.

It is entirely feasible for a more sensitive loop to produce a larger RSSI value, but due to the capacitive pickup of E-field noise, the signal can sound significantly worse, when compared to a smaller loop. Although the smaller loop provides less signal to the receiver, if the capacitive noise pickup is less, the smaller loop will "sound better", even though it has a smaller h_e . This kind of information is very important in evaluating antenna performance.

Suggestions for Experimenters

- Some portable radios (like the Tecsun PL-380 and PL-606) have digital signal strength readouts. Use them! Don't just rely on qualitative judgments of signal reception. While it's useful to describe results qualitatively, write down the signal strength and SNR numbers too. Pay more attention to the signal strength, but the SNR values may also give clues about loop tuning, bandwidth, and common mode noise rejection.
- Don't limit experiments to very weak stations. Measure some stronger stations which don't overload the receiver to get some solid RSSI values. These may be more repeatable than with weak signals.
- Record as much data as possible about the loop, including measured inductance and Q values.
- Try to verify whether critical coupling is achieved. This would be evidenced

by the RSSI value reaching a peak and then dropping again as the receiver is slowly moved closer to the external loop.

- After critical coupling is achieved, re-tune the external loop to resonance and move the receiver off frequency then back. That will ensure everything is tuned to resonance in case the loop coupling has shifted the previously tuned resonance.
- Place each loop in the same location for testing if at all possible, or at least swap locations between loops and re-run the tests to be sure that the location isn't having a significant effect.
- Electrical noise can be very squirrely. When encountered, it may help to experiment with small changes in antenna location and orientation; sometimes moving the loop a few inches or feet, or re-arranging lead wires can make a big difference.

External loops with very high Qs will have very narrow bandwidths. For example, a loop Q of 400 at 1MHz has a total bandwidth of 4kHz – which is a 2kHz one-sided bandwidth. This is narrow enough that it can start to filter out some of the high frequency noise in the demodulated audio and may give the impression of clearer reception. It will have much less effect on the total power received however, which is another reason to record RSSI numbers when available.

FSL Summary

This chapter has attempted to provide some much needed analysis of the workings of FSL antennas. Real world tests provide some confidence that the analysis is accurate.

While in some cases, FSL designs can provide higher values of resonant loop Q (and therefore effective height), there are other ways to achieve that (e.g. Litz wire) without the ferrite sleeve.

In the end, we're not all that enthused about Ferrite Sleeve Loop antennas. It would seem that the reduction in size allowed by the ferrite sleeve is not all that great, and the extra cost and weight are substantial compared to an air core loop.

This conclusion does not consider differences that may exist in the antenna patterns – the ability of the antenna to null-out unwanted signals. Nor does it consider the issue of electrical noise pickup. Our limited testing was unable to reach a conclusion about differences in these behaviors.

Again, this is our opinion and it's based on this analysis and a small number of actual tests which seem to support the analysis. We hope others find this information useful for designing FSL antennas, or for deciding whether to build one of these beasts.

Other Ferritic Schemes

There are several ways in which multiple ferrite rods may be arranged to increase an antenna's effective height. Here we discuss a few of those techniques that may be worth experimenting with.

Linear Stacks

Placing rods end-to-end increases the aspect ratio, and therefore the value of μ_{rod} . If air gaps are kept small enough this can be an effective means of improving performance.

Keep in mind however, that as μ_{rod} increases, so does the effect of ferrite losses on maximum achievable resonant Q. Depending on the situation there can be a point of diminishing returns due to this. Furthermore, as the length increases without bound, μ_{rod} will not exceed μ_i , and this another thing to watch. Using rods with the largest workable value of μ_i and acceptable losses can help in this case.

Fat Stacks

In addition to simply stacking rods end-to-end, it may be advantageous to arrange multiple rods in a bundle parallel to each other, then stack several of these bundles end-to-end⁵. This is effectively a larger diameter rod, and stacking bundles end-to-end keeps the aspect ratio reasonably large.

Rod bundles may be organized in the shape of a polygon. A triangle produces an effect approximately identical to that of a rod with three times the cross-sectional area, and $\sqrt{3}$ times the diameter of an individual rod. Stacking two such structures would give an effective aspect ratio about 15% larger than that of a single rod. Three bundles stacked would have an aspect ratio 73% larger.

A hexagonal arrangement can be made with seven rods – one in the middle and six around the periphery. This has seven times the area and $\sqrt{7}$ times the effective diameter as a single rod. Stacking three such structures in series would have an effective aspect ratio about 13% larger than a single rod, and a stack of five would have an 89% larger aspect ratio.

60kHz Fat Stack Experiment

Ferrite rods with a roughly rectangular cross section, 10x11mm were arranged in bundles of four. Three of these bundles were stacked end-to-end and a Litz wire winding of 115 turns was wound over the center rod. This antenna is pictured in figure 8.10.

⁵See here for example: <http://sarmiento.eng.br/Loop.Ferrite.Rod.Antenna.htm>

The non-resonant effective height works out to 6.1mm. We ran out of Litz wire here, and the inductance measured was 2.77mH. If an additional 6 turns of wire were added to reach 3mH inductance, the effective height would be 6.4mm – only 0.8dB less than the comparable FSL design. Although the pictured fat stack has a higher Q, the FSL’s Q could be made comparable by using Litz wire instead of the stranded wire pictured.

Later, more Litz wire was added, bringing the turn count up to 180, and a theoretical non-resonant $h_e=9.5\text{mm}$.

Tests were done, comparing this to the previously described 83-turn FSL design, and to a large 32-inch octagon antenna. The results came out within 2dB of the expected signal strength in all cases, with the difference likely being due to air gaps between bundles in the stack.

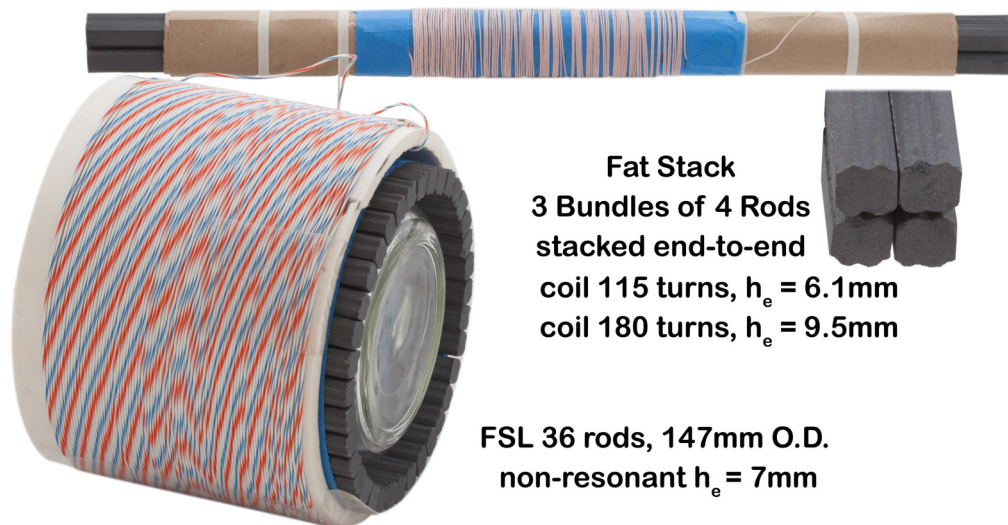


Figure 8.10: Equivalent FSL and Fat Stack antennas

In this experiment, roughly the same effective height was achieved with fewer rods (12 versus 36) when arranged as a fat stack instead of an FSL, and a larger value with 180 turns. Also, note that the fat stack uses considerably less wire – about 40 feet for 121 turns and 60 feet for 180 turns, versus 140 feet for the FSL. As a result, it may also be possible to use smaller gauge Litz wire in the fat stack to achieve a targeted value of Q.

While both of these antennas are capable of achieving resonant Q’s well over 200, such high values make tuning very sensitive and may present problems with temperature dependence of permeability in the ferrite. This problem will be worse with the fat stack design. In either case, it may be necessary to implement some form of automatic tuning in the receiver if Q’s much above 200 are to be effectively implemented.

The larger aspect ratio of the fat stack also means that ferrite losses will have more effect on overall resonant Q. This may rule out the use of some ferrite materials that would be acceptable in the FSL design.

Independent Combinations

There's another way we can think of to improve on the performance of a single rod ferrite loop antenna. It has already been discussed that attempting to stack rods end to end in hopes of increasing μ_{rod} requires the joints to have very small gaps, and yields limited benefit if the component rods have high aspect ratios.

What if the rods are stacked end to end, but with intentional large gaps instead, essentially making them independent? Each rod gets its own coil and they are all connected in series. If four rods are used, each coil would need to have one fourth of the total inductance, and therefore half as many turns. As a result each coil would produce one half the output of the original coil, but there are four coils, so total output would be doubled – a 6dB improvement. All the wiring would need to be short in terms of a wavelength, and this is certainly the case here.

For m stacked rods, the turn count is reduced by \sqrt{m} and the output of each single rod is multiplied by m , so the overall gain is \sqrt{m} , or $(10 \log m)$ in decibels.

How large does the gap between rods need to be to avoid interactions between rods? It might depend on both μ_i and the rod aspect ratio. If neighboring rods enhanced each others' fields, it would increase the inductance, requiring less than half the turn count in each rod's coil. This would eat into the benefit.

We examined two typical cases, the most likely being the stacking of cheap Ukraine/Russian 10x200mm rods with $\mu_i = 400$. The other case, which is much less likely due to the cost, is with 0.5x7.5 inch rods with $\mu_i = 125$. These are US made and cost about \$30US each, whereas four of the cheap rods may be had for \$10 to \$20US.

Stacked 10 x 200mm Rods, $\mu_i = 400$

Simulations of three stacked rods show that a gap of one half rod length (100mm) between rods resulted in only a 0.15 dB increase of flux in the middle of the center rod, and induced voltage in a one-turn coil centered on the rod. The total length for a 4-rod stacking would be 1100mm (a bit over 43 inches).

Working out a full example shows that the non-resonant effective height of a single rod (7.5mm) design can be doubled to 15mm by this technique.

Stacked $1/2$ x $7^{1/2}$ inch Rods, $\mu_i = 125$

Here a spacing of $1/2$ rod length also appears workable, with a total 4-rod stack length of just over 41 inches. This also keeps the field enhancement by neighboring rods to less than 0.2dB.

Perspective

The main advantage to a scheme like this is that it retains the line geometry of the ferrite antenna – albeit producing a much longer line. On the other hand, it doesn't require all that large of an air core design to equal the performance – but without the line geometry, the antenna takes up a much larger volume. This is only true only if the stacked rod antenna doesn't need space to rotate.

In the above example with four 10 x 200mm rods, an antenna with the same effective height can be built with an air core only nine inches in diameter. The bottom line is that the value of a line geometry has to be quite high for this to make sense in any given application.

The takeaway is that there's no free lunch here. Ferrite rods are useful in some situations, but they aren't magic bullets that can perform antenna miracles.

More Ideas

The rods don't have to be stacked in line with each other. A side-by-side arrangement would also work, with rods arranged either linearly, or in some kind of 2-dimensional pattern. Four rods side by side in the pattern of a square is one such example. But now, the array takes up as much or more volume as an equivalent air core loop.

It would be possible to gain 1:1 per rod (i.e. $20 \log m$) if a low-noise amplifier is connected to each rod plus a summing amplifier for the group. And each rod would need to be individually tuned to the proper frequency if a resonant antenna is being built. Here, four rods would yield a 12dB gain over a single rod. That's a lot of cost and effort to save a little space.

Chapter 9

Design Strategies

This chapter presents a variety of approaches for designing electrically small loop antennas. It's unpolished and unfinished. For now, this is mostly just a collection of disconnected and incomplete ideas, presented in the hope that some of them may be useful.

For a stand-alone design, some steps that can be taken up front are as follows:

1. Determine expected signal strength, bandwidth and atmospheric noise levels.
2. Determine overall receiver bandwidth required to keep atmospheric noise level to acceptable levels.
3. Determine required or provided receiver input voltage and impedance.

Sometimes, the goal is different – to improve upon an existing antenna. Steps in this case could be:

1. Measure or estimate parameters of the existing antenna, and from those make an estimate of the resonant or non-resonant effective height.
2. Decide how much improvement is needed.
3. Work out parameters of an antenna that has the desired effective height.

Comparing Two Loops

Consider the formula for resonant h_e with possible inclusion of a ferrite core:

$$h_e = \beta A n \mu_{rod} F_{ext} Q$$

If the antenna is air-cored, then the values of μ_{rod} and F_{ext} can be set to one. Under the presumption that the two antennas are being compared at the same frequency, the ratio of effective heights is

$$\frac{h_{e1}}{h_{e2}} = \frac{A_1}{A_2} \frac{n_1}{n_2} \frac{Q_1}{Q_2} \frac{\mu_{rod1}}{\mu_{rod2}} \frac{F_{ext1}}{F_{ext2}}$$

This shows that for any antenna (air or ferrite-cored) there are three levers for adjusting effective height, the diameter (and area), coil turn count and resonant Q. Where ferrite is involved, rod parameters offer more levers – diameter and length plus intrinsic permeability. Keeping these factors in mind can be useful during the design process.

Non-resonant Loops

This is perhaps the most straightforward type of design task. One way to start is by assuming a fixed length of wire and looking at how h_e varies with either the turn count, or loop radius. These relationships between wire length, turn count, area and diameter or radius may be substituted into the formula for effective height. These three relationships are:

$$n = \frac{l_w}{2\pi r}, \quad r = \frac{l_w}{2\pi n}, \quad A = \frac{l_w^2}{4\pi n^2}$$

First, height may be expressed as a function of wire length and turn count:

$$h_e = \beta A n = \frac{\beta l_w^2}{4\pi n}$$

Then as a function of wire length and loop radius, but with the realization that only certain discrete values of radii will result in an integer turn count,

$$h_e = \beta A n = \frac{\beta \pi r^2 l_w}{2\pi r} = \frac{\beta r l_w}{2}$$

With a fixed length of wire then, effective height varies directly with radius, and inversely with turn count.

In some cases (e.g. AM broadcast band loops), problems with self resonance may end up limiting the amount of wire that can be used. In other cases (e.g. 60kHz loops) this won't often be a concern.

For inductance calculations, a fixed length of wire, l_w , can be specified for the loop, and along with the winding pitch, additional relationships can be specified.

$$l = np = \frac{l_w p}{2\pi r}, \quad \frac{l}{d} = \frac{l_w p}{4\pi r^2}, \quad \text{and} \quad r n^2 = \frac{l_w^2}{4\pi^2 r}$$

Substituting these into one of the above formulas, we can write inductance as a function of radius, winding length and pitch.

$$L = L(r, l_w, p)$$

There's no attempt to actually work out that expression here. Rather, this idea may be of use in developing design software to find inductance based on these inputs, or to find one of the three inputs based on a desired inductance and the other two inputs.

Resonant Loops

This gets a bit more complicate because the Q and bandwidth of the loop now enter the picture. This treatment covers loop construction using solid (or stranded) wire. Litz wire is generally not used in air core loops due to cost, but the reader can infer the effects from discussion below given that Litz wire is much less susceptible to proximity effect.

Parameter Interactions

Understanding how parameters effect each other is helpful in coming up with an acceptable design.

Winding Pitch

Winding pitch has a big effect on self-inductance. Larger pitch values mean less inductance. The effect is roughly linear with the logarithm of pitch. Doubling the pitch will reduce inductance numerically by the same amount, for any initial pitch value.

Increasing winding pitch values above some threshold – typically 2-½ to 3 wire diameters – will not change the AC resistance (and losses) very much. Since at resonance, $Q = \omega L / R_{ac}$, increasing pitch above this threshold reduces both inductance and Q.

Decreasing pitch below the above threshold results in rapidly increasing AC resistance due to proximity effect. Increased losses are enough that they can completely offset the increase in inductance and we find that below some optimum pitch value, Q begins dropping. For resonant designs which attempt to maximize Q, the optimum pitch value is of great interest as long as the resulting Q is not so large as to be problematic for tuning.

These calculations must also take into account additional loading on the loop – resonating capacitor losses and receiver input impedance. At some point, the Q of the loop alone can exceed other system losses, making further increases pointless.

Parameter Scans

The above expressions are approximate and working them out can get tedious. A more general approach which is potentially more accurate is to use some Matlab/Octave

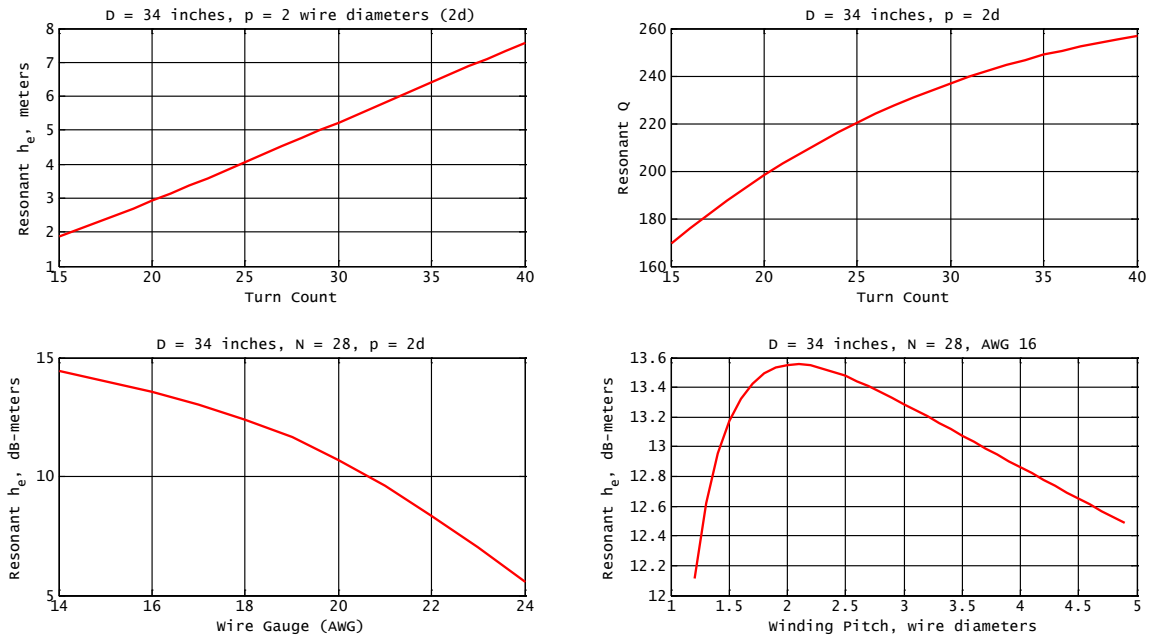


Figure 9.1: Example of parameters scans for 60kHz loop design

scripts to examine loop performance over a range of different parameter values. These calculations can take into account just about all relevant characteristics: inductance, copper losses and load impedance as functions of various parameters. Such a function is provided with in the zip file attached to this PDF document, for designs using solid or stranded copper wire.

The list of input parameters includes operating frequency, loop diameter, turn count, wire gauge, winding pitch, capacitor dissipation factor and load impedance (e.g. receiver input). These parameters can be fixed, or can be a list of different values to examine. From the inputs, the following are determined: inductance, DC and AC resistance, resonating capacitance, self resonant frequency, resonant Q and effective height. Also produced are estimates of thermal noise in the resonant bandwidth, both as a voltage and equivalent E-field strength.

Figure 9.1 shows four different parameter scans generated by the analysis tool. For all of these graphs, the following parameters were held constant:

$$f=60\text{kHz}, \text{ diameter } D=34 \text{ inches}, \text{ capacitor } DF=0.001, \text{ load impedance}=2M\Omega$$

The top two graphs show the variation of resonant effective height and Q with turn count with 16 gauge wire and winding pitch of two wire diameters. The bottom two graphs use a fixed turn count and vary the wire gauge (bottom left) and winding pitch (bottom right). Heights can be shown in linear units as in the top two graphs, or in log units (dB-meters) as in the bottom two.

Again, as an example, the final design chosen might use 16 AWG wire with a 2 wire-diameter winding pitch and would have these characteristics:

D=34.0 in, N=28, 16 AWG wire, p=99 mil, Capacitor DF 0.0010
 Wire used=249 feet, L=1442uH, Rac=1.67 ohm, C=4879pF
 Q=231, he=4.8 m, Thermal noise Vn=0.9uV, En=0.2 uV/m

Equivalent Air and Ferrite Core Loops

Here's another possible method to design an air core loop. We start with a known ferrite loop and wish to build an air loop with larger effective height. The diameter of an air core loop whose effective height is g times the height of the ferrite loop can be derived as follows. Since there is at least one free parameter that must still be chosen, it is assume that a specified length of wire must be used in the air core loop.

$$gh_f = h_a$$

$$g\mu_o\mu_{ext}\omega A_f n_f = \mu_o\omega A_a n_a$$

$$g\mu_{ext}\pi D_f^2 n_f = \pi D_a^2 n_a$$

$$n_a = \frac{l_w}{\pi D_a}$$

$$g\mu_{ext}\pi D_f^2 n_f = D_a l_w$$

$$D_a = g \frac{\mu_{ext}\pi D_f^2 n_f}{l_w}$$

Take a ferrite loop with $\mu_{ext} = 60$, half inch diameter and 225 turns of wire. What diameter is required for an air core loop wound with 300 feet of wire which has ten times the height of the ferrite loop?

$$D_a = 10 \frac{60 \times \pi \times 0.5^2 \times 225}{12 \times 300} \approx 29.45 \text{ inch}$$

and the turn count will be

$$\frac{12 \times 300}{\pi \times 29.45} \approx 38.9$$

Effective Height vs Diameter

$$\begin{aligned}
 d &= \frac{l_w}{n\pi}, \quad n = \frac{l_w}{\pi d} \\
 A &= \frac{\pi}{4} \left(\frac{l_w}{n\pi} \right)^2 = \frac{l_w^2}{4\pi n^2} \\
 h_e &= \beta A n = \frac{\beta l_w^2}{4\pi n} \\
 &= \frac{\beta l_w^2}{4\pi} \frac{\pi d}{l_w} = \frac{\beta l_w d}{4}
 \end{aligned}$$

For a fixed turn count, height varies as wire length squared. For a fixed diameter, height varies as wire length.

Noise vs Loop Geometry

Thermal noise is not always the limiting factor, as atmospheric noise may be more of an issue, especially at lower frequencies. When thermal noise matters, it will be useful to have some expressions for signal-to-thermal noise ratio based on the geometry of the loop. Loop parameters determine effective height, and that determines the signal voltage induced in the loop, so it's just a matter of a few algebraic substitutions.

We'll refer to the external field strength with the suffix "s" for signal. The voltage induced by it is

$$e_s = E_s h_s = E_s \beta A_a n_a$$

The signal-to-thermal noise ratio can be worked out in terms of loop geometry as follows.

$$\begin{aligned}
 \frac{e_s}{e_n} &= \frac{E_s \beta A_a n_a}{\sqrt{8\pi k T B r n \rho}} = \frac{E_s \beta \pi r_a^2 n_a}{\sqrt{8\pi k T B r n_a \rho}} \\
 &= \frac{E_s \beta \sqrt{\pi}}{\sqrt{8k T B \rho}} r^{3/2} \sqrt{n} = \left(E_s \sqrt{\frac{\pi}{8k T B \rho}} \beta \right) r^{3/2} \sqrt{n} \\
 r^3 n &= \left(\frac{e_s}{e_n} \frac{1}{E_s \beta} \right)^2 \frac{8k T B \rho}{\pi} \tag{9.1}
 \end{aligned}$$

This result can be manipulated in several ways to suit the design process. We could for example, hold the parameters on the right hand side of (9.1) fixed which provides a relationship between loop radius and turn count.

In some cases, especially at MW and upper LF frequencies it is not difficult to design a multi-term loop which has a self-resonance frequency that is too low. One way to avoid this is by keeping the total length of wire less than 0.1 to 0.2 λ at the highest operating frequency. When the total length of wire in the loop is specified, it creates a relationship between radius and turn count:

$$n = \frac{l_w}{2\pi r}$$

which can be substituted into (9.1):

$$\frac{r^2 l_w}{2\pi} = \left(\frac{e_s}{e_n} \frac{1}{E_s \beta} \right)^2 \frac{8kTB\rho}{\pi}$$

$$r = \frac{e_s}{e_n} \frac{4}{E_s \beta} \sqrt{\frac{kTB\rho}{l_w}} \quad (9.2)$$

$$\frac{e_s}{e_n} = \frac{E_s \beta r}{4} \sqrt{\frac{l_w}{kTB\rho}} \quad (9.3)$$

These last two expressions are useful whenever the design process specifies a fixed length of wire. At room temperature (300K), equation (9.2) becomes

$$r \approx \frac{e_s}{e_n} \frac{257 \times 10^{-12}}{E_s \beta} \sqrt{\frac{B\rho}{l_w}}$$

For an example, let $f_o = 60\text{kHz}$, $E_s = 10\mu\text{V/m}$, $\rho = 0.05\Omega/\text{m}$ and $B = 500\text{Hz}$.

$$r \approx \frac{e_s}{e_n} \frac{0.102}{\sqrt{l_w}}$$

To achieve a 10:1 signal-to-noise ratio (SNR) with 64 meters of wire,

$$r \approx \frac{10 \times 0.102}{\sqrt{30}} \approx 0.128\text{m}$$

and

$$n = \frac{l_w}{2\pi r} \approx 79.5\text{turns}$$

Noise calculations, paired with effective height specifications can provide a large part of the information needed to nail down a particular loop design.

Given a total length of wire to be used, effective height can be quantified in terms of loop radius.

$$h_e = \beta A n = \beta \pi r^2 \frac{l_w}{2\pi r} = \frac{\beta l_w r}{2} \quad (9.4)$$

$$r = \frac{2}{\beta l_w} h_e \quad (9.5)$$

Continuing with the above example, at 60kHz with 60 meters of wire,

$$r \approx 25h_e, \quad \text{and} \quad h_e \approx \frac{r}{25} \quad \text{and} \quad n \approx 38 \text{ turns}$$

For example, if an effective height of 20mm is required, we get $r = 0.5\text{m}$. And since this is larger than the 0.128m radius required for a 10:1 SNR, it becomes the determining factor.

Now, if the desired h_e cannot be obtained with a reasonable loop radius, the only alternative is to increase the wire length, as long as SRF stays high enough. For example, setting $l_w = 150$ meters gives $r \approx 10.6h_e$.

Ferrite Materials

Ideally, a known ferrite material is chosen which has acceptable losses in the operating frequency range, and an acceptably high initial permeability, μ_i . In some cases, one or more ferrite rods of unknown material may be available, and it is desirable to determine the suitability of the rods for a given design.

One or more test coils may be wound on an unknown rod, then measured on an LCR or impedance meter. The impedance can give a rough idea of μ_i , which may help to narrow down the material. If the rod has a sufficiently high aspect ratio, loss measurements may also give some clues as to the material. On the other hand if the losses are acceptably low, that may be enough information to proceed with the design. Estimates of μ_i made this way can be used in estimating the effective height of a proposed design.

Be aware that winding a coil directly onto the rod with no spacer may result in a lower Q than is possible if there's a gap between the rod and coil. This might lead one to conclude a material is not usable when in fact a larger diameter coil might have acceptable losses with the same rod.

Chapter 10

Example Analyses

Here are a few examples of analyzing loop antennas. Tests were performed on the West coast of the U.S. References to sunrise and sunset may be at either the receiver (West coast) or transmitter site (Colorado).

60kHz Antennas

Analysis of five real-world 60kHz loop antennas is presented here. For the analysis to be valid, information from two different 60kHz receivers is considered.

- A 60kHz receiver module removed from an old atomic clock (Oregon Scientific brand). The module was wired up to an Arduino Uno and a decoding sketch was written for the experiment.
- A second, custom built receiver was also used with two of the antennas. This unit achieves balanced loop operation by connecting a center tap on the loop to RF ground. This architecture created issues with common mode resonance in the loop, so additional damping was required, but it can still achieve higher values of Q than possible with the 60kHz receiver module.

ITU atmospheric noise predicted at the antenna location has F_a in the range of 122-125dB at 60kHz during Winter nights and Summer afternoons respectively. Equation (4.2) predicts atmospheric noise in the range of $30\text{-}50\mu\text{V}/\text{m}$ for the large octagonal loop with a measured Q of 100.

The following antennas used in this experiment. The last two items were also tested with the second, custom-built receiver.

- The original loop with a very small ferrite rod (8 x 60mm). This antenna would only pull in WWVB at certain times of the day, and not even on every day.
- A 6-inch air core loop wound with 83 turns of 22AWG wire. A good signal was received for most of the day, but there were still periods with intermittent or no reception.

- A 14-by-20 inch rectangular air core design, close wound with 36 turns of 20AWG wire using a cardboard box as a form. This worked quite reliably and had good reception at nearly all times of the day with the exception of narrow 30-minute windows near sunrise and sunset.
- 40-inch octagonal loop with 24 turns of 20AWG wire. This worked even better but still lost the signal for short periods of time near sunrise and sunset.
- A ferrite antenna was made using 77-material. The original design had an SRF that was too low (around 300kHz) and suffered from low Q. More careful designs produced results with measured Q as high as 275.

Based on predicted loop performance, estimates of field strength based on a guess at receiver sensitivity are made. We suspect that the receiver module was similar to an MSA6180C which has a published sensitivity at the receiver terminals of $0.4\mu\text{V}$, and input impedance of $600\text{k}\Omega$. The Q for each loop is determined by this impedance value, and by losses in the resonating capacitor.

Another guess made in this analysis is that the published sensitivity value is actually the receiver's noise floor, so it's also assumed that a signal 20dB above that is required for solid reception. Therefore, the E-field sensitivities in figure 10.2 are found by dividing a sensitivity of $4\mu\text{V}$ by the resonant effective height.

Figure 10.1 shows measured inductance, and computed effective heights for these antennas. See below for more information on the entries for the 77 material loops, particularly in regards to circuit modeling of the loop.

The Q values are based on measured data for the coils, combined with loading by estimated capacitor losses ($\tan \delta = 0.07\%$) and the specified receiver input impedance of $600\text{k}\Omega$. For ferrite core antennas, μ_{rod} was estimated to come up with effective height. As such, the h_e values have more uncertainty.

Figure 10.2 shows thermal noise present in the resonant bandwidth, divided by non-resonant effective height, to allow direct comparison to E-field signal strengths.

The receiver module employs a 60kHz crystal to filter the incoming signal so the actual noise bandwidth is only a few Hertz, and thermal noise from any of these loops may not be a factor.

WWVB Field Strength Estimates

These tests were performed on the second floor of a residential building. With the 170mm loop, it was clear that man made noise was an issue as the exact location of the loop was critical. Even with careful placement, an unknown amount of this noise was present. This was not the case with the two larger loops, they could be placed just about anywhere and still get reliable reception.

Based on our estimate of receiver sensitivity, we conclude that the WWVB signal strength can drop below $5\text{-}10\mu\text{V}/\text{m}$ at times around sunrise and sunset, and at other times exceeds $40\text{-}50\mu\text{V}/\text{m}$ at the test location.

Coil	Core	L(μ H)	Q	Effective Height	
				Raw	Resonant
225T, 30AWG	52 material	2044	148	0.50 mm	0.074m
	8x60mm				
83T, 22AWG 36T, 20AWG 24T, 20AWG	Air	1023	144	2.3mm	0.33m
	170mm Dia				
	533x356mm				
	1.016m Octagon				
(Litz Wire)	77 material	3016	275	2.8mm	0.76m
189T, 24AWG	12.7 x 190mm				

Figure 10.1: Example loop particulars

Coil	Core	Thermal	Atmospheric	Sensitivity
		Noise	Noise	
		μ V/m	μ V/m	μ V/m
225T, 30AWG	52 material	13	38	48
	8x60mm			
83T, 22AWG 36T, 20AWG 24T, 20AWG	Air	2.1	39	11
	170mm Dia			
	533x356mm			
	1.016mm Octagon			
Litz wire	77 material	???	???	???
189T, 24AWG	12.7 x 190mm			

Figure 10.2: Example loop sensitivities

At the same time, predicted atmospheric noise levels in the range of 30-50 μ V/m suggest that sensitivity would be limited by it for many of the designs.

Although the data sheet for the receiver module leaves a fair bit of uncertainty in these numbers, this demonstrates how ballpark field strength estimates may be made without expensive instrumentation.

Results with Custom Built Calibrated Receiver

After the first edition of this article was published, a 60kHz BPSK receiver was built with fully calibrated RF and Baseband sections for further testing. The Q of the 40-inch octagon loop was measured in situ to be very close to 100 by externally exciting the loop.

Combined with the calculated non-resonant effective height, more accurate estimates of field strength were possible.

E-field estimates as high as 3mV/m were found on a few nights, and daytime

levels were fairly consistent running in the range of 300-500 μ V/m . Dropouts around sunset and sunrise could result in loss of signal for short durations in the range of 1-10 minutes or so. Loss of signal typically occurred below about 30 μ V/m which is considerably higher than the estimated receiver sensitivity level, and suggests that man-made interference and/or sferics may be involved.

77 Material

Amidon's 77-material is a high permeability MnZn ferrite. An antenna was built using this material and is included in the list above. After some failed designs which resulted in the SRF being too low, two successful designs were built. The difference is in the coils. The parameters common to both designs are shown in figure 10.3.

μ'_i	2000	μ''_i	100
Rod Length	190mm	Rod Diameter	12.7mm
μ_{rod}	113	Receiver Sensitivity	4 μ V
Capacitor tan δ	0.07%	Receiver Input	600k Ω
Coil wire	175/46 Litz (24ga equiv)	Wire Diameter	0.9mm

Figure 10.3: Parameters common to both 60kHz antenna designs

The coil for the first design is wound directly onto the bare rod and the turn count is limited by the need to keep the SRF above 600kHz or so. The data for that is shown in figure 10.4. The noise bandwidth and voltage calculations are based on the resonant loop bandwidth, and would not necessarily apply if the receiver has a smaller internal bandwidth. It is perhaps doubtful that the indicated value of resonant Q (383) could actually be achieved, and perhaps that should be treated as a theoretical maximum.

The second design's coil is wound on a larger diameter form, with about ¼ inch (6.35mm) of space between the coil and ferrite. A higher SRF resulting from the larger diameter permits a much larger turn count. This design has better overall sensitivity as shown in figure 10.5. However, because of the higher inductance and resonant Q, impedance at resonance is much higher and the receiver input impedance has more of an effect on resonant Q.

Although the larger coil has slightly better overall sensitivity (about 2dB worth), it is being limited by the receiver input impedance. If a custom preamp with high input impedance input (e.g. 100M Ω) were used, the parameters for the large diameter coil could theoretically look much better, as shown in figure 10.6. This change makes better use of the available Q and should have 8.7dB better sensitivity than the small diameter coil design. However, Q is so large with this design that tuning and stability will be problematic without some kind of automatic tuning.

Furthermore, actually achieving a value of Q this high would be challenging to say the least. In additional experiments with a custom preamp, we were able to achieve an Q value (measured in situ) of 275 versus a predicted value of 285. It would have

Coil Turns	104	Coil Length	160mm
Coil ID	12.7mm	SRF	700kHz
R_{DC} (calculated)	380 m Ω	R_{DC} (measured)	400 m Ω
L (calculated)	937 μ H	L (measured)	908 μ H
Coil Q (measured)	\approx 750	Equiv R	0.46 Ω
Resonated Q	492	Loaded Q	383
Noise bandwidth	245 Hz	Thermal noise e_n	1.9nV
E-field referenced e_n	1.2 μ V/m	Effective height h_e	1.5 mm
E-field receiver sens	6.8 μ V/m	Resonant h_e	590mm

Figure 10.4: 60kHz antenna with small diameter coil

Coil Turns	189	Coil Length	164mm
Coil ID	25.4mm	SRF	2MHz
R_{DC} (calculated)	1270 m Ω	R_{DC} (measured)	1323 m Ω
L (calculated)	3015.9 μ H	L (measured)	3016.6 μ H
Coil Q (measured)	\approx 960	Equiv R	1.17 Ω
Resonated Q	576	Loaded Q	275
Noise bandwidth	342 Hz	Thermal noise e_n	4.84nV
E-field referenced e_n	1.75 μ V/m	Effective height	2.8 mm
E-field receiver sens	5.3 μ V/m	Resonant h_e	761 mm

Figure 10.5: 60kHz antenna with large diameter coil

been theoretically possible to increase this to 340 or so by modifying the damping in the receiver, but it was not attempted, as tuning the resonance would have been very difficult.

Resonated Q	576	Loaded Q	572
Noise bandwidth	165 Hz	Thermal noise e_n	2.33nV
E-field referenced e_n	0.84 μ V/m	Effective height	2.8 mm
E-field receiver sens	2.5 μ V/m	Resonant h_e	1580 mm

Figure 10.6: 60kHz antenna with large coil and custom preamp

Note that its largest linear dimension (190mm) is about the same as the diameter of the air core loop with similar performance. This illustrates our finding that in general, equivalent ferrite core loop rods must be slightly larger than the diameter of a given air-core antenna.

Hi-Q Tuning

The coil on the larger form was designed so the ferrite rod could be easily slid back and forth inside the coil form. The resonating capacitor was chosen so the rod was slightly off center when tuned to 60kHz. Q was measured in situ with the receiver

powered on and a signal generator driving a small transmitting loop about a meter away from the receiving loop. It was found to be about 275.

Peaking the signal to within 1dB or less of dead center required the rod placement be accurate to 10 mils (0.25mm). Without some kind of signal strength indication, it would difficult or impossible to properly tune the antenna and keep it tuned.

AM Band Example

The Eton Field BT radio has a built-in ferrite loop connected to a Silicon Labs Si4735 single chip receiver. This receiver automatically adjusts input capacitance to tune the loop to resonance. The SI Labs data sheet claims the receiver can accept a loop inductance values between 180 and 450 μ H, so it is entirely feasible to replace the ferrite loop with an external air-core loop¹.

The ferrite antenna's measured Q begins dropping above 400kHz, probably due to ferrite losses since the coil is wound with Litz wire. Perhaps a ferrite material with high μ_i was chosen for the design which has significant losses in the AM band.

Coil	Core	L(μ H)	Q	h_e (mm)	e_n μ V/m
85T, Litz	Ferrite 1x14cm	600	300	3.8	19
101T, Litz		790	400	4.7	27
31T 20AWG	Air 16.8cm round	270	200	7.8	9.2
12T, 22AWG	Air 58cm square	220	400	46	1.4
7T, 20AWG	Air 122cm octagon	160	250	97	0.35

Figure 10.7: AM Band Antenna Examples

Figure 10.7 shows measured and calculated parameters for three antennas: the original ferrite loop, an intermediate size air-core loop, and a large four-foot octagonal air core loop. For the ferrite core, $\mu_{ext} = 59$ was used for calculation of effective height.

Compared to the large octagonal loop, the 16.8cm round loop is about 20dB less sensitive, and the Eton Field BT's ferrite antenna about 26dB less. Tests performed with a Tecsun PL-380 radio hard-wired to each of these antennas seems to confirm these relative sensitivities within 3dB or so. However, this assumes the radio tunes each coil to the same Q value and that is far from certain.

Parameter	Value	
Shape	Octagon	
Area	1.16 m ²	
Circumference	3.96m	
Equivalent circular diameter	1.230m	
Turn count	7	
Wire length	27.65m (0.16λ@1700kHz)	
Average Winding pitch	7.26mm	
Non-resonant h_e @ 540kHz	97mm	
Resonant h_e @ 540kHz, Q=50	4.9m	
Wire	20ga, 0.812mm dia	
Parameter	Estimated	Measured
Inductance	161.8μH	159.3μH
Q @ 400kHz	216	204
SRF	4.27MHz	4.07MHz
DC Resistance	1.00	0.95 Ω

Figure 10.8: Air core loop for Eton Field BT

4 foot Air-Core Loop for Eton Field BT

The estimated SRF was determined as 80% of that expected for a free-hanging, disconnected loop. Measured SRF of the loop with connections implies an equivalent parallel capacitance of 9.6pF. A capacitance of 51pF is required to resonate at 1710kHz, leaving headroom of about 33pF for stray and wiring capacitance.

¹The Field BT's ferrite antenna inductance is much higher than the acceptable range published in the Silicon Labs Si473x data sheet. It is not clear whether this is an error in the design or data sheet, or if some circuit modifications were incorporated by Eton to accommodate this large value of inductance. Regardless, 210μH air core loops work well over the entire AM band.

Appendix A

Symbols

All units are MKS (meters, kilograms, seconds, Hertz, Henries, Farads, etc) unless otherwise noted. Although we attempt to delineate coil and ferrite rod parameters with d and f subscripts, that may not be the case everywhere and in some cases the meaning is implied by the context.

r, r_c, r_f Coil or ferrite rod radius

d, d_c, d_f Coil or ferrite rod diameter

l, l_c, l_f Coil winding or ferrite rod length

A Area, either that inside the coil, or that of a cross-section of ferrite core

n Number of turns in coil

p Winding pitch – distance between adjacent turns in the coil

w Coil wire diameter

f Frequency

ω Radian frequency

ϵ_o Permittivity of free space, about 8.854pF/m

Z_o Impedance of free space, approximately 377 Ω

E Electric field RMS intensity, volts/meter

H Magnetic field RMS intensity, Teslas

h_e Effective height, meters

Q Component or circuit Q factor

R Resistance

Permeability symbols are shown in a separate list here as they come with many different subscripts. All the different variants are explained in the text.

μ_o Permeability of free space, $4\pi \times 10^{-7}$ H/m

μ_i Initial permeability of ferrite material

μ_a Apparent permeability of cylindrical ferrite rod

μ_{ext} Apparent external permeability of ferrite rod with coil

μ_{int} Apparent internal permeability of ferrite rod with coil

μ With any other subscript, represents a permeability relative to μ_o

Appendix B

Double-Tuned Transformers

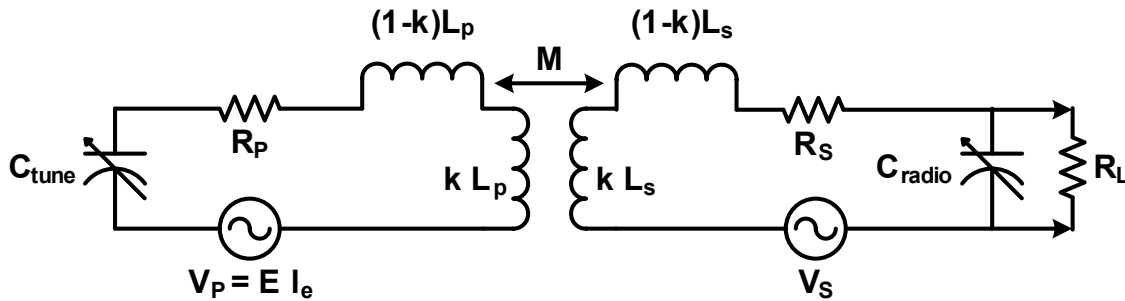


Figure B.1: Double tuned transformer model

There are several resources on the internet which provide a full analysis of the double-tuned transformer that is used to model two tuned, magnetically coupled loop antennas here, as in figure B.1.

This analysis assumes both primary and secondary inductance are tuned to the same frequency, f_c (with corresponding radian frequency ω_c). The critical coupling factor, k_c results in the largest possible voltage across R_L .

Maximum gain occurs with critical coupling, where $k = k_c$, but the classic flat-top response only occurs here when the primary and secondary Q values are about equal. With wildly different Qs, the flat-top condition will occur at a higher value, when $k > k_c$.

In typical usage, the Q values of primary and secondary are chosen to be the same, $Q_p = Q_s$. However, in this case, Q_s is determined by the portable radio and is often unknown. For AM broadcast signals, one may guess that it is likely no more than 50-100 or so, since larger values will start to attenuate high frequencies in the audio modulation. It may also vary with frequency, but that's also unknown.

Here are the equations to determine the critical coupling factor, k_c , and we note that for typical situations, the best possible gain at resonance is about equal to the

inverse of k_c .

$$\begin{aligned} N &= \sqrt{\frac{L_s}{L_p}} & Q_p &= \frac{\omega_c L_p}{R_p} \\ Q_{s1} &= \frac{\omega_c L_s}{R_s} & Q_{s2} &= R_L \omega_c C_{radio} \\ Q_s &= \frac{Q_{s1} Q_{s2}}{Q_{s1} + Q_{s2}} & k_c &= \frac{1}{\sqrt{Q_p Q_s}} \\ \frac{V_{R_L}}{V_P} &\approx \sqrt{Q_p Q_s} = \frac{1}{k_c} \end{aligned}$$

Appendix C

Noise Bandwidth

Here we provide a justification of the noise bandwidth for the antenna tuned circuit model used in this paper. The approximation used is

$$B_{noise} = \frac{\pi}{2} B_{3dB}$$

The ratio between noise and 3dB bandwidths is termed the *noise bandwidth ratio* and is assumed to be a constant equal to $\pi/2$ herein.

Normalized to a maximum magnitude of one, the voltage output of the tuned antenna versus frequency is:

$$\frac{1/Q}{1 - \theta^2 + j\theta/Q} \tag{C.1}$$

where $\theta = \omega/\omega_o = f/f_o$

The magnitude-squared of the denominator is

$$X(\theta) = \theta^4 - (2 - 1/Q^2)\theta^2 + 1 \tag{C.2}$$

To find noise bandwidth we need to integrate the magnitude squared

$$\frac{1}{Q^2} \int_0^\infty \frac{d\theta}{X(\theta)} = \frac{1}{Q^2} \int_0^\infty \frac{d\theta}{\theta^4 - (2 - 1/Q^2)\theta^2 + 1} \tag{C.3}$$

The integrand is a ratio of polynomials with four poles in the denominator (two repeated pairs). This integral may be evaluated using the Residue Theorem, which yields the value of the integral from negative to positive infinity.

$$\int_{-\infty}^\infty \frac{d\theta}{X(\theta)} = 2 \int_0^\infty \frac{d\theta}{X(\theta)}$$

We only want the integral from zero to infinity, so the result will need to be divided by two. Due to the repeated poles, a partial fraction expansion of $1/X(\theta)$ must be

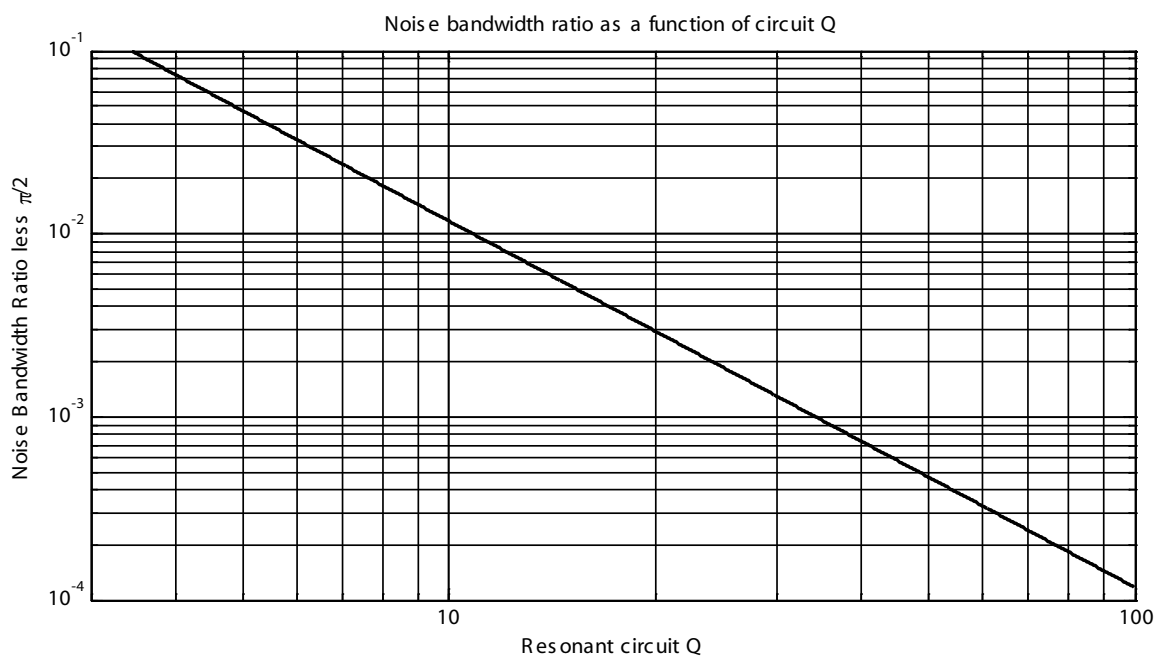


Figure C.1: Noise bandwidth ratio dependence on Q

created; then the residuals at every pole in the upper half of the complex plane (those with non-negative imaginary parts) are summed.

For large values of Q the noise bandwidth is very close to the 3dB bandwidth multiplied by $\pi/2$. The actual ratio is always larger than this value, never smaller. This result is only applicable to the tuned antenna circuit shown in figure 5.1. Note that this circuit passes the noise voltage through un-attenuated at low frequencies – this is the reason that the ratio is always larger than $\pi/2$.

This problem was solved in Matlab for values of Q between about 3 and 100 and the results are shown in figure C.1. This shows that for values of Q even as low as three, errors in computed noise levels are insignificant if a fixed value of $\pi/2$ is used for the ratio. The error here at $Q = 3$ is only about 1/4 dB in the noise ratio.

Appendix D

Antenna Noise Output

Figure D.1 shows the gain of the antenna tuned circuit relative to the gain at resonance. For each value of Q , there are two plots – one for thermal noise and another for external signals such as atmospheric noise, man-made noise and signals. Plots for external noise sources are depressed at low frequency since the antenna’s effective height drops linearly as frequency drops.

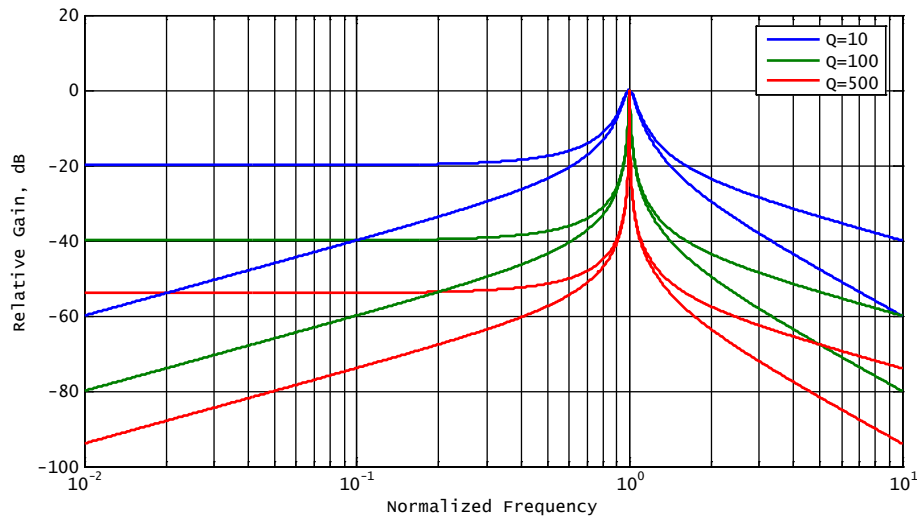


Figure D.1: Noise Gain of Tuned Antenna

Equivalent Noise Bandwidth

As worked out in the preceding appendix, thermal noise power is accurately estimated by taking the noise bandwidth to be the 3dB bandwidth multiplied by $\pi/2$. We assume the Q is high enough that VLF atmospheric noise is rejected by the loop.

Example

Design an air-core resonant receive antenna for WWVB signal at 60kHz.

- Receiver is MAS6180C with $600\text{k}\Omega$ input impedance and sensitivity of $1\mu\text{V}$.
- Expected level of atmospheric noise at 60kHz is $Fa = 115\text{dB}$.
- Thermal noise should be at least 10dB below atmospheric.
- A narrowband incoming signal at $10\mu\text{V}/\text{m}$ should be at least as strong as atmospheric noise.
- A narrowband incoming signal at $10\mu\text{V}/\text{m}$ should be at least 10dB above receiver sensitivity, or $3.2\mu\text{V}$ at the receiver input.

These requirements at receiver input. Internally, the receiver may have smaller bandwidths, and that's not considered here. Minimum resonant effective height is easily determined as

$$h_{e\ min} = \frac{3.2\mu\text{V}}{10\mu\text{V}/\text{m}} = 0.32\text{m}$$

From (4.2) we determine that

$$E_{atm} \approx 44.8\text{dB}\mu\text{V}/\text{m} - 10 \log_{10} Q, \quad \text{or} \quad e_{atm} \approx \frac{175\mu\text{V}/\text{m}}{\sqrt{Q}}$$

Determination of Q

Limiting atmospheric noise to $10\mu\text{V}/\text{m}$ requires $Q = 17.5^2 = 306$, which is a bit on the high side. Although this is feasible, loops with such high Q can be hard to tune and keep tuned. In this case, it may be a better option to settle for a lower Q, in the range from 100-150 or so, and ask the receiver do a bit more filtering (that's not always possible of course). For this example, the target value for Q is set to 150, which requires a non-resonant effective height of $0.32\text{m}/150$ or about 1.3mm. Resulting atmospheric noise will be about $14\mu\text{V}/\text{m}$.

Limits on Effective Loss Resistance

Atmospheric E-field noise density within loop bandwidth is $566\text{nV}/\text{m}/\sqrt{\text{Hz}}$ from equation 4.1. Multiplying this by the non-resonant h_e yields the atmospheric noise voltage density induced in the loop, within the loop's bandwidth. It works out to $736\text{pV}/\sqrt{\text{Hz}}$. Thermal noise density should be kept 10dB below this, or $233\text{pV}/\sqrt{\text{Hz}}$. We can solve for resistance in the formula for thermal noise density,

$$R = \frac{v_{th}^2}{4KT} = \frac{233 \times 10^{-12}}{4 \times 1.38 \times 10^{-23} \times 300} \approx 3.3\Omega$$

This is the maximum equivalent noise resistance for the entire resonant loop circuit connected to the receiver required to keep thermal noise 10dB below atmospheric.

Thermal Noise Contributions

There are three thermal noise sources: resistive losses in the loop and capacitor, and receiver input resistance. The contribution from any one source is determined by shorting the other two and computing resulting noise voltage density. Each contribution is then summed in root-sum-squared fashion. Sometimes, one or more of the thermal noise sources is negligible compared to the total, but it's easiest just to compute the total noise assuming all three are significant.

Coming up with a Design

There are a lot of design parameters in this design, and some means of simplifying the process is needed. One approach is to pick values for all but one parameter, then create graphs of various performance measures versus variations in that parameter. For for this example, the coil radius, wire gauge and turn spacing will be fixed, and performance measures examined with varying turn count. If the desired performance cannot be achieved, then one or more of the fixed parameters can be adjusted and new graphs created. Rinse and repeat.

In this case, solid copper wire is assumed with adequate turn spacing so that proximity effects may be ignored in calculating the resistance at 60kHz. Thus, only skin effect need be considered. Designs using Litz wire could use tighter turn spacing and would need to take a different approach.

The initial parameters chosen are a coil radius of 5-½ inches, with 22 AWG wire spaced four wire diameters. For this example, these values are somewhat arbitrary, and in an actual design they would be driven by various constraints are not considered here. For each turn count, we compute:

- Coil Inductance
- AC Resistance
- Effective Q, including resistor input resistance, and resonating capacitor losses
- Bandwidths (3dB and noise)
- Thermal noise at receiver input
- Effective height, and resonant effective height
- Atmospheric noise level at receiver input

From this data plots are generated of resonant effective height and atmospheric-to-thermal noise ratio, versus turn count. The range of turn counts examined must be determined by trial and error.

The results show that the resonant Q values achievable with solid copper wire are about as high as is reasonable for stable loop tuning (150-200). Higher values of Q might require frequent re-tuning, or a means to automatically tune the loop through firmware or other method.

The wire diameter had to be increased, to as much as 14 gauge to get higher Q values at lower turn counts.

Ferrite-Coupled Example

Note: this example may contain errors and will be verified and cleaned up in a subsequent version of this document.

This is intended to boost signals in the AM broadcast band between 540 and 1700kHz. The loop is large enough that a receiver with internal ferrite loop will fit inside the form to access the strongest magnetic fields. To avoid problems with the receiver's ferrite rod reducing the SRF too low, a minimum target air core SRF of 5MHz was used. A total wire length of about 20m was chosen – about 0.11λ at 1700kHz.

The outer shield of a small coax cable was used to construct the loop. Due to the relatively large coax shield diameter, it has a very small AC resistance – only about $0.05\Omega/\text{m}$ at 1700kHz. This is equivalent to using AWG 10 wire to wind the coil, and due to skin effect the AC resistances are comparable. Neglecting proximity effects, the total AC resistance will be one ohm or less over the band of frequencies. Therefore, the overall Q is too high at resonance and additional resistance is added to achieve a 3dB bandwidth of about 12kHz.

A section cut from a scrap fiberglass water softener tank provided the coil form with an outside diameter just over nine inches. This is large enough for the portable receiver to fit inside the form and receive the best signal boost.

Thermal noise has been computed at room temperature using the noise bandwidth of the tuned loop, not the 3dB bandwidth. The resulting noise voltage is converted to an equivalent E-field strength through the effective height of the antenna – which varies linearly with frequency. The equivalent thermal noise is larger at the low end of the band because the antenna's effective height is smaller there.

For computing the extra resistance for a specific bandwidth,

$$B = \frac{f_o}{Q} = \frac{f_o R}{2\pi f_o L} = \frac{R}{2\pi L}$$

so,

$$R = 2\pi BL$$

Winding inside diameter	232mm	9.13 in
Turn count	27	
Total wire length	19.67 m	64.54 ft
Wire diameter	2.49mm	98 mil
Winding pitch	5.48mm	220 mil
SRF (estimated)	6.1 MHz	
Inductance (measured)	140 μ H	
Added R	10 Ω	
3dB and noise bandwidths	12kHz	18kHz
Tuning capacitor	570 to 57pF	
Thermal noise	4.4 to 1.4 μ V/m	

Figure D.2: Ferrite Coupled Design Example

Receiver Bandpass Filtering

60kHz receivers often use a 60kHz crystal to filter out excess noise. This may create an excessively narrow bandwidth and slow down carrier amplitude transitions. Is it feasible to use a wider bandwidth?

Estimating Crystal Q

Not many datasheets will specify the Q value. Some (e.g. from Abracon) will give the shunt capacitance and the ratio between shunt and motional capacitance. This allows computation of impedance at resonance and Q based on specified motional resistance.

Using data for the Abracon ABS25 crystal, the possible range of Q at 60kHz would be from about 13,000 to 53,000 for a bandwidth range of 4.6Hz to 1.1Hz. At 1.1Hz bandwidth would require about at 10ppm frequency tolerance, and typical commercial 60kHz crystals are 20ppm tolerance at best, so it may be safe to assume that typical bandwidths are between 2.4 and 4.6Hz. These bandwidths may be too narrow and it's likely that a series resistance is added to the crystal to reduce the Q and get something more reasonable. Even so, it's still likely the resulting bandwidth is only 20Hz or less.

These narrow bandwidths have a significant impact on how fast the receiver can respond to carrier amplitude changes.

MAS6180C

Input impedance is 600k ohms and with high-Q ferrite antenna, this impedance results in a 6dB signal amplitude loss and the effective Q is reduced and bandwidth is about

250-300Hz instead of the 140Hz with a higher input impedance.

In this situation antenna L is 3.950mH, R is 2.8 ohms and C for resonance is 1.7813nF. The effective output impedance of the antenna at resonance is about 800k ohms.

The MAS6180C receiver's input impedance cuts the antenna Q about in half, and reduces gain by 6dB.

Appendix E

Exact Resonant Loop Analysis

It's necessary to state what is meant by resonance before beginning here. There are (at least) two possible definitions:

- The frequency at which capacitive and inductive reactances cancel each other in the series circuit.
- The frequency at which the phase angle of the terminal impedance is zero.

For high-Q circuits, there's not a lot of difference between these two. Below, the first definition is used, and this will result in some reactance being present at the antenna terminals at resonance.

One of the goals is to determine the effect of load impedance on the tuned circuit. To be valid for high-Q loop designs, this analysis must also include losses in the resonating capacitor. With this additional consideration, the equations become complex to the point that it's more work to write them down than it is to compute the desired parameters using CAD tools (we use Matlab/Octave in examples) or SPICE simulations.

Previous Versions

Prior versions of this document included a lot of math to work out exact equations for the loaded resonant loop. It was decided that this was much too complex and error prone, and the appendix has been rewritten in favor of numerical calculations performed with the aid of computers.

Determining Effective Q

One approach as suggested in figure E.1 is to first compute the equivalent impedance of the resonating capacitor in parallel with the receiver's input impedance¹.

¹Shown as a parallel R-C circuit in the schematic, but it can be any complex impedance.

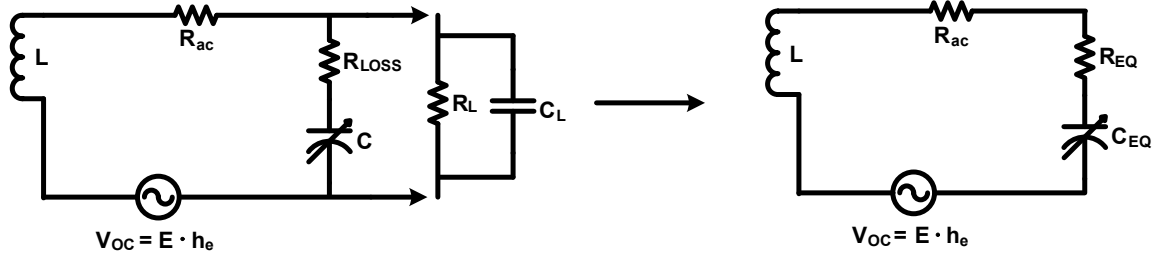


Figure E.1: Thevenin equivalent of tuned loop at resonance

The resulting simplification is shown on the right side of the figure, with the values C_{EQ} and R_{EQ} . The equivalent capacitance will be pretty close to the original value for high-Q designs, but can vary significantly when the Q is lower. As such, it's best to use the equivalent capacitance in computing the resonant frequency,

$$\omega_o = \frac{1}{\sqrt{L C_{eq}}}$$

Now the loaded Q at resonance is easily obtained:

$$Q = \frac{\omega_o L}{R_{ac} + R_{eq}} = \frac{1}{\omega_o C_{eq} (R_{ac} + R_{eq})} \quad (\text{E.1})$$

Example

Consider a loop tuned to resonance at 1MHz with an inductance of 200 μH , loss resistance of 5 Ω , capacitor of 126.6pF with $\tan \delta = 0.0003$. Then add load impedances of 600k and 100k Ω , all in parallel with 2pF. Find the change in Q and resonant frequency caused by the loading. Working the numbers is an exercise left for the reader, but our answer is shown in the table below.

First, compute the impedance of the load using the initial estimate of resonant frequency, $\omega_o = 1/\sqrt{LC}$.

$$Z_L = R_L \parallel \frac{1}{j\omega_o C_L}$$

Then combine this with the resonating capacitor's impedance,

$$Z = \left(R_{loss} + \frac{1}{j\omega_o C} \right) \parallel Z_L = \left(\frac{\tan \delta}{\omega_o C} + \frac{1}{j\omega_o C} \right) \parallel Z_L$$

The imaginary part of the result, Z can be interpreted as the impedance of an ideal capacitor, C_{eq} at frequency ω_o . Then, optionally re-compute the resonant frequency

$$\omega_1 = \frac{1}{\sqrt{LC_{eq}}}$$

and the effective Q follows from there. For high-Q circuits, the actual resonance will not be very different from the desired value. It is possible to adjust the capacitor value and re-compute to get the actual resonance closer to the desired value. Typically this is not necessary.

Below we show the results for this example, where the receiver input capacitance (2pF) was subtracted from the resonating capacitor to compensate for that.

	$R_L = \infty$	$R_L = 600\text{k}\Omega$	$R_L = 100\text{k}\Omega$
Frequency Error	0 Hz	2.8 Hz	83 Hz
Resonant Q	234	157	59.4

Typical Matlab/Octave Code

Here's how this might be computed using one of these CAD tools.

```
f=1e6; w=2*pi*f; s=1i*w;
L=200e-6; R=5;
C=1/(w*w*L); % capacitor for resonance at 1MHz
C=C-2e-12; % compensation for rx input capacitance
tanD=0.0003; % capacitor loss tangent
Zin=1/(1/600e3+s*2e-12); % receiver input impedance @ 1MHz
Zc=1/(s*C)+tanD/(w*C); % capacitor impedance including losses
Zeq=1/(1/Zin+1/Zc); % equivalent impedance of capacitor || rx input impedance
Req=real(Zeq);
Ceq=-1/(w*imag(Zeq));
Q=w*L/(Req+R); % loaded Q of the circuit
w1=1/sqrt(L*Ceq); % actual resonant frequency
freqErr=(w1-w)/w; % relative frequency error
% if desired, adjust C and repeat until frequency error is acceptably low
C=C*(1+freqErr)^2;
```

Note: prior versions of this document had misleading or incorrect values for the example, because the 2pF load capacitance was not accounted for in choosing the value for the resonating capacitor.

Q Away From Resonance

Only for the sake of curiosity, the expressions for the Q of a RLC series resonant circuit at frequencies away from resonance are worked out here.

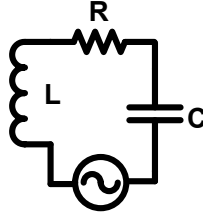


Figure E.2: Series RLC circuit to be analyzed

The total series loop impedance is

$$Z = sL + \frac{1}{sC} + R = \frac{s^2LC + sRC + 1}{sC}$$

For a an applied voltage of one volt RMS, loop current is

$$I = \frac{1}{Z} = \frac{sC}{s^2LC + sRC + 1}$$

Capacitor voltage is the loop current multiplied by the capacitor impedance,

$$V_C = \frac{1}{s^2LC + sRC + 1}$$

Energy dissipated in the resistor over the period of a cycle at frequency f is the power in the resistor multiplied by the length of one cycle:

$$E_R = \frac{|i|^2 R}{f} = 2\pi \frac{R}{\omega |Z|^2}$$

The capacitor voltage and inductor current always differ by 90 degrees, and peak energy storage will occur when either the capacitor voltage or inductor current is maximum. Away from resonance, energy stored will vary with time, but will be at a maximum when either the inductor current or capacitor voltage is maximum, depending on whether the frequency is above or below resonance, respectively.

These are RMS currents and voltages, so the peaks are larger by $\sqrt{2}$. Peak energy in the inductor is then

$$E_L = \frac{1}{2}L \left(|i|\sqrt{2} \right)^2 = \frac{L}{|Z|^2}$$

and for the capacitor,

$$E_C = \frac{1}{2}C \left(|V_C|\sqrt{2} \right)^2 = \frac{C}{\omega^2 C^2 |Z|^2} = \frac{1}{C\omega^2 |Z|^2}$$

At frequencies below resonance, E_C is larger, while E_L is the big one at higher frequencies. So, for low frequencies,

$$Q = 2\pi \frac{E_C}{E_R} = \frac{\omega|Z|^2}{2\pi R} \frac{1}{C\omega^2|Z|^2} = \frac{1}{R\omega C} = \frac{X_C}{R}$$

And at high frequencies,

$$Q = 2\pi \frac{E_L}{E_R} = \frac{\omega|Z|^2}{2\pi R} \frac{L}{|Z|^2} = \frac{\omega L}{R} = \frac{X_L}{R}$$

At resonance, Q is minimum and equal to either expression. Above, Q increases linearly with frequency, and it increases inversely with frequency below resonance.

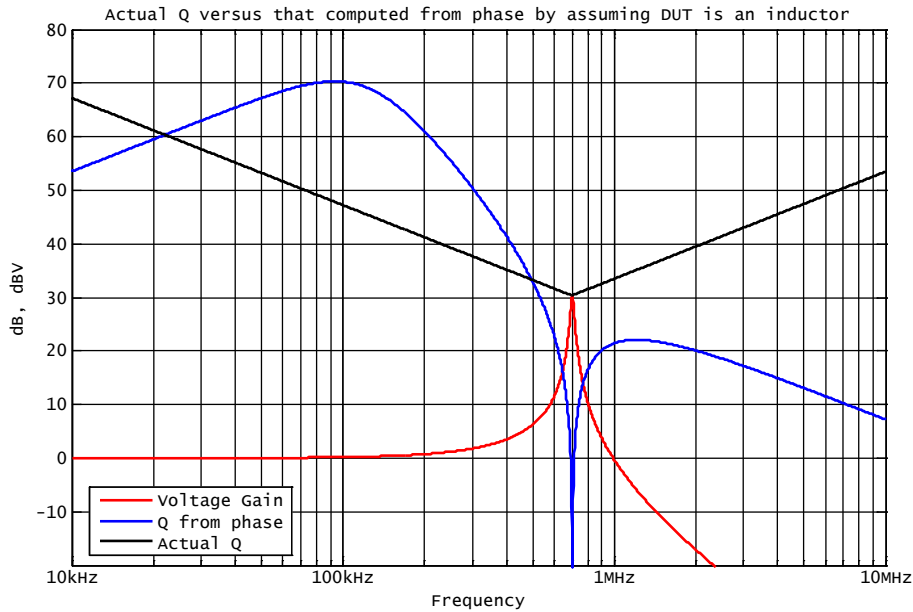


Figure E.3: Example Calculation of Q

The difference between computing Q correctly away from resonance and that based on the phase angle of terminal impedance can be seen in figure E.3. The black V-shaped line is the true Q while the blue plot is based on the impedance phase angle looking across the capacitor, under the assumption that the impedance is due to an inductor with series resistor. The blue plot does indeed indicate an extremely low Q at resonance, while the actual value is about 31 (30dB).

In summary, having the value of Q away from resonance is not all that useful but going through the exercise helps in understanding the definition of Q.

The SiLabs Si473x Receiver

Several inexpensive AM-band receivers are available which are based on the Si473x RF receiver IC (e.g. Tecsun PL380). Although these contain an internal ferrite loop antenna, it is not difficult to remove or disconnect that, and make direct connection to an external loop antenna. This works quite well, but predicting the resulting performance is problematic because the effective input resistance of the Si473x chip is not specified.

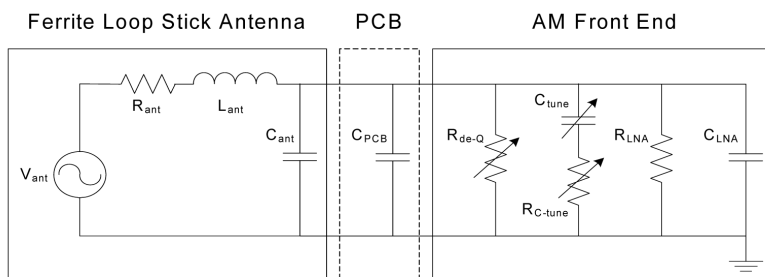


Figure E.4: SiLabs Si473x AM Antenna Input Model (from AN383)

Figure E.4 is copied from SiLabs application note AN383, and is their model of the AM antenna input. It is stated that the value of R_{de-Q} may be adjusted by the radio (w/o any user input) to reduce the level of strong signals.

Predicting the performance of a loop antenna connected to this receiver requires knowing the values of R_{de-Q} , R_{C-tune} , R_{LNA} , and none of these are specified by SiLabs. This makes it impossible to compare the stand-alone performance of loops with different values of inductance, loss resistance and effective height. In essence, the loop and Si473x receiver form a black box, and it is only possible to make comparisons between different loop/receiver combinations.

There is a possible loophole in this however. If two loops with identical values of inductance are used to receive weak signals, some guesses about the Si473x internal configuration can be made:

- The value of C_{tune} will be the same for both loops.
- As a result, the value of R_{C-tune} will be the same in both cases.
- For small amplitude signals, R_{de-Q} will be set to the maximum possible value.

The last assumption is the most questionable one. Although SiLabs states that R_{de-Q} is used to reduce input levels for large signals, it may also be possible that for very high-Q loops it may be used to reduce tuning sensitivity. The tuning capacitance is digitally controlled, and there's no specification of the tuning resolution, so R_{de-Q} could also be used to lower the loop Q in some cases. On the other hand, the value

of R_{LNA} could preclude this possibility entirely. Again, this is all just an educated guess.

At any rate, some experiments could be performed under these assumptions, and compared to predicted performance to get a sense for their validity.

Appendix F

Miscellaneous

Inductance Calculations

The calculation of inductance of air core loops for this article were done using Robert Weavers's methods, and in particular the `Lcoil` function as defined in [Weaver]. In our limited experience, these methods generally yield results which match measured inductances to an accuracy of 1% or better.

One benefit of using this method is that the algorithm allows for each turn of the coil to have a unique wire diameter, axial position and radius. Although varying the wire diameter within the coil is not of much interest, this method can be used to analyze spiral and conical coils, as well as coils with uneven turn spacings and radii.

At its heart, the algorithm uses a simple calculation of the inductance between two circular current filaments. In the Matlab/Octave scripts, this is the `MaxwellMut` function. Calling it with a specially computed turn spacing argument allows determination of the mutual inductance between each turn and itself.

The overall calculation simply involves adding up the mutual inductance between every possible pair of turns (including each turn with itself). By giving each turn a unique wire diameter, radius and axial position, the inductance of a non-uniform coil design is easily computed. See the function `LcoilArbitrary` for an example.

Skin Effect

These two formulas are often used for computing skin depth and the resulting resistance of solid copper wire. See Wikipedia on the topic of *Skin Effect* for example.

$$\delta = \sqrt{\frac{2\rho}{\omega\mu} \left(\rho\omega\epsilon + \sqrt{1 + \rho\omega\epsilon} \right)} \quad (\text{F.1})$$

$$J = J_s e^{-(1+j)d/\delta} \quad (\text{F.2})$$

For those interested in higher accuracy in all cases, a paper published by Dr. David Knight [ITU-R] provides an algorithm accurate to parts-per-billion. Use of those methods instead of the above formula makes little difference (hundredths of a percent) for the examples presented in this article.

Skin/Proximity Effects, Medhurst & Inductance

A couple of observations are made here which some may find useful, the first having to do with skin depth and AC resistance of straight wires.

At low frequencies where the wire diameter is much less than the skin depth, the resistance of a wire varies inversely with cross-sectional area. Doubling the diameter, quadruples the area, and cuts the resistance by a factor of four. At high frequencies where the wire is large compared to skin depth, conduction only happens around the periphery of the wire, so resistance is proportional to circumference; doubling the diameter doubles the circumference and cuts resistance in half. This can be seen in figure F.1, and the breakpoint between the two slopes occurs where the wire diameter is about equal to three skin depths.

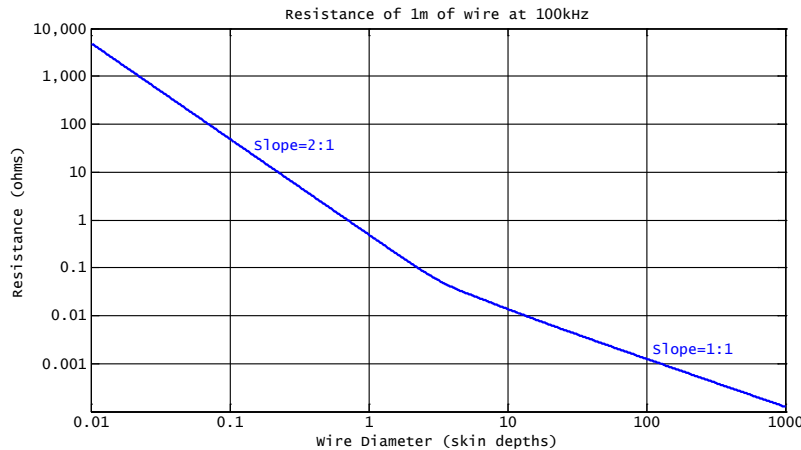


Figure F.1: AC Resistance vs Wire Diameter

Proximity Effect on Inductance

The next observation applies to coils where the wire diameter is a significant fraction of the coil diameter, perhaps more than a couple percent. At low frequencies, current is uniformly distributed in the wire, and inductance calculations using the mean diameter with L_{coil} (see [Weaver]) are quite accurate.

As frequency increases, currents in the wire become concentrated towards the axis of the coil due to proximity effect. This has the effect of reducing the effective

diameter of the coil. If the wire diameter is more than a few percent of coil diameter this causes a noticeable decrease of inductance.

Tests on an air-core coil close-wound with 16 AWG magnet wire (1.3mm dia) demonstrate this effect. The coil of 47 turns with mean diameter of 18mm exhibits roughly a 10% decrease in inductance due to this effect, as seen on the right side of figure F.2. Calculations with Lcoil indicate this corresponds to a reduction in effective diameter by $\frac{2}{3}$ of the wire diameter.

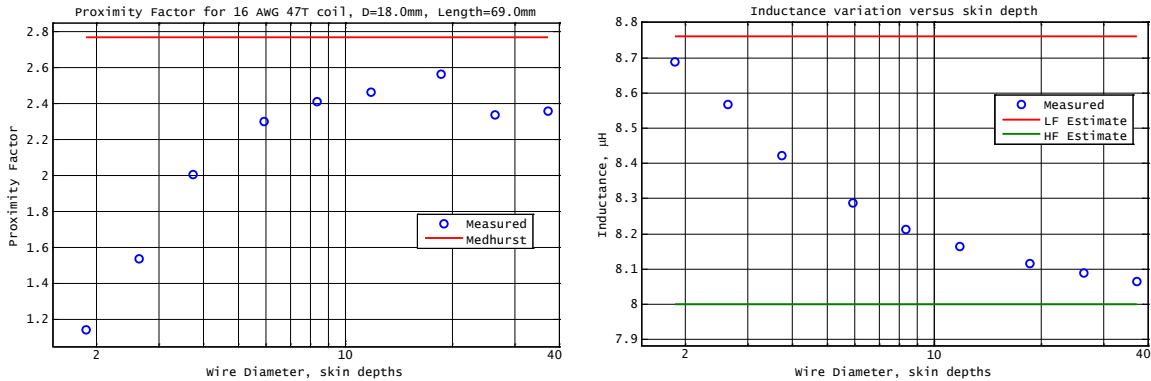


Figure F.2: Medhurst Accuracy (left)

Proximity Effect on Inductance (right)

The curve labeled “LF Estimate” is made using the mean diameter of the coil (18mm), while the “HF Estimate” uses a diameter reduced by $\frac{2}{3}$ of the wire diameter (17.14mm).

Accuracy of Medhurst Estimates

The same coil described above provides an example where Medhurst’s estimate of proximity effect is about 15% in error. The left side of figure F.2 shows proximity effect as a function of wire diameter for this coil. Resistance versus frequency for this coil is what was measured, but the x-axis shows the wire diameter relative to skin depth at each test frequency.

Proximity factor seems to level off at about 2.4, but there appears to be some other effect at work, causing some minor variation for wire diameters between 15 and 40 skin depths.

These tests steered well clear of the coil’s self-resonant frequency, but in many cases that will add another set of complications to the behavior.

Core Area

Ferrite rods often are circular but with two flats on opposite sides of the diameter. To include that in the area use these formulas. Let r be the rod radius and f the distance across the flats.

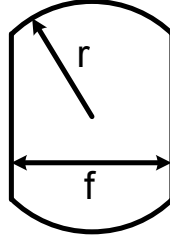


Figure F.3: Ferrite core cross section

Angle between center of flat and one edge is

$$\phi = \cos^{-1} \frac{f}{2r} = \cos^{-1} \frac{f}{d}$$

Width of the flat is

$$w = 2r \sin \phi$$

Area of cut-out is area of sector less area of triangle which has base formed by flat of width w and height of $f/2$

$$A_{cut} = \phi r^2 - \frac{wf}{4} = \phi r^2 - \frac{fr \sin \phi}{2} = r^2 \left(\phi - \frac{f \sin \phi}{2r} \right)$$

The area of the ferrite rod is then the circular area less twice the cut area:

$$\begin{aligned} A_{rod} &= \pi r^2 - r^2 \left(2\phi - \frac{f \sin \phi}{r} \right) = \pi r^2 \left(1 - \left[\frac{2\phi}{\pi} - \frac{f \sin \phi}{\pi r} \right] \right) \\ &= \pi r^2 \left(1 - \frac{2}{\pi} \left[\phi - \frac{f}{d} \sin \phi \right] \right) \end{aligned} \quad (\text{F.3})$$

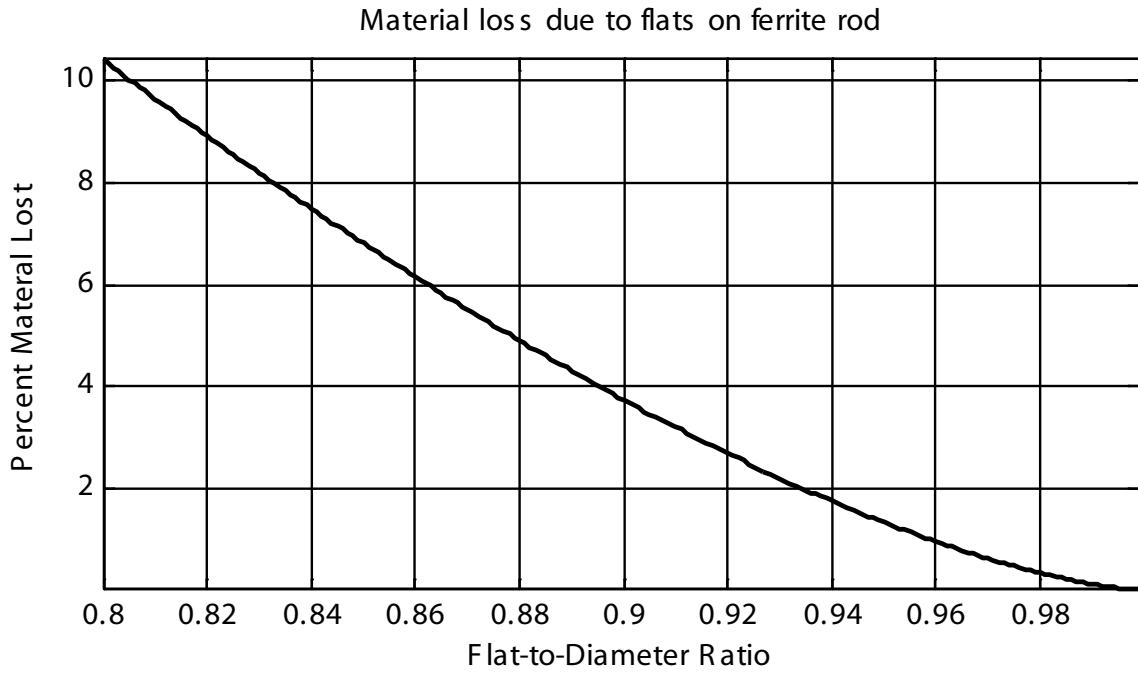


Figure F.4: Effect of flats on round ferrite rods

The percent loss of material due to the presence of flats on the rod is plotted in figure F.4. The x-axis is the ratio between distance across the flats and the diameter of the rod.

Effective Size of Ferrite Sleeve

When composed of multiple round rods or flat bars, the sleeve has less total ferrite area in cross section than would a solid sleeve. The ratio of these areas and the dimensions of a sleeve having the same average diameter are easily worked out.

Rod Construction

Let R be the average sleeve radius – O.D. plus I.D. over two, r the rod radius and n the number of rods in the sleeve. The cross section of a solid sleeve with same I.D. and O.D. is

$$A_{full} = \pi((R + r)^2 - (R - r)^2) = 4\pi Rr = \pi Dd$$

where D and d are the average and rod diameters. The actual cross sectional area is simply

$$A_{true} = n\pi r^2$$

So the fraction of the sleeve outline filled with ferrite is

$$\alpha = \frac{n\pi r^2}{4\pi Rr} = \frac{nr}{4R} = \frac{nd}{4D} \quad (\text{F.4})$$

where we can use diameters instead of radii in the comparison.

Take an actual design from DeBock which has 23 10mm diameter rods with a sleeve OD of 3.5 inches (89mm). The fraction of the sleeve outline comprised of ferrite is:

$$\frac{23 \times 10}{4 \times 89} \approx 0.646$$

This reveals that 64.6% of the outline is filled with ferrite.

The next question is, what sleeve thickness with the same average radius would have the same cross sectional area of ferrite? Let r_{eq} be half of this equivalent thickness.

$$n\pi r^2 = 4\pi Rr_{eq}$$

$$r_{eq} = \frac{n\pi r^2}{4\pi R} = \frac{nr^2}{4R} = \alpha r \quad (\text{F.5})$$

$$d_{eq} = 2r_{eq} = \alpha d \quad (\text{F.6})$$

Continuing the example, we find that

$$d_{eq} = \frac{23 \times 10^2}{4 \times 89} \approx 6.46$$

A ferrite sleeve with thickness of 6.46mm has the same cross sectional area as the actual configuration. The average diameter of the design is (89-10) or 79mm and the equivalent sleeve would have OD of (79+6.46) or 85.46mm and ID of (79-6.46) or 72.54mm.

This effectively changes the L/D ratio by the change in OD, and changes the remaining area as well.

A second example uses 64 8mm rods on a 7-inch (178mm) OD circle. For this, we have $D = 178 - 8 = 170$ mm, $\alpha \approx 0.719$. The effective sleeve thickness is $d_{eq} = \alpha d \approx 5.75$ mm. This has an effective OD of $R + d_{eq} \approx 175.75$ mm.

Bar Construction

A similar analysis is done here, but it's assumed that the flat bars are not really flat, but have a small radius matching the circle that they're placed on.

Again, the average radius, R is used, and w will represent the bar width, with t being the thickness. The total amount of ferrite around this circle is the bar width times the number of bars. The ratio of this to the circumference of a circle of average radius R is what you'd have if the sleeve were solid. That leads to this:

$$\alpha = \frac{nw}{2\pi R}$$

where w is the bar width. From there the effective OD and ID of the equivalent solid sleeve are given by

$$R \pm at$$

where t is the bar thickness. Where very thin bars are used, it may not matter too much if the FSL design OD or average diameters are used.

For an example, consider a two-inch ID design built with eight flat bars, each 20mm wide and 3mm thick. The average diameter would be 2 inches plus 20mm or 53.8mm. The circumference of that circle is 169mm while the total of all bar widths is 8×20 mm or 160mm. That gives $\alpha = 160/169 \approx 0.95$. Thus, the sleeve thickness used to compute effective external permeability would be 0.95×3 mm or about 2.85mm.

These adjustments may not always make a significant difference, but it's worthwhile to make a quick calculation just to see. Finally, there's some error here because we assume the bars are curved to match the circle and not flat. How much that matters depends on the number of bars.

Alternate Technique

Another approach is to estimate the average gap between bars around the circle and divide that by bar width to get the value of $(1 - \alpha)$.

Mensuration of the Octagon

We define f as the distance between opposite sides, w as the distance between opposite apex, and s as the length of one side.

The area is calculated by finding the area of the triangle formed by the lines labeled $f/2$, $s/2$, and $w/2$ in figure F.5. There are 16 such triangles in the octagon so multiplying by 16 gives the total area.

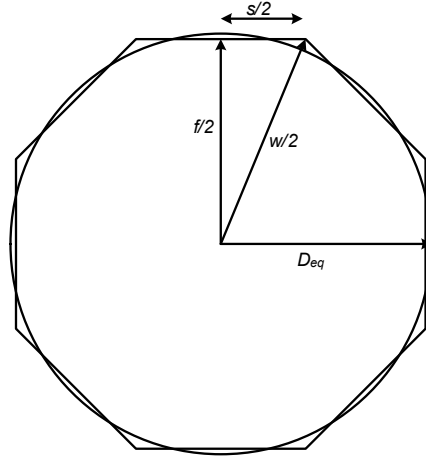


Figure F.5: Octagon Dimensions

Assume we are given the distance across the flats, f . The angle at the center from the center of a side to the adjacent apex is $\phi = 2\pi/16 = \pi/8$. The length of the line from center to the center of a side is $f/2$, and the length of the side s is:

$$\tan \phi = \frac{s/2}{f/2}, \text{ or } s = f \tan \phi$$

The area of that right triangle is one half width times height:

$$A_t = \frac{1}{2} \frac{s}{2} \frac{f}{2} = \frac{\tan \phi}{8} f^2$$

And the total area of the octagon is sixteen times that:

$$A = (2 \tan \pi/8) f^2 \approx 0.8284 f^2 \approx \frac{29}{35} f^2$$

and the diameter of a circle having the same area is

$$D_{eq} = \sqrt{\frac{4}{\pi} 2 f^2 \tan \pi/8} = f \sqrt{\frac{8}{\pi} \tan \pi/8} \approx 1.0270 f$$

The circumference is just eight times the length of a side:

$$C = 8s = 8f \tan \pi/8 \approx 3.3137f$$

The distance between opposing apex points, w , is:

$$w = f \sec \pi/8 \approx 1.0824f$$

Given the diameter of an equivalent circle, the octagon dimensions across flats and apex points is:

$$f \approx 0.9737D_{eq} ; \quad w \approx 1.0539D_{eq}$$

Appendix G

Axial Field Polynomial Fits

These are fourth order polynomials and the independent variable, x is position relative to center of rod, with zero being the center and one being the end. Since fields are symmetrical about the center, only one side of the rod is considered.

$$H(x) = \sum_{k=0}^4 c_k x^k$$

μ_i	l_f/d_f	c_4	c_3	c_2	c_1	c_0
63	5.00	-1.5329	2.2676	-1.6685	0.2008	0.9927
	7.07	-1.5844	2.3210	-1.6975	0.1972	0.9907
	10.00	-1.6731	2.4038	-1.7114	0.1970	0.9835
	14.14	-1.9721	2.8987	-1.9955	0.2718	0.9840
	20.00	-2.2592	3.2286	-2.0779	0.3060	0.9815
	28.28	-2.6284	3.6011	-2.0674	0.2960	0.9848
125	5.00	-1.4836	2.2123	-1.6690	0.1962	0.9929
	7.07	-1.4814	2.1935	-1.6758	0.1860	0.9911
	10.00	-1.4865	2.1646	-1.6565	0.1764	0.9842
	14.14	-1.6577	2.4838	-1.8835	0.2357	0.9853
	20.00	-1.7416	2.5166	-1.8567	0.2451	0.9852
	28.28	-1.8268	2.4409	-1.6560	0.1984	0.9884
250	5.00	-1.4578	2.1837	-1.6696	0.1939	0.9930
	7.07	-1.4275	2.1283	-1.6659	0.1802	0.9913
	10.00	-1.3883	2.0430	-1.6320	0.1658	0.9846
	14.14	-1.4903	2.2745	-1.8360	0.2173	0.9860
	20.00	-1.4583	2.1556	-1.7655	0.2140	0.9864
	28.28	-1.3698	1.8427	-1.4893	0.1483	0.9902

μ_i	l_f/d_f	c_4	c_3	c_2	c_1	c_0
500	5.00	-1.4448	2.1695	-1.6701	0.1927	0.9930
	7.07	-1.4000	2.0955	-1.6613	0.1772	0.9915
	10.00	-1.3380	1.9821	-1.6207	0.1605	0.9848
	14.14	-1.4043	2.1703	-1.8152	0.2081	0.9863
	20.00	-1.3118	1.9786	-1.7288	0.1985	0.9870
	28.28	-1.1300	1.5537	-1.4287	0.1238	0.9911
1000	5.00	-1.4389	2.1634	-1.6708	0.1922	0.9931
	7.07	-1.3867	2.0799	-1.6595	0.1758	0.9915
	10.00	-1.3129	1.9520	-1.6156	0.1579	0.9849
	14.14	-1.3608	2.1188	-1.8059	0.2035	0.9865
	20.00	-1.2374	1.8917	-1.7134	0.1909	0.9873
	28.28	-1.0081	1.4149	-1.4067	0.1120	0.9916
2000	5.00	-1.4388	2.1643	-1.6727	0.1922	0.9931
	7.07	-1.3820	2.0754	-1.6602	0.1754	0.9915
	10.00	-1.3012	1.9387	-1.6140	0.1567	0.9849
	14.14	-1.3394	2.0938	-1.8019	0.2013	0.9865
	20.00	-1.2002	1.8490	-1.7065	0.1871	0.9874
	28.28	-0.9468	1.3476	-1.3983	0.1062	0.9918
4000	5.00	-1.4495	2.1808	-1.6802	0.1934	0.9930
	7.07	-1.3876	2.0864	-1.6670	0.1764	0.9915
	10.00	-1.2994	1.9391	-1.6168	0.1568	0.9849
	14.14	-1.3302	2.0842	-1.8014	0.2005	0.9866
	20.00	-1.1819	1.8287	-1.7038	0.1854	0.9875
	28.28	-0.9163	1.3148	-1.3949	0.1033	0.9919

The field value estimates produced by these curve fits must be integrated over the range of x-values corresponding to the position occupied by the coil and divided by the coil length to get an average value of the field within the coil. That answer is relative to the field at the center of the rod. See the chapter on ferrite core loops for more on applying these curve fits.

Appendix H

Worked Examples

Calculations for three of the example antennas are worked out in detail here.

The bandwidth that is used for thermal (and atmospheric) noise in any calculation will depend on the situation. In some cases, the resonant bandwidth is appropriate, in others the receiver or other system bandwidth might be the correct choice.

60kHz Thermal Noise

Noise calculations shown below are not the entire story for the 60kHz examples because the receiver's bandwidth may be much more narrow – for example there may be a crystal filter with a bandwidth of just a few Hertz.

Atmospheric Noise

A value of $F_a = 60\text{dB}$ from ITU figure 15b is used for all calculations. This gives values for F_a of 70 and 120dB for frequencies of 60kHz and 540kHz respectively.

MW Receiver Sensitivity

The MW antenna calculations are based on a Silicon Labs Si4374 receiver. The specified input sensitivity of $25\mu\text{V}$ is specified at 26dB (S+N)/N power ratio (400:1) (2kHz IF bandwidth). Here, our use of the term SNR will mean the ratio of signal plus noise power to noise power. The relationships between SNR and signal and noise *voltages* are as follows:

$$\text{SNR} = (s^2 + n^2)/n^2, \quad \text{or,} \quad n = \frac{s}{\sqrt{\text{SNR} - 1}}, \quad \text{and} \quad s = n\sqrt{(\text{SNR} - 1)}$$

In this case the SNR of 26dB is roughly a 400:1 power ratio, which corresponds to a receiver noise floor voltage of

$$n \approx \sqrt{\frac{(25\mu\text{V})^2}{400 - 1}} \approx 1.25\mu\text{V}$$

This is a reasonable SNR value for a listenable signal, but for DXing purposes, stations may often be identified with higher noise levels. Therefore, calculations in in this appendix will use an SNR of 10dB or a 10:1 power ratio, and we have

$$s \approx \sqrt{(1.25\mu\text{V})^2(10 - 1)} \approx 3.8\mu\text{V}$$

60kHz Loop Q

Examples for LF tuned loops are worked for the case of two different types of tuning capacitor. Due to the large capacitance required, air dielectric capacitors are not practical. Film capacitors are the perhaps the best choice here, and the two dielectrics considered are PPS (polyphenylene sulfide) and PP (polypropylene). Typical values for the dissipation factor ($\tan \delta$) at 100kHz are 0.6% for PPS dielectric, and low-loss PP capacitors are readily available with $\tan \delta \leq 0.07\%$ at 100kHz. Some PP capacitors are rated with loss as low as 0.02% but are not always readily available, so the larger figure is used here.

Reactance of the capacitor at 60kHz is calculated, and this value is multiplied by $\tan \delta$ to determine the effective series resistance. This is then added to the loop's AC resistance. Calculations will show the values for PPS and PP film capacitors respectively enclosed in braces and separated by a comma, for example like this: {3.20, 1.22}.

MW Loop Q

One of the unknowns for this receiver is the final Q of the tuned loop antenna. It's important to know this because it has a direct bearing on the overall effective height of the system.

None of the documentation indicates that the Si4374 receiver adds any resistance across the loop to intentionally lower the Q. However, there are obviously varactors or equivalent in the receiver and these may result in a lowered Q value. For the purposes here, it's assumed the tuned loop has a Q of 50, regardless of the actual Q of the unloaded loop. It would require an in-situ measurement of the Q across the AM band to be certain.

FSL Test Antennas

The rods used are not exactly round or square, so the cross sectional area was determined by measuring the volume of water displaced by a single rod, then dividing by its length. The result is very close to that of a round rod with a diameter of 12mm.

With 36 rods, the total cross sectional ferrite area is

$$A_f = 36 \times \pi \times 0.006^2 \approx 4.072 \times 10^{-3} \text{ m}^2$$

Since the sleeve is not solid, the thickness of a solid sleeve with the same cross sectional area as the rods is computed. The first step is to compute the percentage of the overall outline filled with ferrite. This can be computed from (F.4):

$$\alpha = \frac{36 \times 0.012}{4 \times 0.136} \times 100\% \approx 79.41\%$$

Using (F.6), the sleeve thickness which contains the same cross sectional area and has a mean diameter of 136mm is:

$$d_{eq} = \alpha d \approx 0.7941 \times 0.012 \approx 0.00953$$

Thus, the inside and outside diameters of the sleeve are

$$D_i = 136 - 9.53 = 126.47\text{mm}, \quad D_o = 136 + 9.53 = 145.53\text{mm}$$

From equation (8.1), the percentage of the sleeve containing ferrite (compared to a solid rod) is:

$$1 - \left(\frac{D_i}{D_o}\right)^2 \approx 24.48\%$$

The average permeability for these rods is somewhere around $\mu_i \approx 300^1$. The estimated apparent permeability is $\mu_{sleeve} = 3.88$.

¹They were shipped from China, very poorly packaged and likely were subjected to a lot of shock and vibration which can lower permeability significantly. Advertised $\mu_i=800$, but the actual value seems much lower. In this application however, the reduced value of μ_i has little effect.

Sleeve Calculation Summary

Ferrite Rods	12x140mm, qty 36
Sleeve Form	ID of 6-inch PVC pipe, 6.000in / 152mm
Average Sleeve Dia	136mm
Effective sleeve thickness	9.53mm
Effective sleeve OD	145.53mm
Effective sleeve aspect ratio	1.051
Effective sleeve ID	126.47mm
Sleeve fill percentage	24.48%
Rod μ_i	250
μ_{sleeve}	3.88
Coil Form OD	6.626in / 168mm

Figure H.1: Ferrite Sleeve Parameters

60kHz Coil

This consists of 83 turns of 22AWG stranded wire wound on a 6-inch PVC pipe section. The following parameters were measured using this coil.

Parameter	Air Core	Ferrite Sleeve Core
Inductance	1.03mH	2.89mH
Resonant Q	128.8	133.9
Loaded Q	50	50

Figure H.2: 60kHz Coil Parameters

Series resistance was added in each case to lower the Q to 50, so the expected difference in signal strength should be solely due to differences in h_e .

AM Broadcast Band Coils

This consists of 20 turns of Litz wire (47 strands 40 AWG) close wound on a 6-inch PVC pipe section. An additional 10-turn winding was added next to the 20-turn winding, and these could be connected in series to verify the linearity of the receiver's RSSI display with the air core.

An additional air core coil was wound with 29 turns of Litz wire (47/40) on a 10-inch form with 0.1 inch winding pitch. This is expected to have roughly the same non-resonant height as the FSL antenna (20-turn coil).

For these calculations, there is no attempt to factor in differences in Q; as with the 60kHz tests, the Q of each setup is reduced by resistors in series with the coil, in this case targeting a Q of 100.

The antennas will be compared at 560kHz, where

$$\beta = \frac{2\pi \times 560,000}{2.997 \times 10^8} \approx 0.0117$$

The effective height is given by

$$h_e = \beta A n \mu_{sleeve},$$

where μ_{sleeve} is one for air core antennas.

Coil	Form OD	A	n	μ_{sleeve}	h_e
6-inch PVC	168mm	0.0222 m ²	30	1	7.8mm
10-inch fiberglass	254mm	0.0507 m ²	29	1	17.2mm
6-inch FSL	147mm	0.0166 m ²	20	3.9	15.1mm

Regarding weight, measurement of ferrite density is about 4.69g/cm³. Each rod weighs about 74.3g and the total sleeve with 36 rods has a weight of 2.67kg (5 lbs, 14 oz).

Large 60kHz Rectangular Air Core Loop

Form	Rectangular, 533x356mm (21x14 inches)
Coil	36T insulated 20ga copper, closely spaced
Inductance	1355uH
Resistance at 60kHz	3.20Ω

Loaded Q

$$\omega = 2\pi \times 60,000 \approx 377\text{krad/s}$$

$$C_{tune} = \frac{1}{(377\text{k})^2 \times 1335\text{uH}} \approx 5.19\text{nF}$$

$$R_c = \omega L \times \{0.006, 0.0007\} \approx \{3.1, 0.36\}\Omega$$

$$R_{ser} = 3.50, 0.79\Omega \quad (\text{from Matlab/Octave})$$

$$R_{loss} = 3.2 + \{3.1, 0.36\} = \{6.7, 4.0\}\Omega$$

$$Q = \frac{\omega L}{R_{loss}} = \frac{377\text{k} \times 1355\mu\text{H}}{\{6.7, 4.0\}\Omega} \approx \{76, 128\}$$

$$B_{3dB} = \frac{f_c}{Q} = \frac{60\text{kHz}}{\{76, 128\}} \approx \{790, 470\}\text{Hz}$$

$$B_{noise} = \frac{\pi}{2} B_{3dB} \approx \{1200, 740\}\text{Hz}$$

Effective Height

$$\beta = \frac{\omega}{c} = \frac{377\text{k}}{3 \times 10^8} \approx 0.00126$$

$$A = 0.533 \times 0.356 \approx 0.190\text{m}^2$$

$$h_e = \beta A n = 0.00126 \times 0.190 \times 36 \approx 8.6\text{mm}$$

$$h_e(\text{resonant}) = h_e Q = 8.2 \times \{76, 128\} \approx \{0.65, 1.1\}\text{m}$$

At this point, estimated receiver sensitivity of $4\mu\text{V}$ may be referred back to an E-field value by dividing it by the resonant effective height,

$$E_{sens} = \frac{4\mu\text{V}}{\{0.65, 1.1\}\text{m}} \approx \{6.1, 3.7\}\mu\text{V}/\text{m}$$

Thermal Noise

At a temperature of 300K, with noise bandwidth of 670Hz and resistance of $(3.76 + 1.05 \approx 4.8\Omega)$.

$$\sqrt{4kT} \approx 129\text{pV}/\sqrt{\Omega \text{ Hz}}$$

$$e_n = \sqrt{4kTBR} = 129\text{pV} \times \sqrt{\{1200, 740\} \times \{6.7, 4.0\}\Omega} \approx \{12, 7.0\}\text{nV}$$

$$E_n = \frac{e_n}{h_e} = \frac{\{12, 7.0\}\text{nV}}{8.6\text{mm}} \approx \{1.3, 0.81\}\mu\text{V}/\text{m}$$

Atmospheric Noise

$$E_{atm} = 120 + 30 \log_{10}(60,000) - 10 \log_{10}(\{76, 128\}) - 213.5 \approx \{31, 29\} \text{ dB}\mu\text{V}/\text{m}$$

Using PP capacitors instead of PPS film improves resonant effective height and reduces thermal noise by about 4.5dB. This may or may not be significant depending on the level of atmospheric noise present.

Small 60kHz Ferrite Loop

This is an analysis of the antenna that was found in an atomic clock receiver.

Ferrite Rod	7.700mm dia, 6.723mm across flats, 59.2mm long
Coil	225T 30ga copper wire, 2 layers
	Bottom layer 38.5mm long
	Top layer 16.5mm long, centered over bottom layer
Inductance	2100uH
Equivalent Parallel C	105pF
Resistance at 60kHz	3.76Ω

Core Area

Using equation (F.3),

$$\phi = \cos^{-1} \frac{6.732}{7.700} = 0.5092$$

$$A = \pi(7.700/2)^2 \left(1 - \frac{1}{\pi} \left[2 \times 0.5092 - \frac{6.732 \sin(0.5092)}{7.700/2} \right] \right) \approx 44.1\text{mm}^2$$

$$r_{eq} = \sqrt{\frac{A}{\pi}} = \sqrt{\frac{44.1}{\pi}} \approx 3.747\text{mm}$$

$$l/d = \frac{59.2}{2 \times 3.747} \approx 7.90$$

Permeabilities

$$A_L = \frac{0.0021}{225^2} \approx 41.5\text{nH/T}^2$$

$$\mu_{int} = \frac{A_L l_f}{\mu_o A_f} = \frac{41.5\text{nH/T}^2 \times 0.0592\text{m}}{1257\text{nH/m} \times 44.1 \times 10^{-6}\text{m}^2} \approx 44.3$$

There's a bit of a problem here as μ_{int} has come out unreasonably high. Even with $\mu_i = 2000$, we calculate $\mu_{rod} = 39.2$ for the given aspect ratio $l/d = 7.90$. However, this is a two layer coil and equations for that have not been developed here.

In order to get some ballpark numbers, we will use $\mu_{rod} = \mu_{ext} = 40$. The results should not be off by more than a factor of two.

Loaded Q

$$\omega = 2\pi \times 60,000 \approx 377\text{krad/s}$$

$$C_{tune} = \frac{1}{(377\text{k})^2 \times 2100\mu\text{H}} \approx 3.35\text{nF}$$

$$R_c = \omega L \times 0.006, 0.0007 \approx \{4.75, 0.55\}\Omega$$

$$R_{ser} = \{5.8, 1.6\}\Omega \quad (\text{from Matlab/Octave})$$

$$Q = \frac{\omega L}{R} = \frac{377\text{k} \times 2100\mu\text{H}}{3.76 + \{5.8, 1.6\}} \approx \{83, 148\}$$

$$B_{3dB} = \frac{f_c}{Q} = \frac{60\text{kHz}}{\{83, 148\}} \approx \{720, 410\}\text{Hz}$$

$$B_{noise} = \frac{\pi}{2} B_{3dB} \approx \{1100, 640\}\text{Hz}$$

The transformed receiver input impedance (1.045 ohms) is not the major determining factor in loaded Q, but it does pull it down noticeably. Using PPS instead of PP film capacitors has a significant detrimental effect.

Effective Height

$$\beta = \frac{\omega}{c} = \frac{377\text{k}}{3 \times 10^8} \approx 0.00126$$

$$h_e = \mu_{ext} \beta A n = 40 \times 0.00126 \times 44.1 \times 10^{-6} \times 225 \approx 0.50\text{mm}$$

$$h_e(\text{resonant}) = h_e Q = 0.50 \times \{83, 148\} \approx \{41, 74\}\text{mm}$$

At this point, estimated receiver sensitivity of $4\mu\text{V}$ may be referred back to an E-field value by dividing it by the resonant effective height,

$$E_{sens} = \frac{4\mu\text{V}}{\{0.041, 0.074\}\text{m}} \approx \{97, 54\}\mu\text{V/m}$$

There is a 5.1dB gain in sensitivity to be had by choosing PP over PPS film dielectric capacitors here.

Thermal Noise

At a temperature of 300K,

$$\sqrt{4kT} \approx 129\text{pV}/\sqrt{\Omega \text{ Hz}}$$

$$e_n = \sqrt{4kTBR} = 129\text{pV} \times \sqrt{\{1100, 630\} \times \{9.6, 5.4\}} \approx \{9.4, 7.1\}\text{nV}$$

$$E_n = \frac{e_n}{h_e} = \frac{\{13, 7.5\}\text{nV}}{0.50\text{mm}} \approx \{13, 7.5\}\mu\text{V/m}$$

Atmospheric Noise

$$E_{atm} = 120 + 30 \log_{10}(60,000) - 10 \log_{10}(\{83, 148\}) - 213.5 \approx \{31, 28\} \text{ dB}\mu\text{V/m}$$

40-inch Octagonal 60kHz Loop

Frequency	60kHz
Form	Octagonal, 1.016m (40 inches) across flats
Coil	24T 20ga PVC insulated wire
Spacing	3.2mm (1/8 inch)
Inductance	1345 μ H
Resistance at 60kHz	3.1 Ω
Parallel capacitance	13.6pF
SRF	1.19MHz

Loaded Q

$$\omega = 2\pi \times 60\text{kHz} \approx 377\text{krad/s}$$

$$C_{tune} = \frac{1}{(377\text{k})^2 \times 1345\mu\text{H}} \approx 5.233\text{nF}$$

$$R_c = \omega L \times \{0.006, 0.0007\} \approx \{3.04, 0.355\}\Omega$$

$$R_{ser} = \{3.5, 0.78\}\Omega \quad (\text{from Matlab/Octave})$$

$$Q = \frac{\omega L}{R} = \frac{377\text{k} \times 1345\mu\text{H}}{\{3.5, 0.78\}\Omega} \approx \{77, 131\}$$

$$B_{3dB} = \frac{f_c}{Q} = \frac{60\text{kHz}}{\{77, 131\}} \approx \{780, 460\}\text{Hz}$$

$$B_{noise} = \frac{\pi}{2} B_{3dB} \approx \{1200, 720\}\text{Hz}$$

Effective Height

$$\beta = \frac{\omega}{c} = \frac{377 \times 10^3}{3 \times 10^8} \approx 0.00126$$

$$A = 8 \left(\frac{d}{2} \right)^2 \tan \frac{\pi}{8} = 8 \left(\frac{1.016}{2} \right)^2 \times 0.4142 \approx 0.855 \text{m}^2$$

$$h_e = \beta A n = 0.00126 \times 0.855 \times 24 \approx 25.8 \text{mm}$$

$$h_e(\text{resonant}) = h_e Q = 0.0258 \times \{77, 131\} \approx \{2.0, 3.4\} \text{m}$$

At this point, a receiver sensitivity of $4\mu\text{V}$ may be referred back to an equivalent E-field value by dividing it by the resonant effective height,

$$E_{sens} = \frac{4\mu\text{V}}{\{2.0, 3.4\} \text{m}} \approx \{2.0, 1.2\} \mu\text{V/m}$$

Thermal Noise

At a temperature of 300K, with noise bandwidth of 650Hz and resistance of (3.53Ω),

$$\sqrt{4kT} \approx 129 \text{pV}/\sqrt{\Omega \text{ Hz}}$$

$$e_n = \sqrt{4kTBR} = 129 \text{pV} \times \sqrt{\{780, 460\} \text{Hz} \times \{3.5, 0.78\} \Omega} \approx \{11.5, 6.8\} \text{nV}$$

$$E_n = \frac{e_n}{h_e} = \frac{\{11.5, 6.8\} \text{nV}}{25.8 \text{mm}} \approx \{0.45, 0.26\} \mu\text{V/m}$$

Atmospheric Noise

$$E_{atm} = 120 + 30 \log_{10}(60,000) - 10 \log_{10}(\{77, 131\}) - 213.5 \approx \{31, 29\} \text{ dB}\mu\text{V/m}$$

4-foot Octagonal MW Loop

Frequency range	540 to 1700kHz
Form	Octagonal, 1.18m (46.5 inches) across flats
Coil	7T 20ga magnet wire
Spacing	7.2mm
Inductance	156 μ H
Resistance at 540kHz	2.3 Ω
Receiver	Silicon Labs Si4734, 3.8 μ V sensitivity

Performance will be worst at the low end of the band so calculations are performed at 540kHz. The turn count (7) cannot be made any larger without lowering the SRF to a point where the receiver cannot tune the top end of the band.

Loaded Q

Assuming that the actual Q is forced by the receiver to be 50,

$$\omega = 2\pi \times 540\text{kHz} \approx 339\text{Mrad/s}$$

$$C_{tune} = \frac{1}{(339\text{M})^2 \times 156\mu\text{H}} \approx 550\text{pF}$$

$$B_{3dB} = \frac{f_c}{Q} = \frac{540\text{kHz}}{50} \approx 10.8\text{kHz}$$

$$B_{noise} = \frac{\pi}{2} B_{3dB} \approx 17\text{kHz}$$

$$R_{noise} = \frac{\omega L}{50} \approx 11\Omega$$

Effective Height

$$\beta = \frac{\omega}{c} = \frac{3.39 \times 10^6}{3 \times 10^8} \approx 0.0113$$

$$A = 8 \left(\frac{d}{2} \right)^2 \tan \frac{\pi}{8} = 8 \left(\frac{1.18}{2} \right)^2 \times 0.4142 \approx 1.16 \text{m}^2$$

$$h_e = \beta A n = 0.0113 \times 1.16 \times 7 \approx 92 \text{mm}$$

$$h_e(\text{resonant}) = h_e Q = 92 \times 50 \approx 4.6 \text{m}$$

At this point, a receiver sensitivity of $3.8 \mu\text{V}$ may be referred back to an equivalent E-field value by dividing it by the resonant effective height,

$$E_{sens} = \frac{3.8 \mu\text{V}}{4.6 \text{m}} \approx 0.82 \mu\text{V/m}$$

Thermal Noise

This is examined from two viewpoints. First, we assume a direct connection to a receiver which limits the resonant Q to a value of 50. At a temperature of 300K, with noise bandwidth of 670Hz and resistance of (11Ω) – using the resistance equivalent used to reduce loop Q down to 50.

$$\sqrt{4kT} \approx 129 \text{pV}/\sqrt{\Omega \text{ Hz}}$$

$$e_n = \sqrt{4kTBR} = 129 \text{pV} \times \sqrt{17 \text{kHz} \times 11} \approx 55 \text{nV}$$

$$E_n = \frac{e_n}{h_e} = \frac{55 \text{nV}}{8.6 \text{mm}} \approx 6.4 \mu\text{V/m}$$

Thermal noise in this bandwidth is higher than the receiver's sensitivity, and this will slightly degrade the overall system sensitivity.

Atmospheric Noise

$$E_{atm} = 120 + 30 \log_{10}(60,000) - 10 \log_{10}(50) - 213.5 \approx 11.5 \text{ dB}\mu\text{V/m}$$

Atmospheric noise is about 6dB higher than thermal, and this may end up being the limit on sensitivity.

Amplifier Noise Requirements

It's possible to examine the requirements necessary to buffer and/or amplify the loop's output output with a low noise operational amplifier.

With the same assumptions as above, we instead computed the thermal noise density at the resonant frequency – at the output of the resonated loop.

$$\begin{aligned}e_n &= Q \sqrt{4kT} \sqrt{R} \\ &= 50 \times 129pV \times \sqrt{11\Omega} \\ &\approx 21nV/\sqrt{Hz}\end{aligned}$$

It's not difficult to find high input impedance op-amps with noise density values better than this. It's also necessary to keep the amplifier's input current noise from swamping the thermal noise. Even if the amplifier input impedance is infinite, the loop terminals will have an impedance of 120k Ω (calculated with Matlab/Octave), so the input noise current will be converted to voltage across this impedance. The thermal noise would be equaled by the following current noise passing through this impedance:

$$i_n = \frac{e_n}{120,000} \approx 180fA/\sqrt{Hz}$$

One possible choice of amplifier is the Analog Devices AD8067 with voltage noise below 7nA/ \sqrt{Hz} and current noise less than one fA/ \sqrt{Hz} . It's also capable of a gain of 26dB out throughout the AM band and can easily drive a 50 Ω resistive load. These are available for \$4-5US each in small quantities as of 2020.

FSL Examples

Figure H.3 shows some of the details of the calculations for effective height of the example FSL designs discussed in the chapter on FSL antennas. All dimensions are in millimeters. All ferrite is assumed to have intrinsic permeability $\mu_i = 400$. Figure 8.6 contains more detail on the FSL designs listed here.

FSL Design Name	Fill	Sleeve Geometry			uRod	Effective Height	
		OD	Thick	Aspect		Est	Sim
3-inch Micro	0.709	73.9	5.7	0.88	3.70	12.0	11.4
3.5-inch Long John	0.647	85.4	6.5	2.34	9.15	29.6	28.8
5-inch Short-rod	0.740	124.9	5.9	0.52	2.48	19.1	18.7
5-inch Ultra Light	0.709	124.7	5.7	1.12	4.40	29.3	28.5
7-inch AM-Band	0.720	175.6	5.8	0.80	3.28	33.2	32.6
17-inch DXpedition	0.747	429.3	7.5	0.47	2.21	67.0	66.0
3-inch Bar	0.771	81.9	2.3	1.22	4.57	21.2	18.9
5-inch Bar	0.852	126.6	2.6	0.79	3.16	27.5	25.2
7-inch Bar	0.895	177.5	2.7	0.56	2.46	29.4	27.4
3-inch PL-380 Model	0.895	56.6	2.7	1.77	6.66	12.6	11.0

Figure H.3: Details on FSL calculations

- Fill is the fraction of the sleeve outline cross section that is actually filled with ferrite as opposed to gaps between the rods or bars.
- Sleeve geometry is the *effective* size of the sleeve, which compensates for the fill fraction.
- uRod is the computed apparent fluxmetric permeability, μ_{rod} , for a sleeve of the indicated geometry, and was used to estimate effective height.
- Two different effective heights are shown:
 - A value computed using the methods described chapter 8.
 - The simulated value using a physical model matching the actual FSL design.

Appendix I

Matlab/Octave Scripts

The 7-zip archive attached to this PDF document contains scripts useful for analysis and design of electrically small loop antennas. Scripts are organized into several directories:

AirCoreLoops Functions for analyzing air core loops.

Fext For computing values F_{ext} with ferrite core loops.

uRod Functions to compute μ_{rod} for ferrite core designs.

ITU Digitized ITU data on atmospheric noise.

More information about these scripts will be added in future versions of this document.

Air Core Loops

General Analysis

This is an overarching function which will perform many of the calculations needed to analyze the behavior of one or more air core loops.

Estimation of SRF

This, and associated scripts are a copy of the files provided in our article on self resonance in solenoids. The top-level function is named `EstimateSRF`. See [osengr-2] for more about this and associated scripts.

Inductance Calculations

These functions are based on Robert Weaver's excellent series of articles [Weaver] at electronbunker.ca. Functions to accurately estimate solenoid inductance for uniformly wound solenoids, as well as more arbitrary constructions are provided.

Rather than being based on formulas fit to data, these functions work by computing the mutual inductance between every pair of turns in the solenoid, including between each turn and itself. Exact solutions to Maxwell's equations are used, and this provides very accurate results as long as the winding pitch is not too steep (that's the case for a majority of air core loop designs).

This method also lends itself to situations where the solenoid turns are not evenly spaced, and turn diameters are unequal, such as with spiral or conically shaped coils. The function `LcoilUniform` contains an example of this kind of calculation.

Bibliography

- [Attwood] Attwood, S.S., *Electric and Magnetic Fields*, John Wiley and Sons (1949)
- [CIA] Central Intelligence Agency (?), *Final Report on the Ferrite Antennas for Very Low Frequencies*
- [Balinis] Balanis, Constantine A., *Antenna Theory, Third Edition*, Wiley Interscience 2005, ISBN 0-471-66782-X
- [Bolton] Bolton, Timothy, *Optimal Design of Electrically Small Loop Antenna Including Surrounding Medium Effects*, Georgia Tech Masters Thesis
- [Bolton-1] Ibid, pp50-63.
- [Cross] R. Cross, *Ferrite Rod Receiving Loop Antenna Analysis and Modeling*, spreadsheet and documentation, Sept. 2007.
http://raylcross.net/murod_mm/index.html
- [Cross-1] Bolton, Timothy, Excel spreadsheet
https://raylcross.net/murod_mm/MUMMROD.XLS
- [DeBock-1] DeBock, Gary, *FSL Antenna Design Optimization*, March, 2012,
<http://www.mediafire.com/?6oyoldllrbiwf91>
- [DeBock-2] DeBock, Gary, Puyallup, WA, October 2011,
7 Inch Diameter "Affordable" FSL Antenna
- [DeBock-3] DeBock, Gary, Puyallup, WA, May 2012,
8" Ferrite Sleeve Loop Antenna Demonstration,
<https://www.youtube.com/watch?v=iqYZcRXGxM>
- [DeBock-4] DeBock, Gary, *Gary DeBock's guide to building the ultimate FSL antenna for the Tecsun PL-380*,
<https://swling.com/blog/2016/01/dx-fiend-gary-debocks-guide-to-building-the-ultimate-fsl-antenna-for-the-tecsun-pl-380/>

- [Dowell] Dowell, P.L., *Effects of eddy currents in transformer windings*, Proceedings of the IEE, Vol 113, No. 8, August 1966, pp.1387-1394
- [Ferroxcube] Ferroxcube, *Soft Ferrites Introduction*, September 1, 2008
- [ITU-R] International Telecommunication Union,
Radio Noise, Recommendation ITU-R P.372.13 09/2016,
https://www.itu.int/dms_pubrec/itu-r/rec/p/R-REC-P.372-13-201609-1!!PDF-E.pdf
- [Knight-1] Knight, David W., *Practical continuous functions for the internal impedance of solid cylindrical conductors*, DOI: 10.13140/RG2.1.3865.1284
- [Knight-2] Knight, David W., *Solenoid Impedance and Q*
- [Nan] Nan, Xi and Sullivan, Charles, *An Improved Calculation of Proximity-Effect Loss in High Frequency Windings of Round Conductors*, IEEE Power Electronics Specialists Conference, June 2003, pp. 853-860.
- [Medhurst-1] Medhurst, R. G., *H.F. Resistance and Self-Capacitance of Single-Layer Solenoids* part 1, *Wireless Engineer*, February 1947, pp.35-43
- [Medhurst-2] Medhurst, R. G., *H.F. Resistance and Self-Capacitance of Single-Layer Solenoids* part 2, *Wireless Engineer*, March 1947, pp.80-92
- [Payne] Payne, A.H. *Losses in Ferrite Rod Antennas*, <http://g3rbj.co.uk>
- [Popiel] Popiel, Jerry,
Jerry's Mediumwave DXing Powerhouse Mini FSL Antenna,
<https://swling.com/blog/tag/tecsun-pl-380-ferrite-sleeve-loop/>
- [Snelling] Snelling, E.C., *Soft Ferrites, Properties and Applications, section 4.3, Open Magnetic Cores* Iliffe Books, Ltd. 1969.
- [Tongue] Tongue, Ben, *About Maximizing the Q of solenoid inductors that use ferrite rod cores*, Internet article,
<http://www.bentongue.com/about-maximizing-the-q-of-solenoid-inductors-that-use-ferrite-rod-cores-including-charts-of-magnetic-flux-density-and-flux-lines-with-some-actual-q-and-inductance-measurements-from-simulations-in-fe/>
- [Weaver] Weaver, Robert,
Numerical Methods for Inductance Calculation,
Internet article, <http://electronbunker.ca/eb/CalcMethods.html>
- [Weaver-1] Ibid, <http://electronbunker.ca/eb/CalcMethods1b.html>

- [osengr-1] Open Source Hardware Engineering,
Inductance of Solenoids on Ferrite Rods,
<https://www.osengr.org/Articles/Ferrite-Rod-Inductance.pdf>
- [osengr-2] Open Source Hardware Engineering,
Self-Resonance Frequency of Single-Layer Air Core Solenoids,
<https://www.osengr.org/Articles/Solenoid-Self-Resonance.pdf>
- [Krauss] Krauss, Bostian, Raab,
Solid State Radio Engineering,
John Wiley & Sons, 1980, ISBN 0-471-03018-X
- [Green] Green, Leslie,
RF Inductor Modeling for the 21st Century,
EDN Magazine, September 2001, pp67-74,
<https://www.edn.com/rf-inductor-modeling-for-the-21st-century/>